Time of flight neutron scattering and the path to NIMROD

Daniel Bowron

ISIS Facility
Science and Technology Facilities Council
Rutherford Appleton Laboratory
Chilton, Didcot
Oxfordshire
OX11 0QX

The neutron diffraction experiment

Total Structure Factor

Atomic concentrations and scattering lengths

$$F(Q) = \sum_{\alpha,\beta} c_\alpha c_\beta b_\alpha b_\beta (S_{\alpha\beta}(Q) - 1)$$

Partial Structure Factors

$$S_{\alpha\beta}(Q) - 1 = 4\pi\rho \int_0^\infty r^2 (g_{\alpha\beta}(r) - 1) \frac{\sin(\mathrm{Qr})}{\mathrm{Qr}} \mathrm{dr}$$

Atomic density

Partial Pair Distribution Functions

Schematic of a neutron scattering experiment

$Q = 4\pi/\lambda \sin\theta$

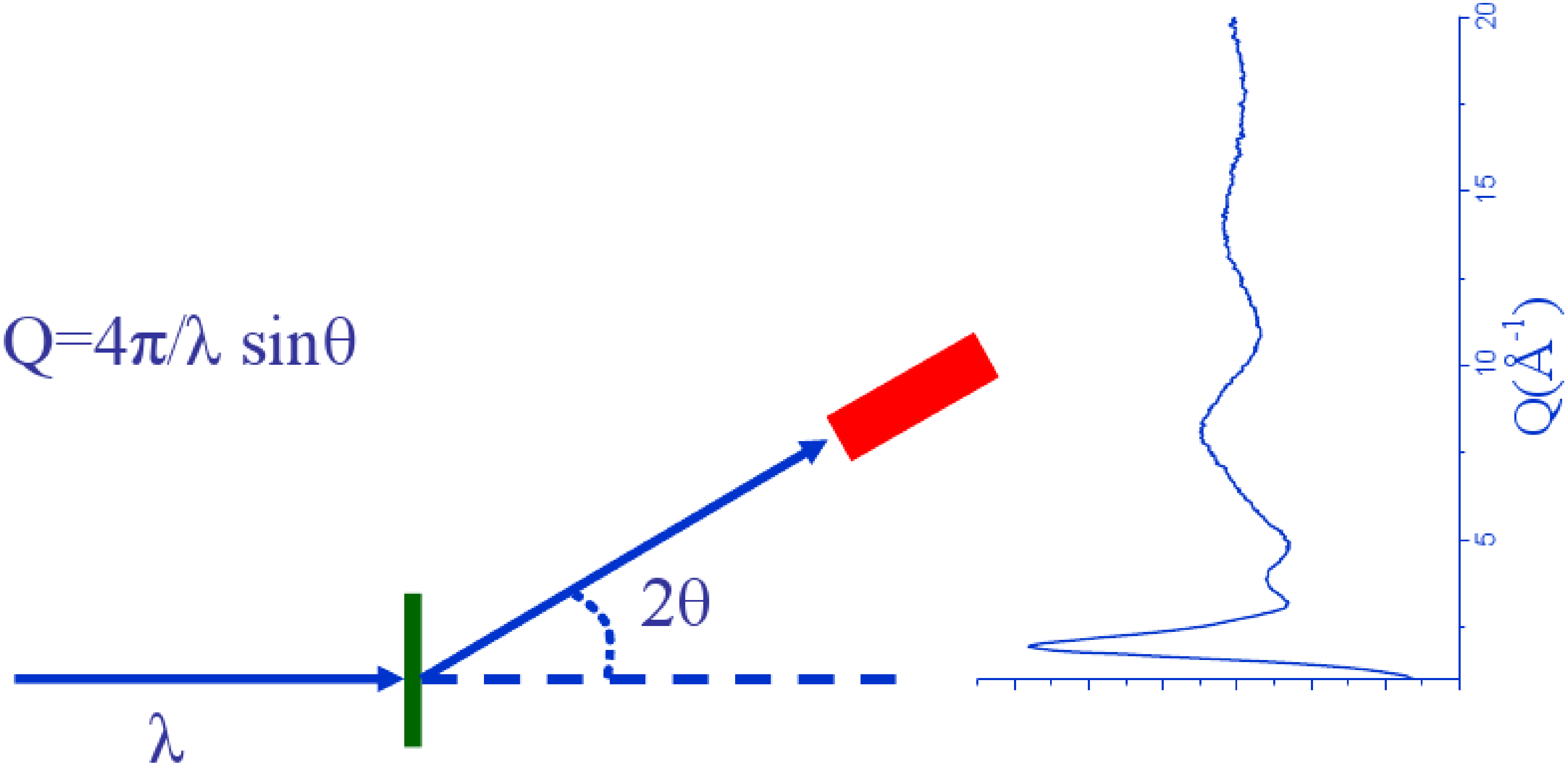

Schematic of the D4C neutron diffractometer at the ILL

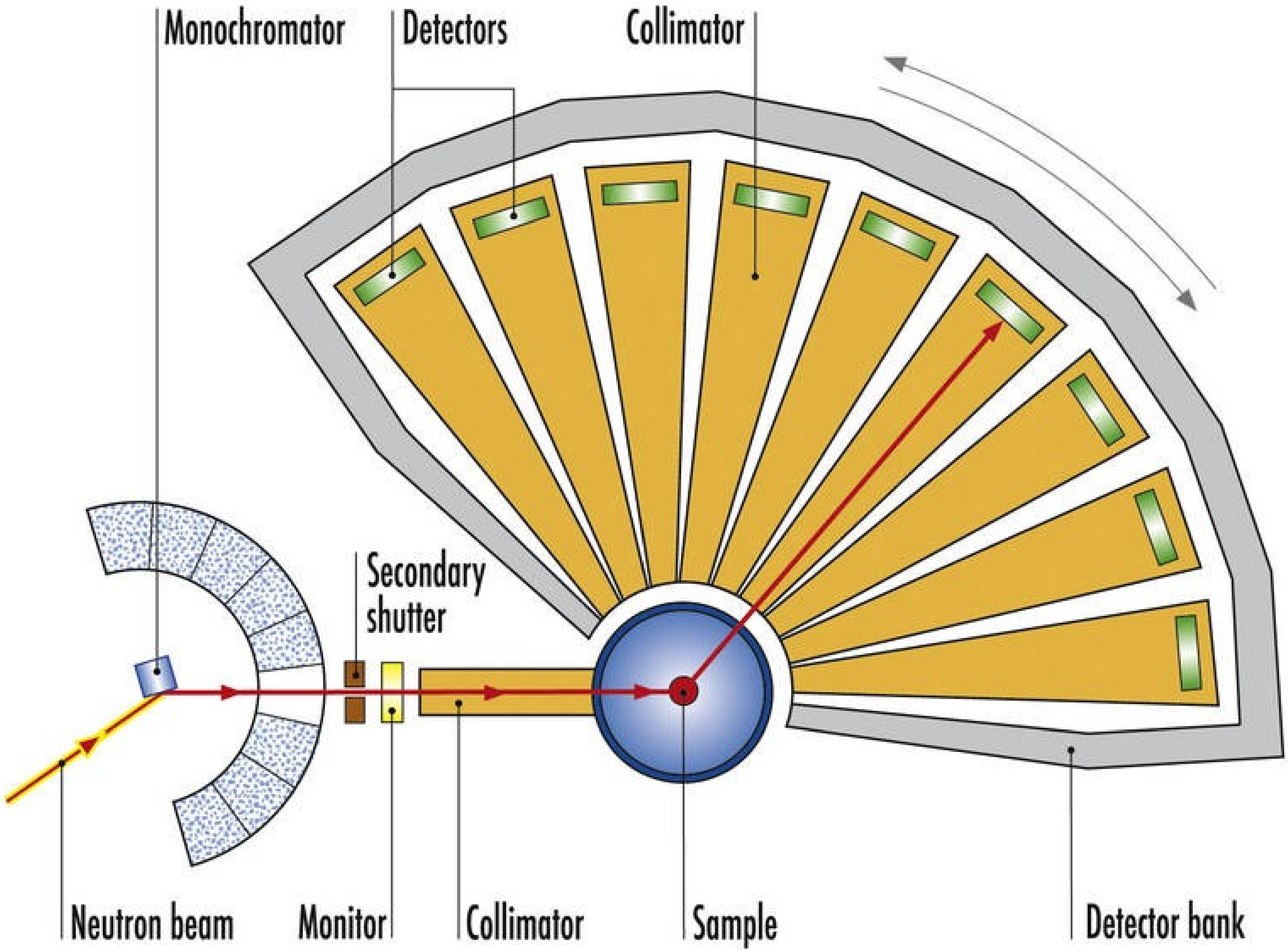

Schematic of the SANDALS diffractometer at ISIS

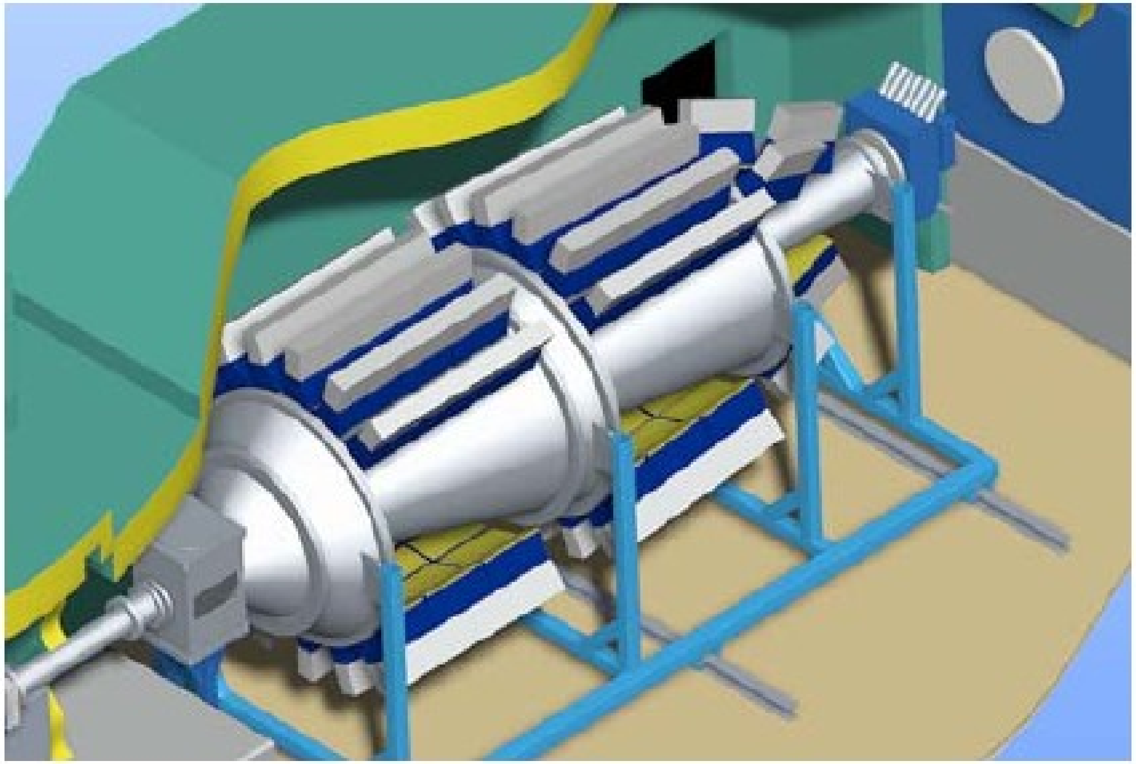

Time of flight neutron scattering

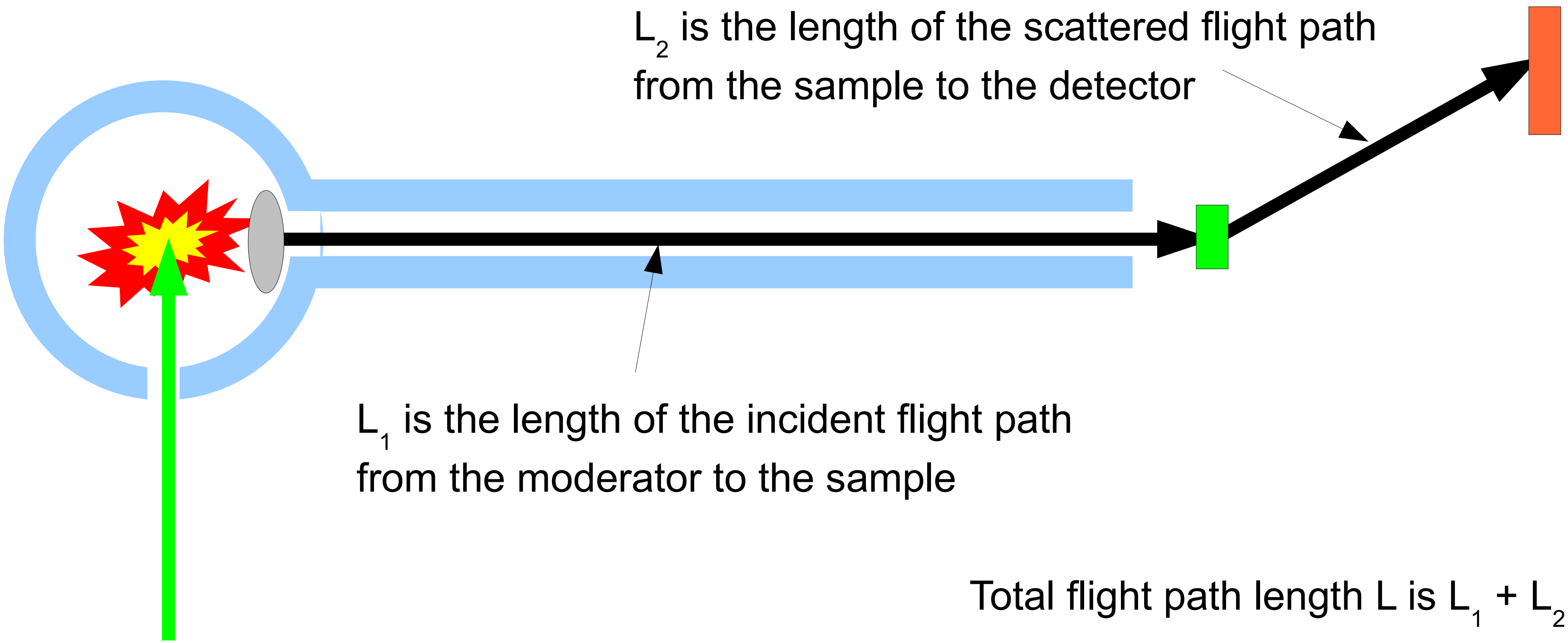

Total flight path length L is $L_1 + L_2$

The time of flight (TOF) is the time in μs taken for a neutron to travel 1m (μs m^{-1})

The time of arrival at the detector, t_0 , is the TOF (μs m^{-1}) multiplied by the total flight path (m)

Time of flight neutron scattering: Some useful relationships

Time of arrival

$$t_0 = \mathrm{TOF}\,.\,L$$

Neutron wavelength

$$\lambda = 0.0039562.\mathrm{TOF} = 0.0039562.\frac{t_0}{L}$$

$$t_0 = 252.77\,\lambda\,L$$

Neutron velocity

$$v = \frac{10^6}{\mathrm{TOF}}$$

Neutron wave vector

$$k = \frac{2\pi}{\lambda} = \frac{1588.2}{\mathrm{TOF}}$$

Neutron energy

$$E = \frac{81.807}{\lambda^2}$$

$$v\left[m\,s^{-1}\right]\,,\;t_0\,[\mu s]\;,\mathrm{TOF}\left[\mu s\,m^{-1}\right]\,,\;L\,[m]\;,\;\lambda\left[\text{Å}\right],$$
$$k\left[\text{Å}^{-1}\right]\,,\;E\,[\mathrm{meV}]$$

Time of flight neutron scattering: Typical values

Wavelength	Energy	Time of arrival (L=10m)	Speed
20Å	0.205 meV	50554 μs	197.8 ms^{-1}
10Å	0.818 meV	25277 μs	395.6 ms^{-1}
5Å	3.273 meV	12638.5 μs	791.2 ms^{-1}
4Å	5.113 meV	10110.8 μs	989.0 ms^{-1}
3Å	9.090 meV	7583.1 μs	1319 ms^{-1}
2Å	20.452 meV	5055.4 μs	1978 ms^{-1}
1Å	81.807 meV	2527.7 μs	3956 ms^{-1}
0.5Å	327.228 meV	1263.9 μs	7912 ms^{-1}
0.25Å	1.309 eV	631.9 μs	15825 ms^{-1}
0.1Å	8.181 eV	252.8 μs	39557 ms^{-1}
0.05Å	32.723 eV	126.4 μs	79114 ms^{-1}

Time of flight neutron scattering: Spectral profile

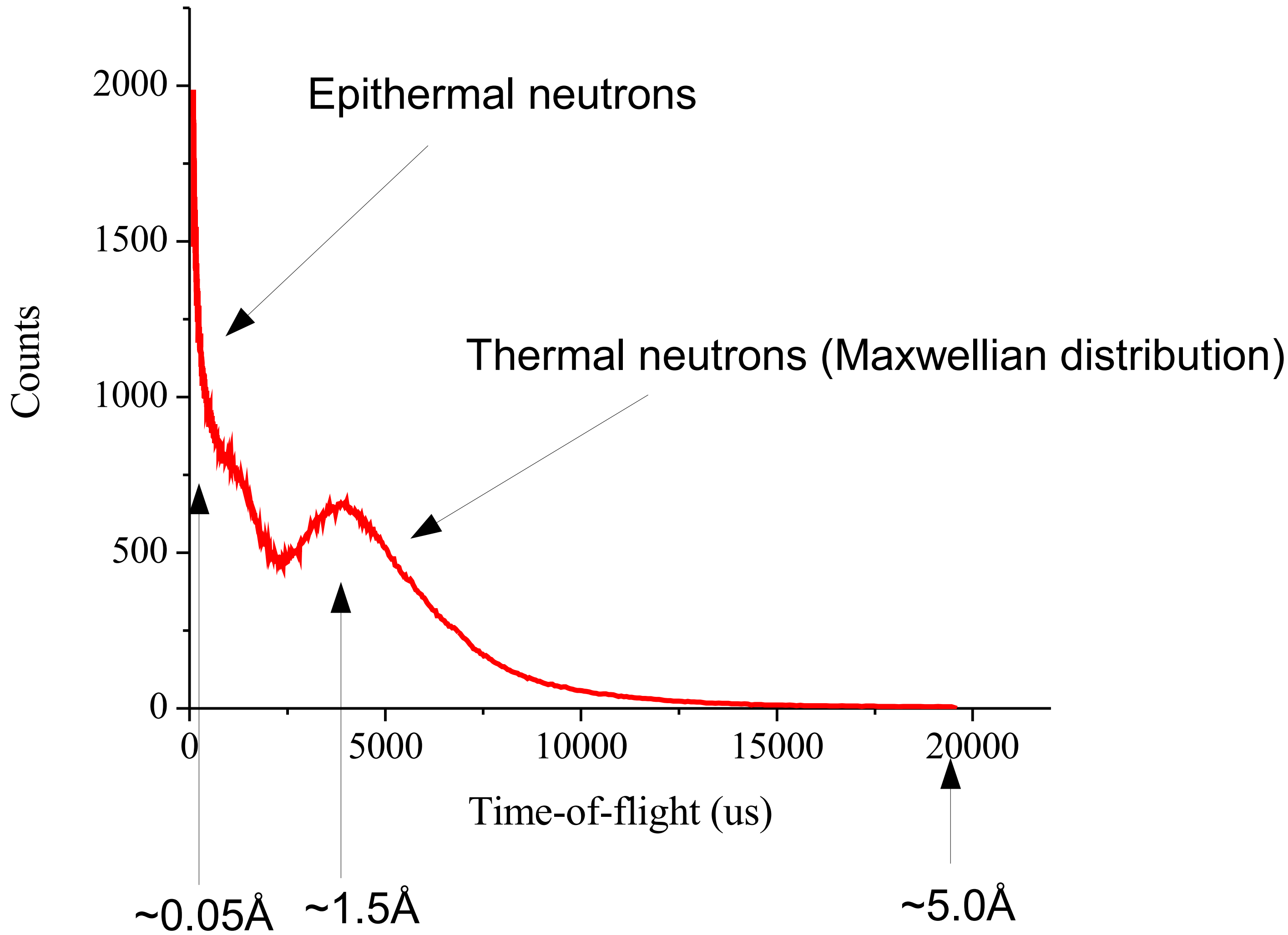

Time of flight neutron scattering: Spectrum parametrization

$$\Phi_{\text{Epithermal}}(E) = \frac{\Phi_0}{E^A}$$

$$\Phi_{\text{Maxwellian}}(E) = J\frac{E}{T^2}\exp\left\{\frac{-E}{T}\right\}$$

$$\Phi_{\text{Total}}(E) = \Phi_{\text{Maxwellian}} + \Delta(E)\Phi_{\text{Epithermal}}$$

$$\Delta(E) = \frac{1}{\left[1+\exp\left\{\frac{W_1}{\sqrt{E}} - W_2\right\}\right]}$$

$$\Phi(\lambda) = \Phi(E)\left(\frac{\delta E}{\delta\lambda}\right) = 2\Phi(E)\left(\frac{E}{\lambda}\right)$$

Time of flight neutron scattering: Spectrum parametrization

Methane moderator

$$\Phi_0\,(\text{at } 750\text{MeV}) \rightarrow 2.7\left[10^{10} n(\text{eVsr}100\text{cm}^2\mu\text{As})^{-1}\right]$$

$$A \rightarrow 0.92$$

$$J \rightarrow 5.7\left[10^{10} n(\text{sr}100\text{cm}^2\mu\text{As})^{-1}\right]$$

$$T\,(\text{eV}) \rightarrow 0.011$$

Proton beam energy

$$W_1\,(\text{eV})^{\frac{1}{2}} \rightarrow 1.7$$

Typical moderator view

$$W_2 \rightarrow 7.0$$

Time of flight neutron scattering: Spectrum parametrization

Methane moderator

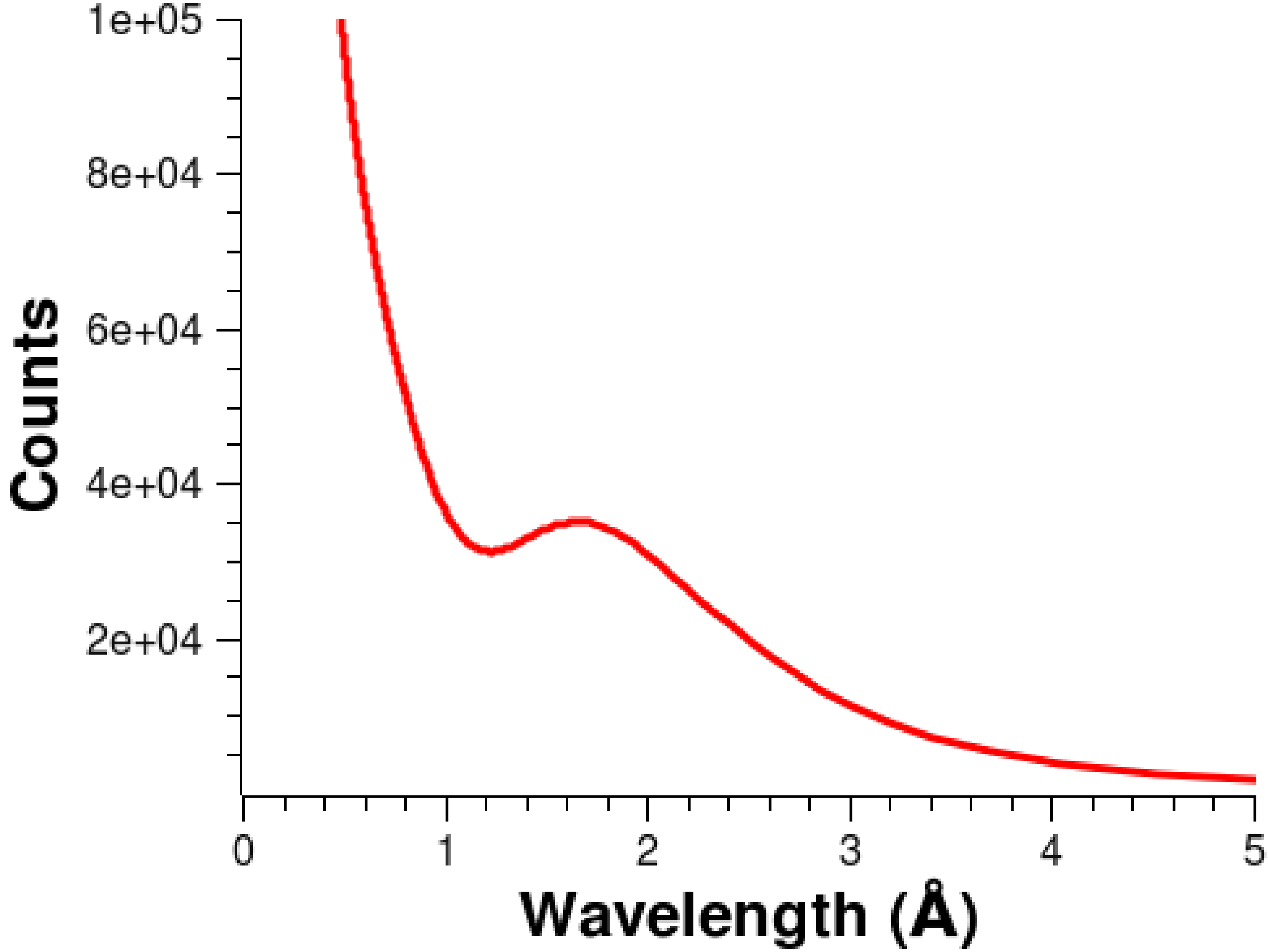

Light element optimized diffractometers
SANDALS type

Utilise:
(1) relatively small forward scattering angles: 1º to 40º
(2) high energy neutrons $0.05Å \leq \lambda \leq 5.0Å$
(3) wide accessible Q-range $0.1Å^{-1} \leq Q \leq 50Å^{-1}$
(4) flat plate sample geometry
(5) moderate resolution $\Delta Q/Q \approx 2\%$

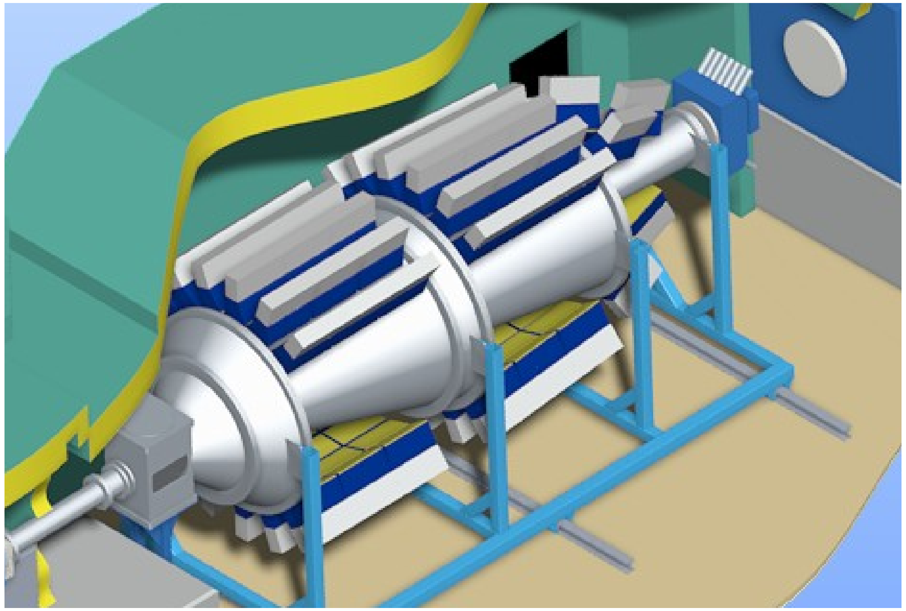

Distribution of Q-ranges across the detector banks

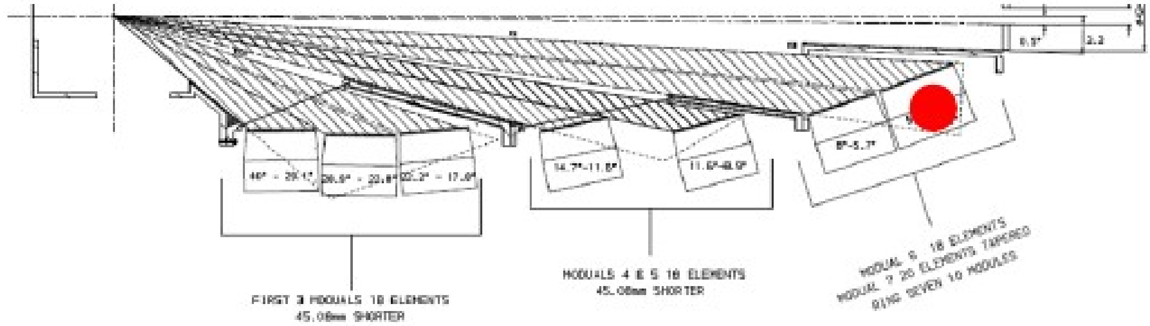

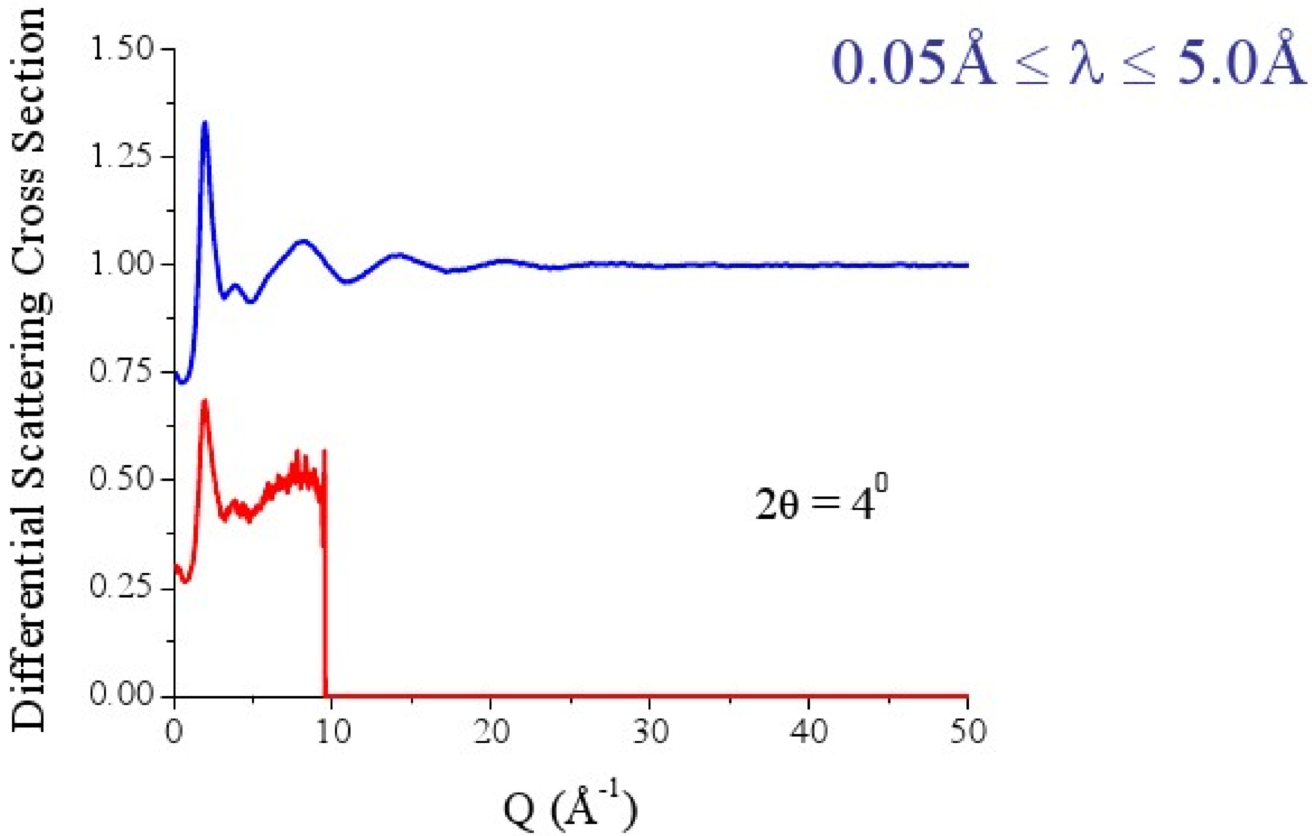

Distribution of Q-ranges across the detector banks

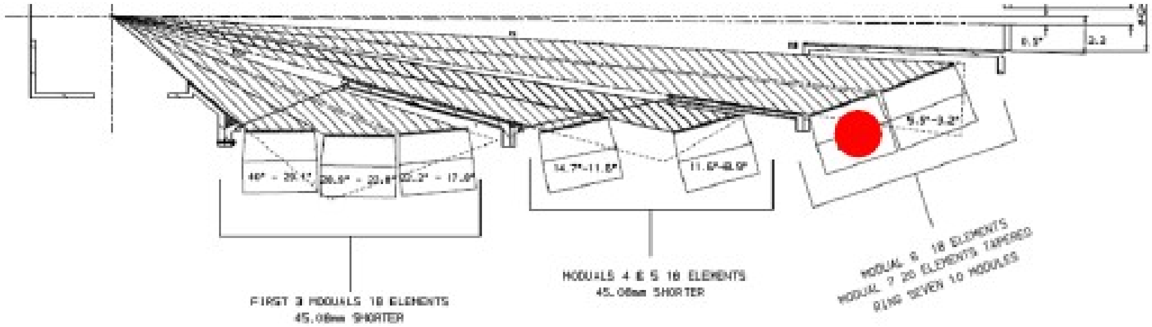

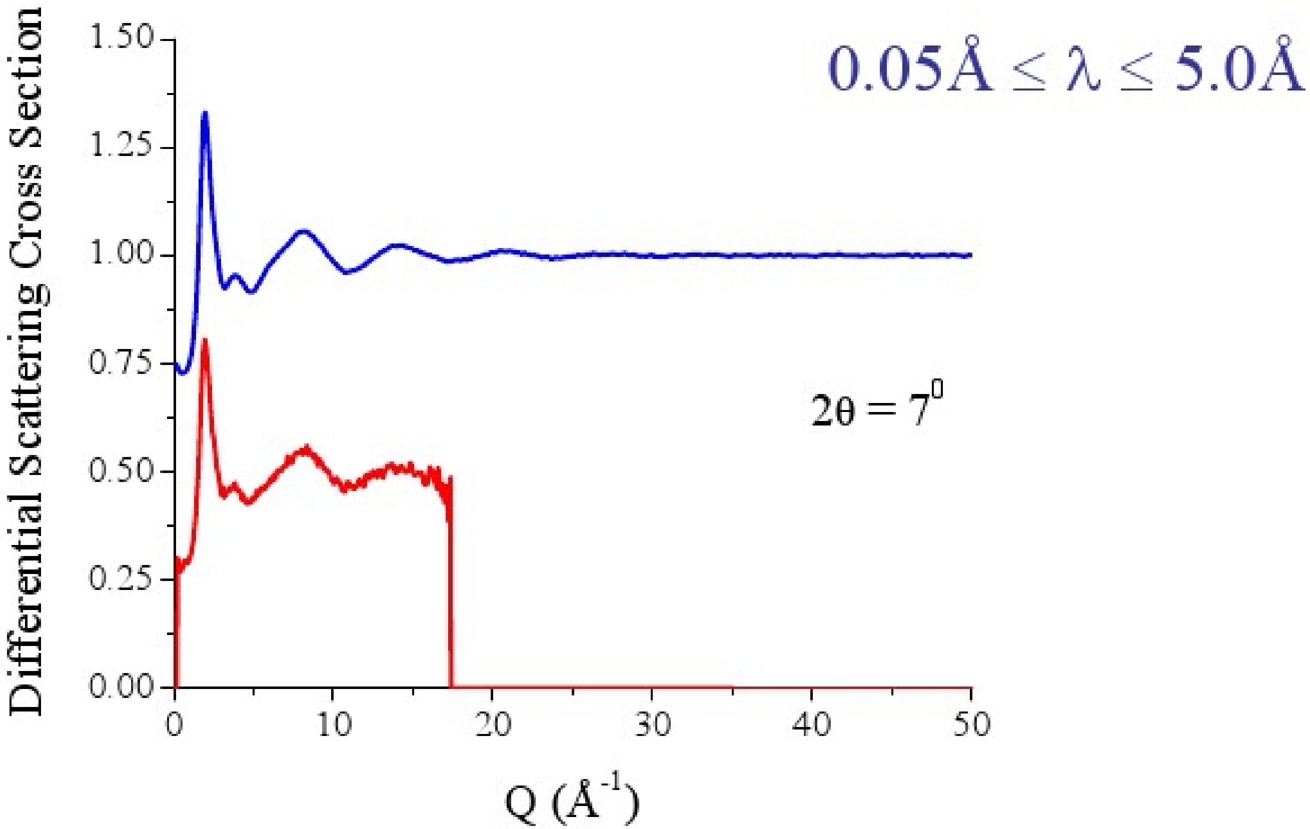

Distribution of Q-ranges across the detector banks

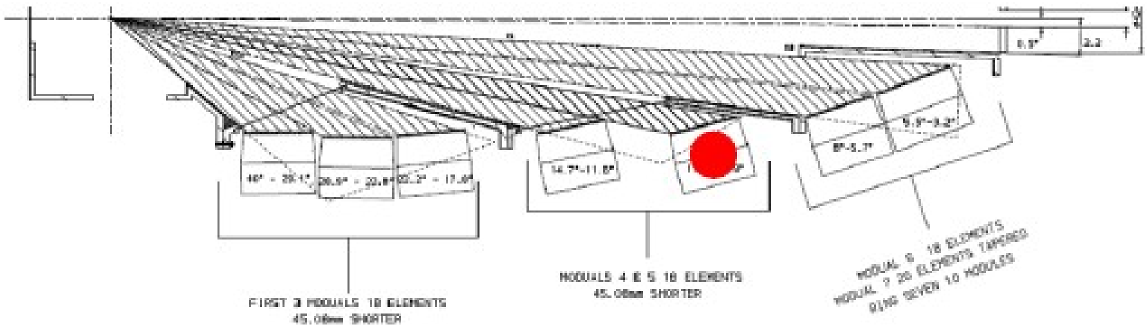

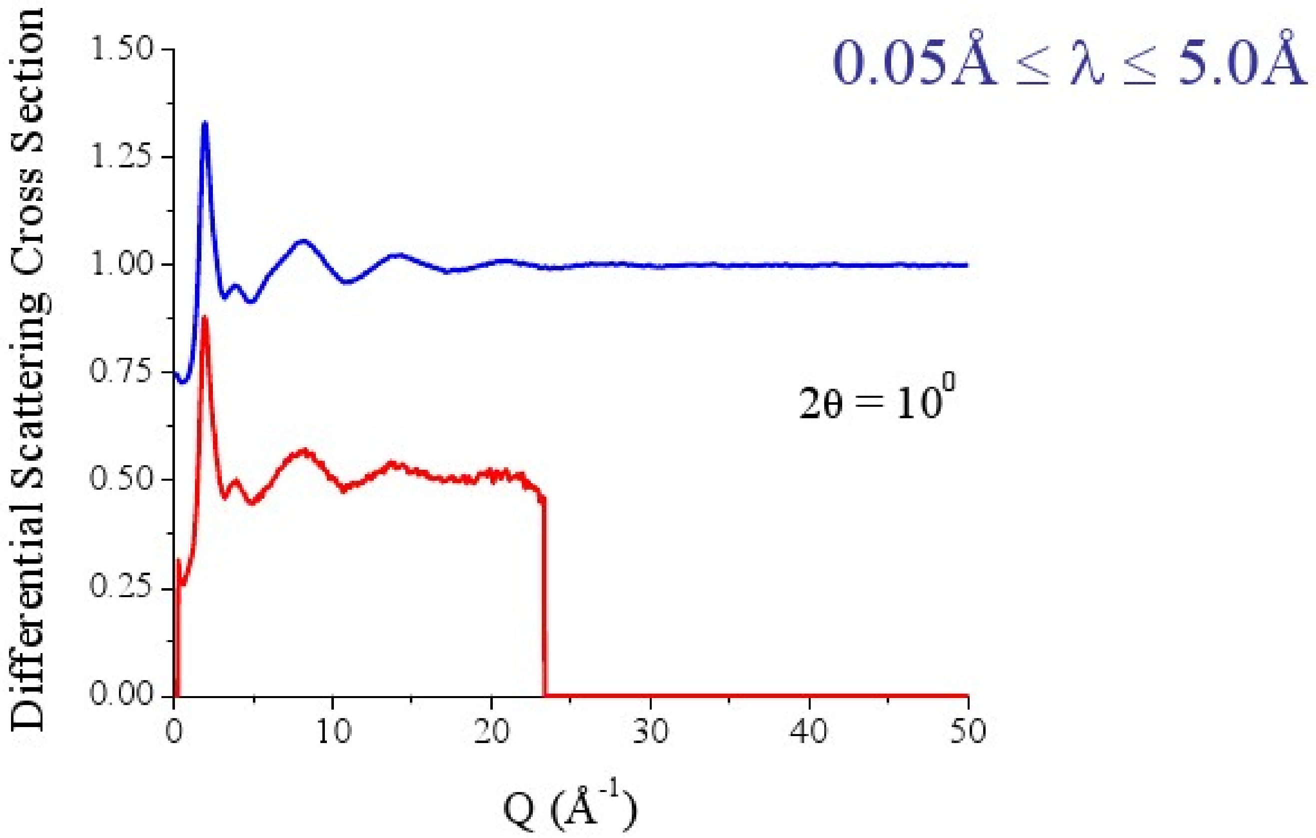

Distribution of Q-ranges across the detector banks

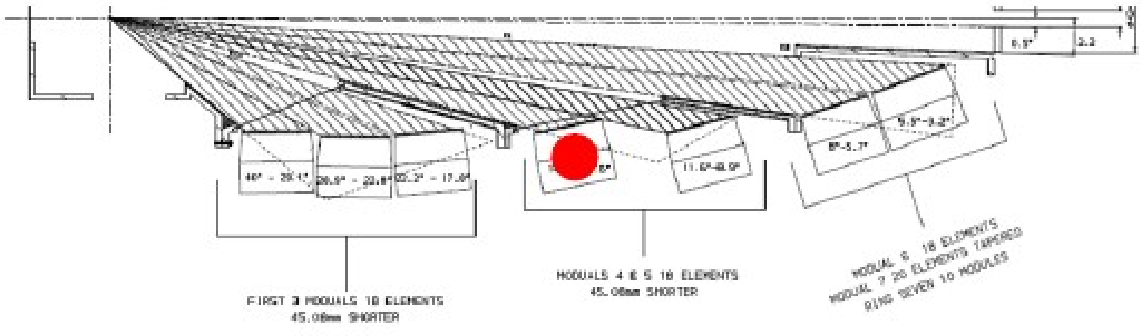

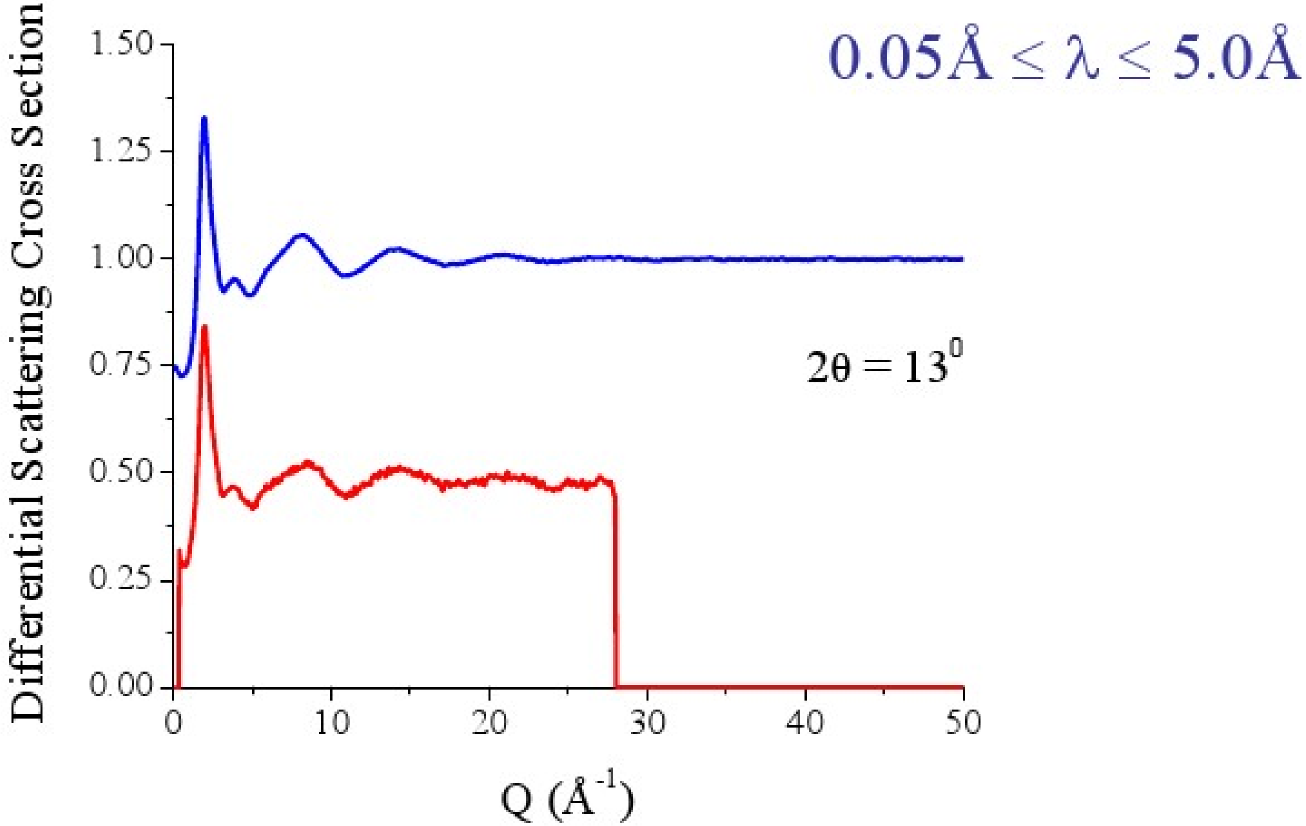

Distribution of Q-ranges across the detector banks

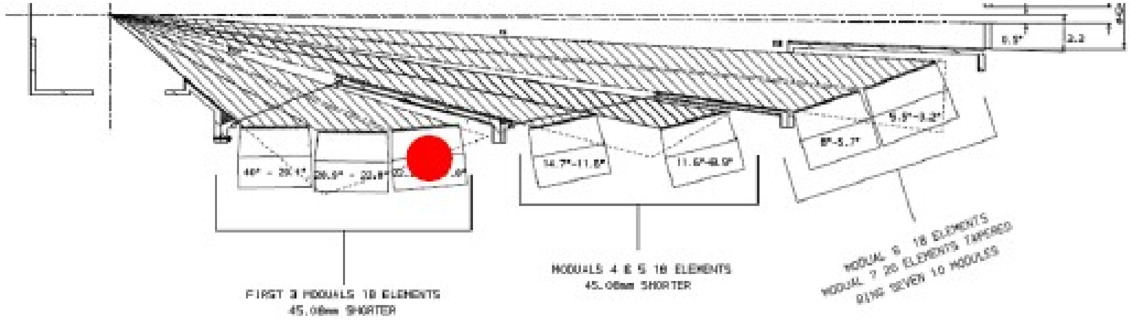

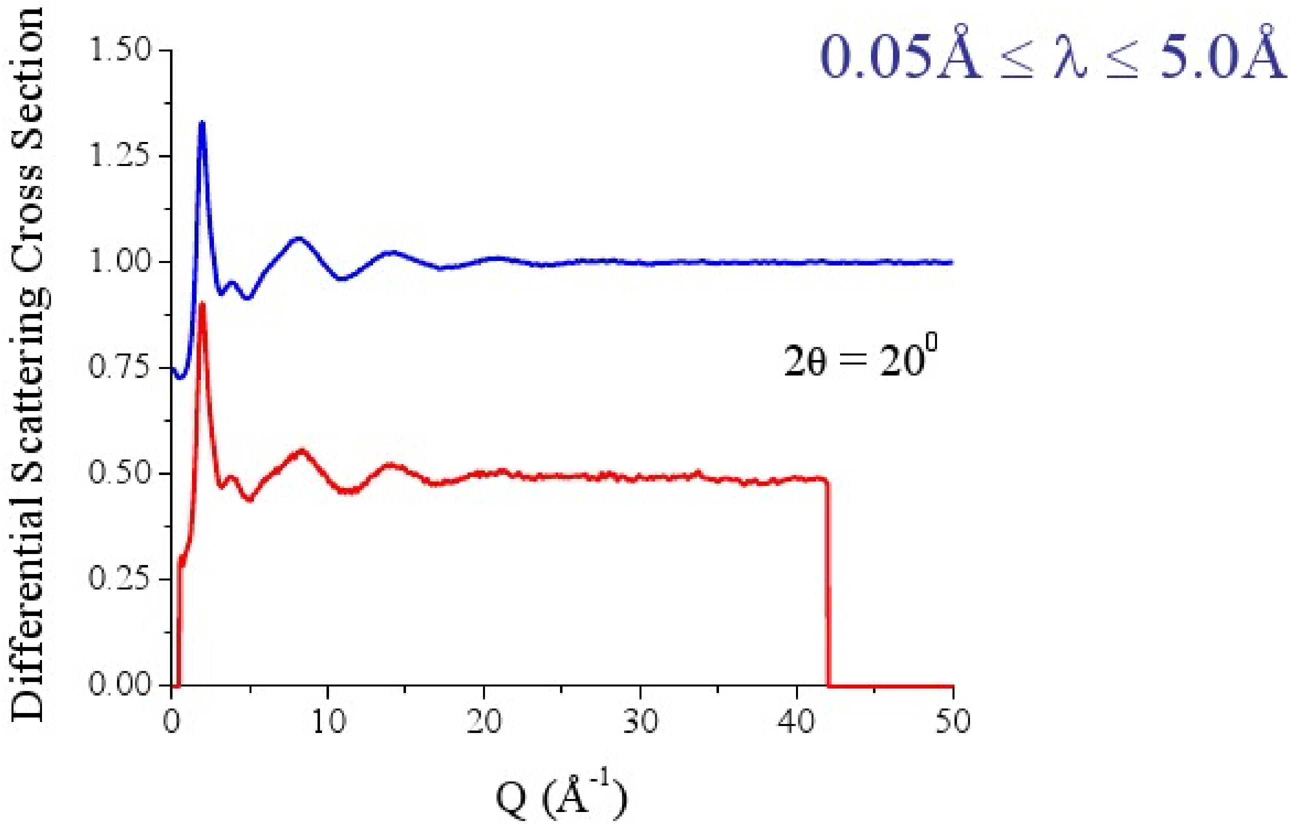

Distribution of Q-ranges across the detector banks

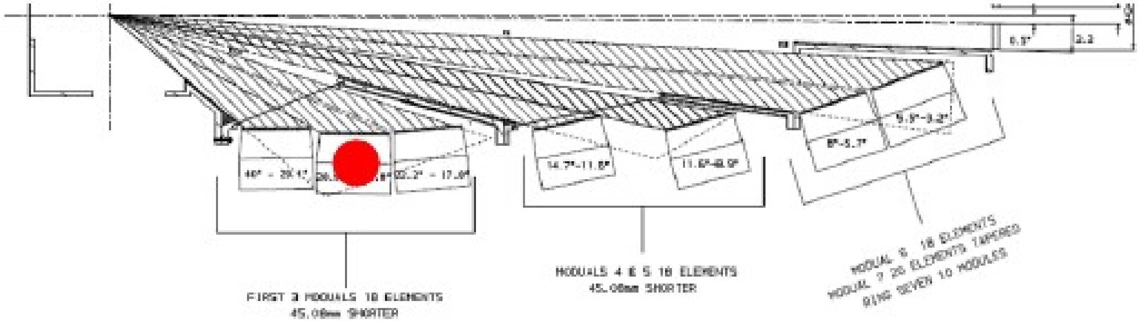

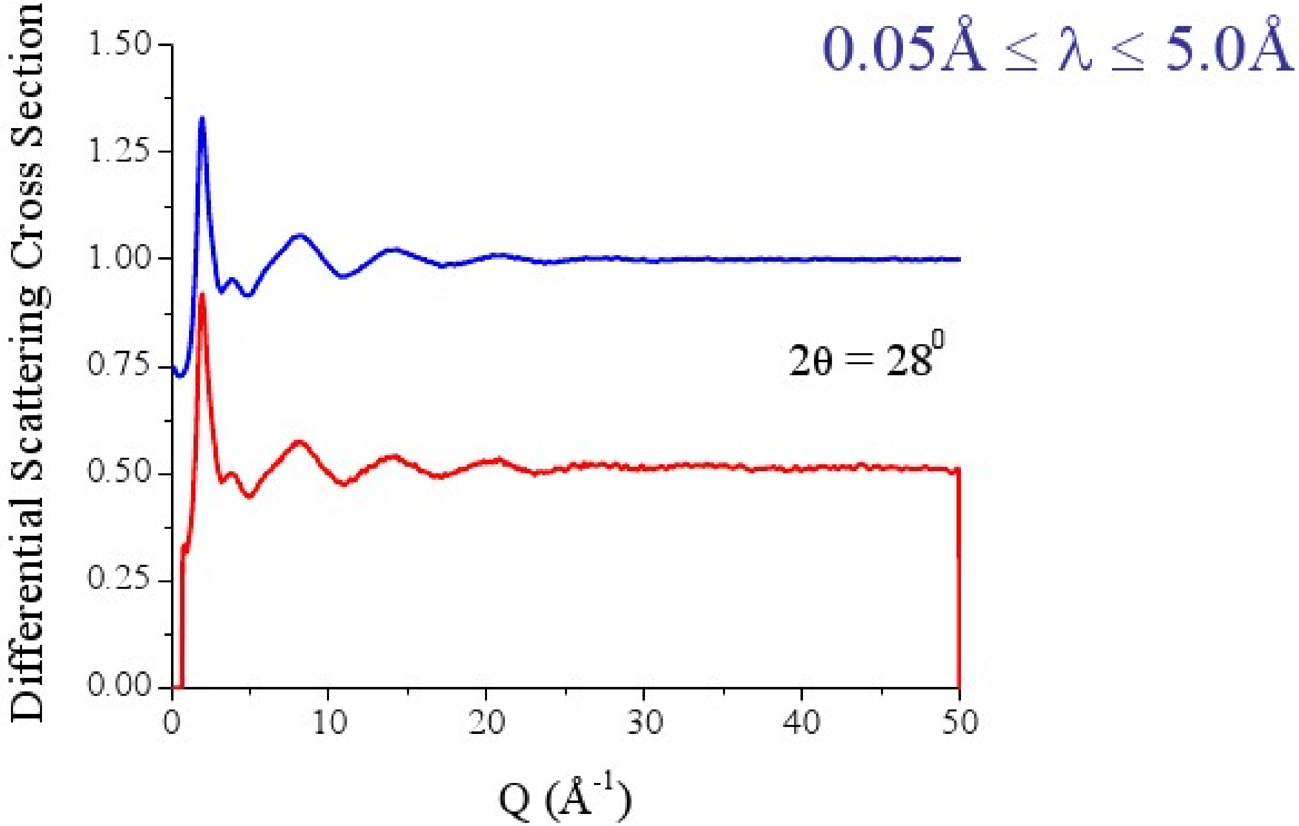

Distribution of Q-ranges across the detector banks

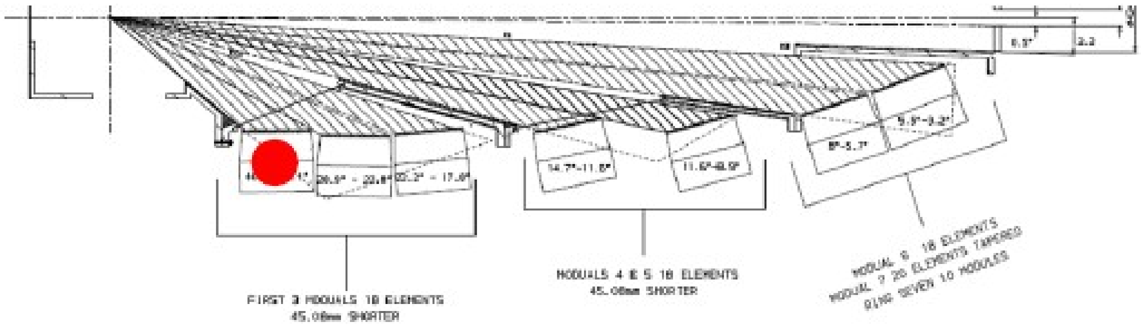

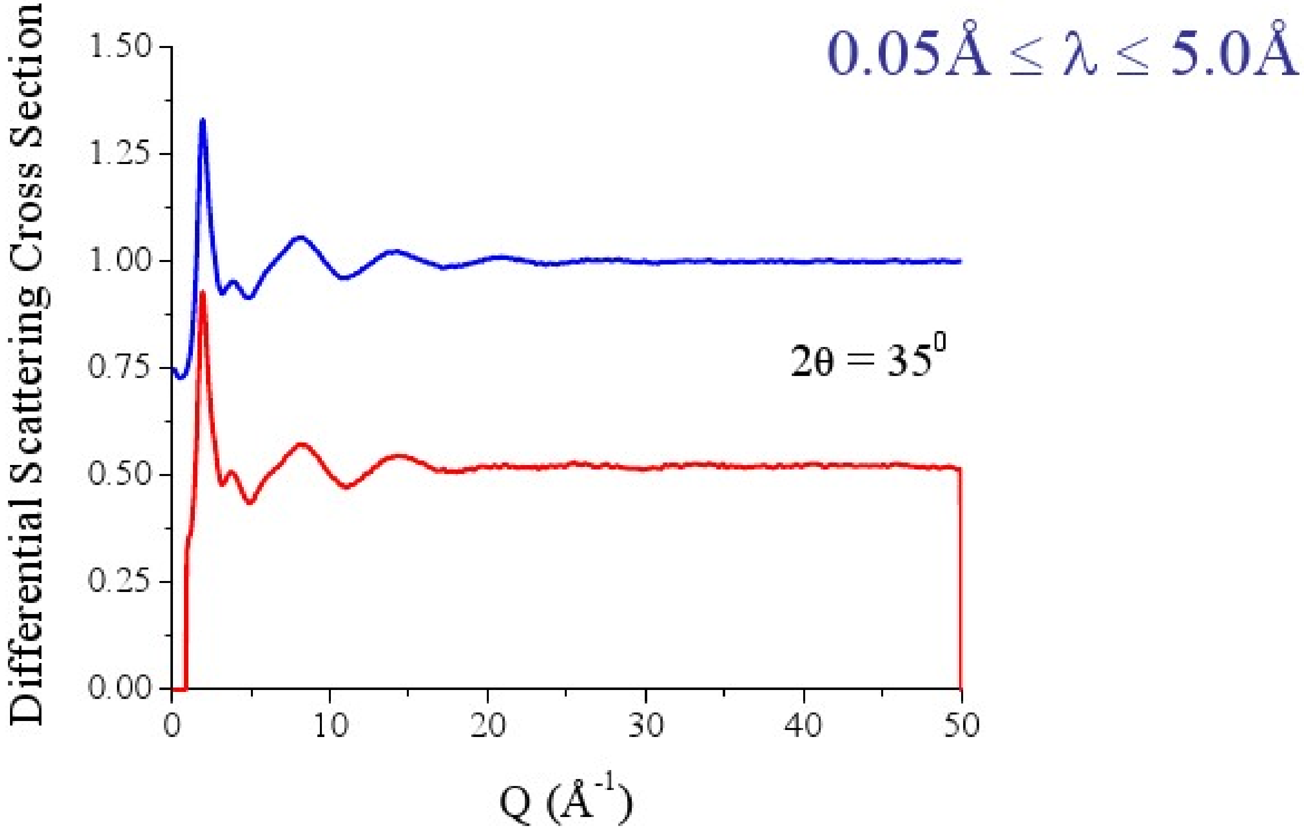

Science & Technology Facilities Council

ISIS

Real space resolution of a neutron scattering instrument

$$F(Q) = \rho_0 \int_0^\infty 4\pi r^2 g(r) \frac{\sin Qr}{Qr} dr$$

$$g(r) = \frac{1}{(2\pi)^3 \rho_0} \int_0^\infty 4\pi Q^2 F(Q) \frac{\sin Qr}{Qr} dQ$$

$$g(r) = \frac{1}{(2\pi)^3 \rho_0} \int_0^{Q_{\max}} 4\pi Q^2 F(Q) \frac{\sin Qr}{Qr} dQ$$

$$Q = \frac{4\pi}{\lambda} \sin\theta$$

Reactor Experiment $\quad 2\theta = 130^\circ \; \lambda = 0.5A \rightarrow Q_{\max} = 22.8A^{-1}$

Pulsed Source Experiment $\quad 2\theta = 40^\circ \; \lambda = 0.05A \rightarrow Q_{\max} = 86A^{-1}$

Real space resolution of a neutron scattering instrument

Reactor θ_{max} = 140° λ = 0.5Å

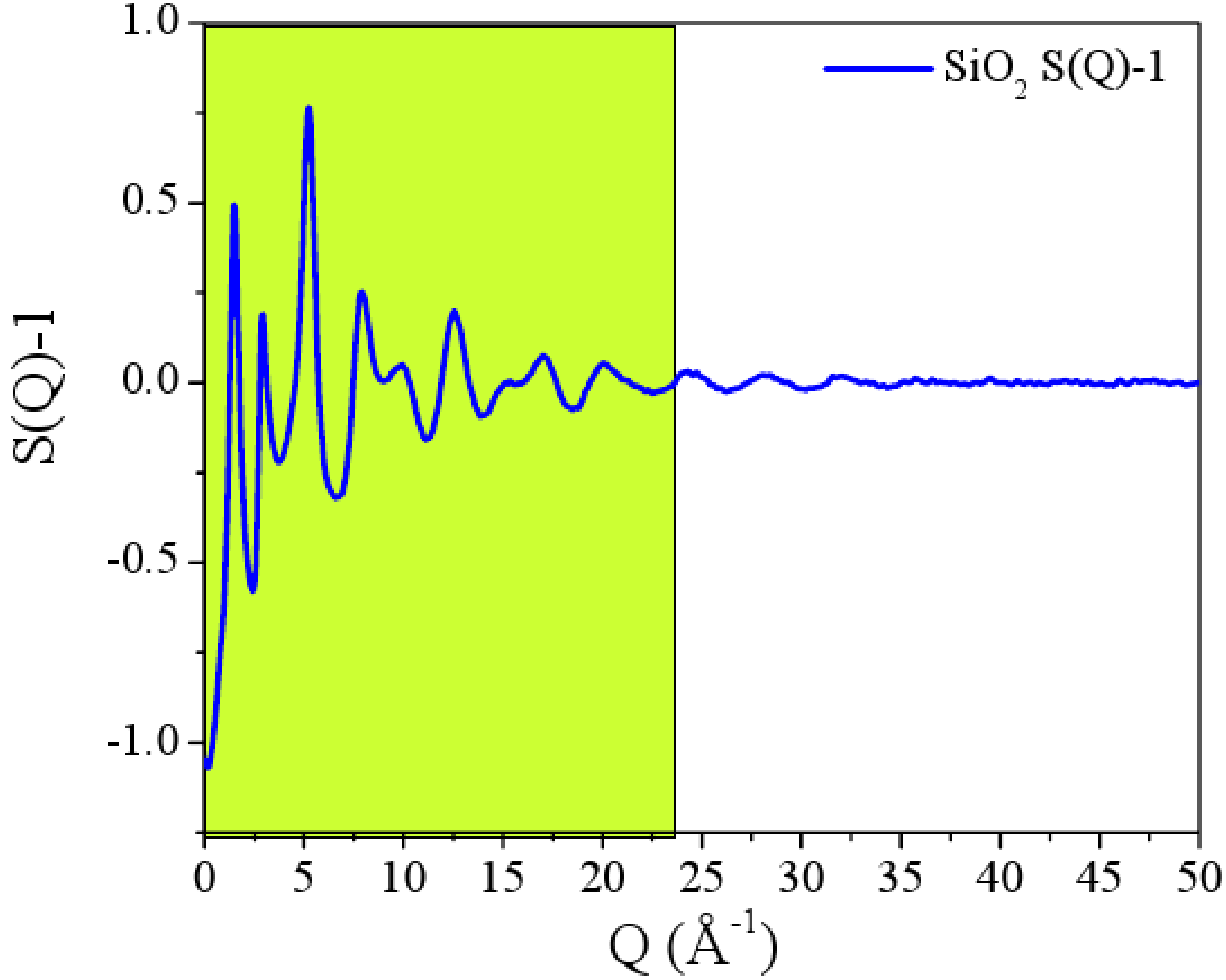

Real space resolution of a neutron scattering instrument

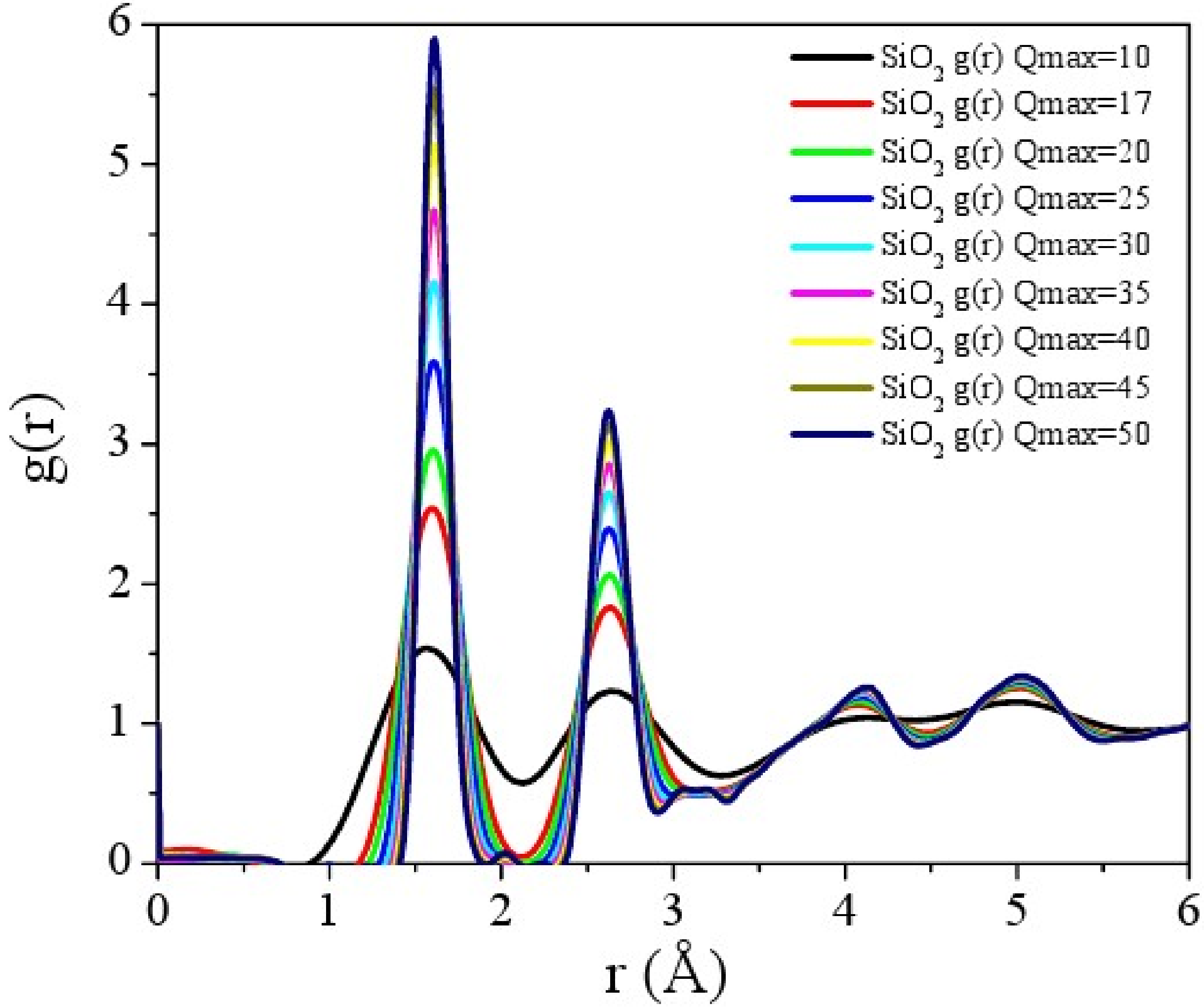

Real space resolution of a neutron scattering instrument

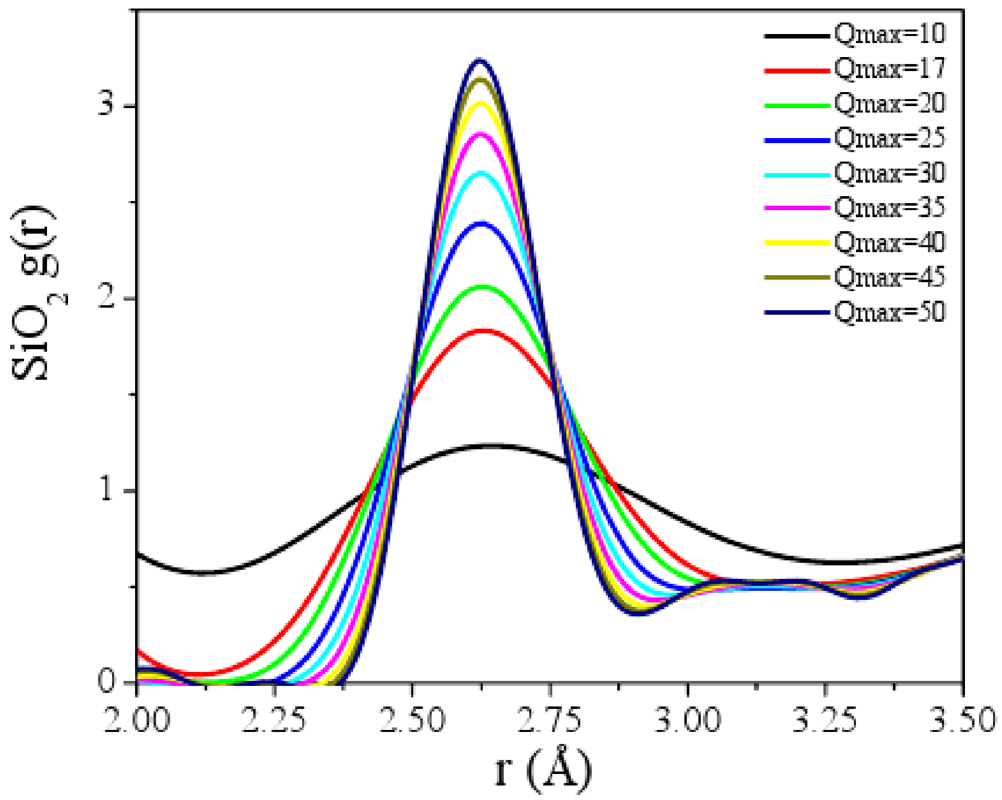

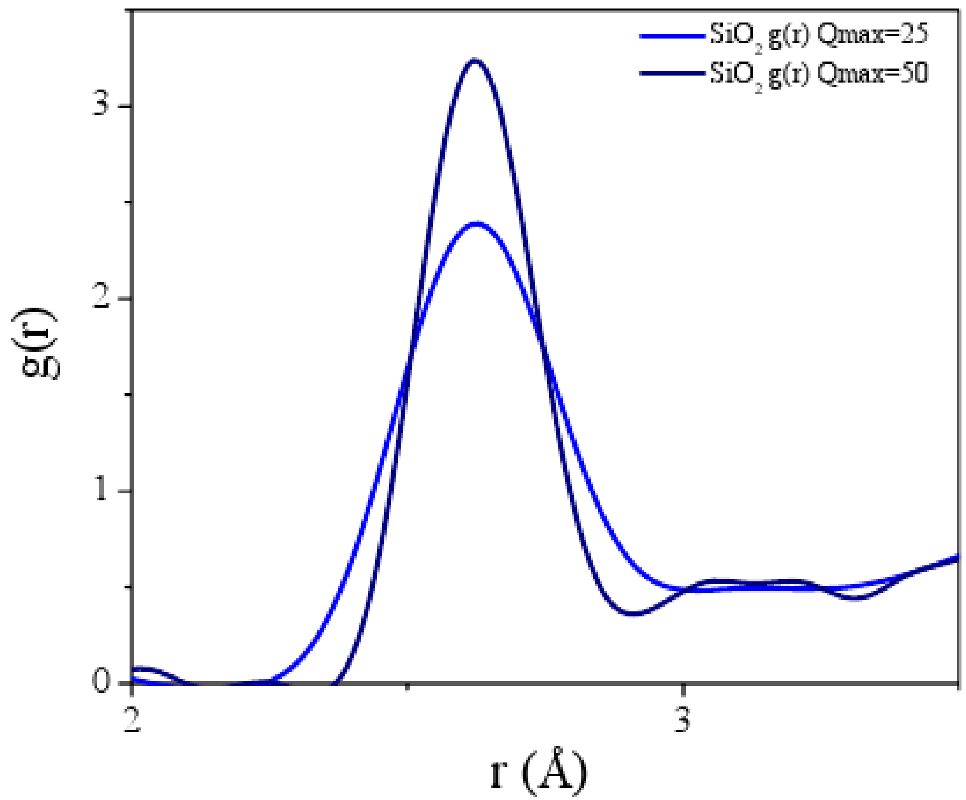

Q-resolution of a neutron scattering instrument

$$Q = \frac{4\pi}{\lambda}\sin\theta$$

$$\Delta Q = \left(\frac{\delta Q}{\delta\theta}\right)\Delta\theta + \left(\frac{\delta Q}{\delta\lambda}\right)\Delta\lambda$$

$$\Delta Q = Q[\cot\theta\Delta\theta + \Delta\lambda/\lambda]$$

Under the conditions that the wavelengths of the scattered neutrons are measured by time of flight with detectors at fixed scattering angle 2θ, it can be shown that the resolution $\Delta Q/Q$ of the TOF neutron diffractometer is roughly constant as a function of TOF.

Q-resolution of a neutron scattering instrument

Δθ/θ

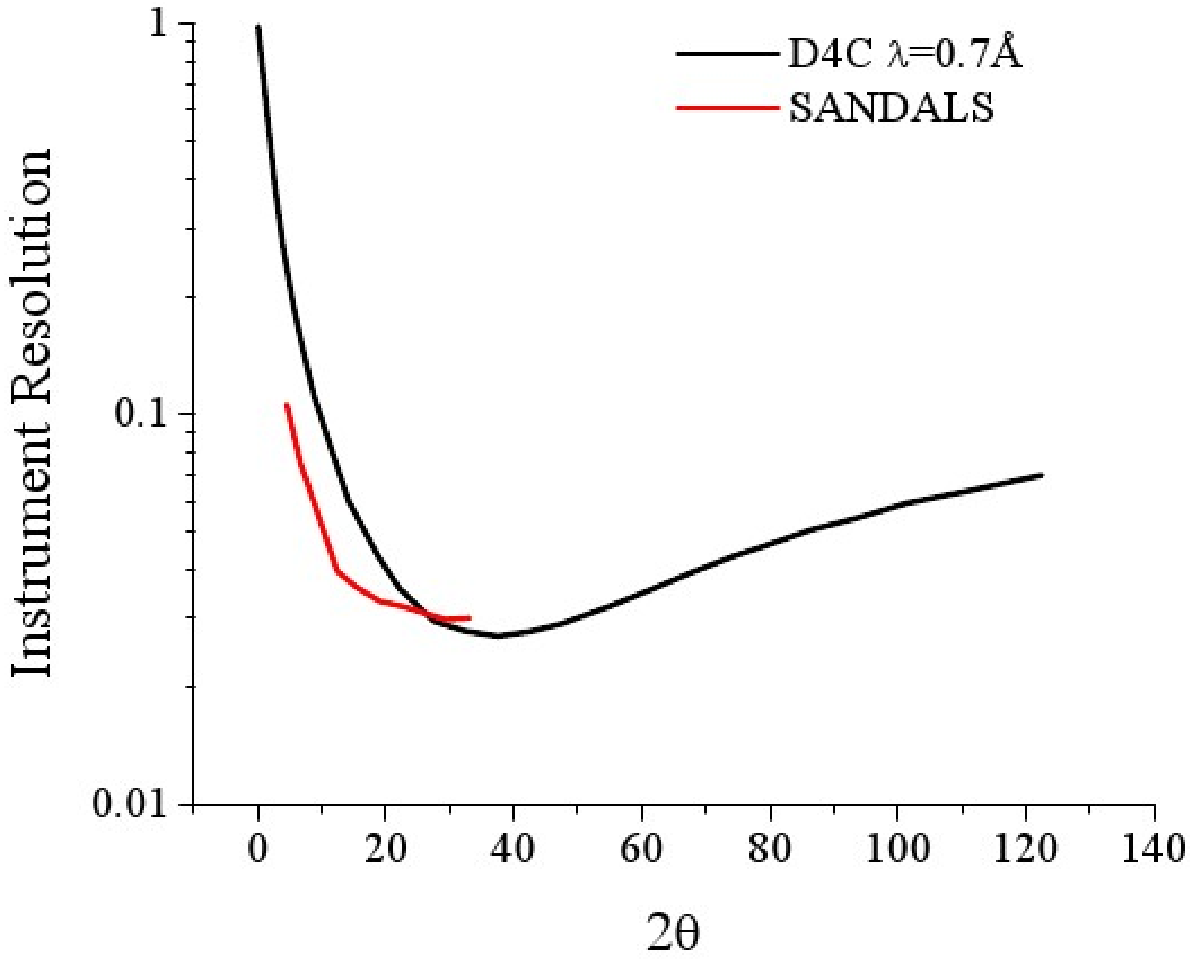

Q-resolution of a neutron scattering instrument

ΔQ/Q

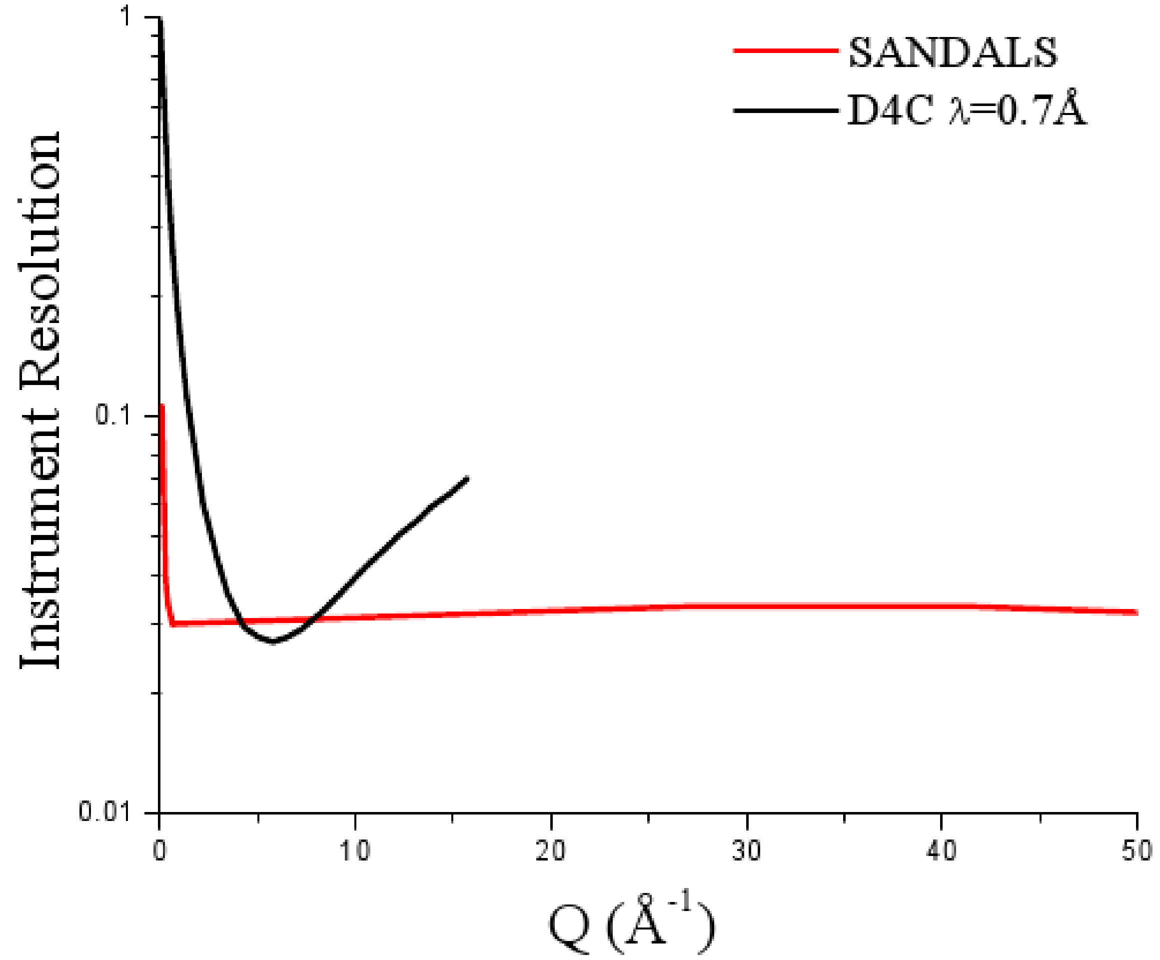

Q-resolution is particularly important for total scattering studies

In total scattering studies it is important to accurate measure both the sharp Bragg and the diffuse scattering components.

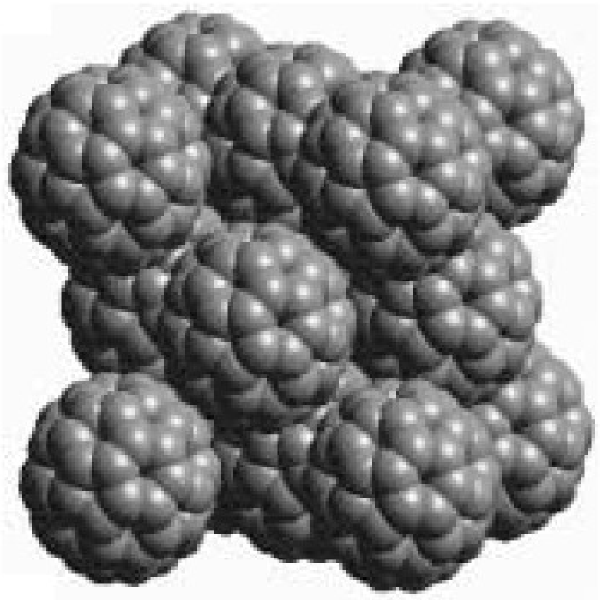

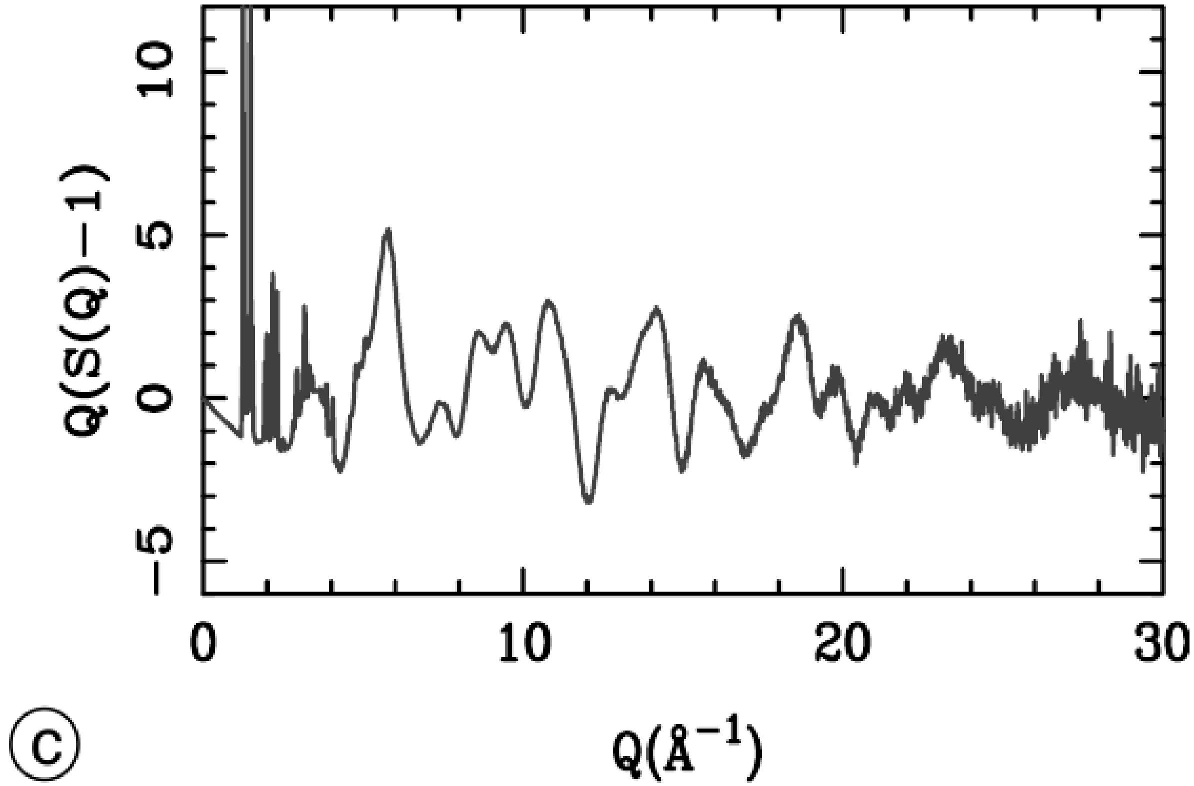

Th. Proffen, S. J. L. Billinge, T. Egami and D. Louca, Z. Kristallogr. **218** (2003) 132–143

Light element optimized diffractometers
SANDALS type

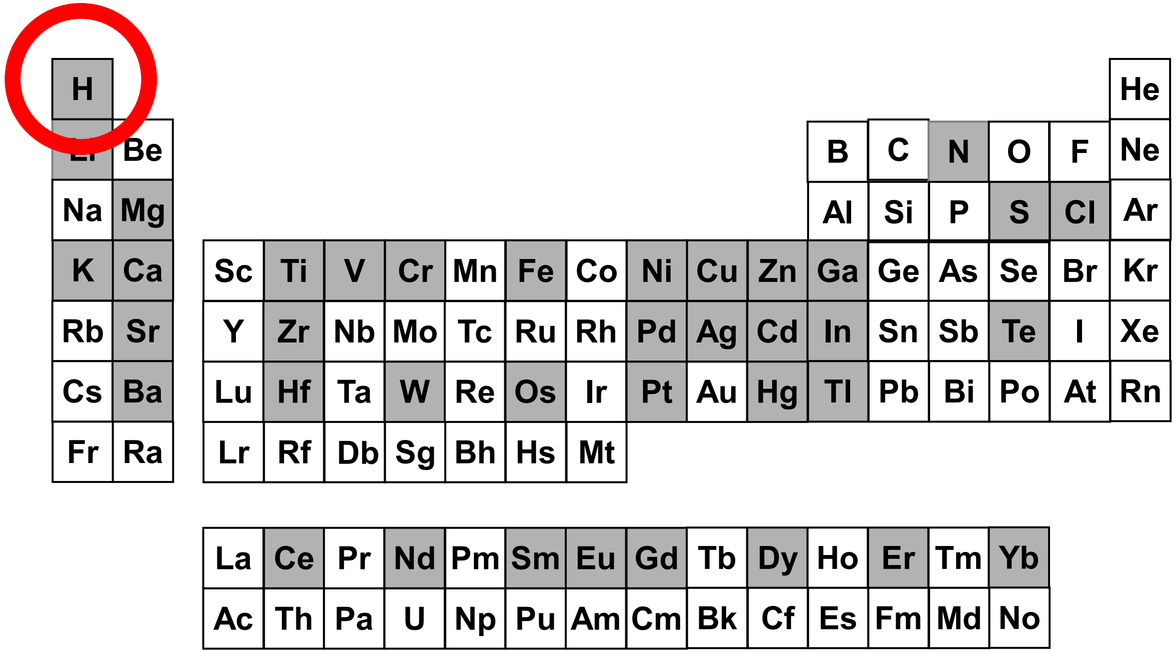

Elements with isotopes that potentially can be used for NDIS ion solvation studies ($\Delta\ b_c \geq 1$fm)
J.E.Enderby, *Chem. Soc. Revs.* 159 (1995)

Science & Technology Facilities Council

ISIS

Inelasticity !
The challenge for light element neutron diffraction

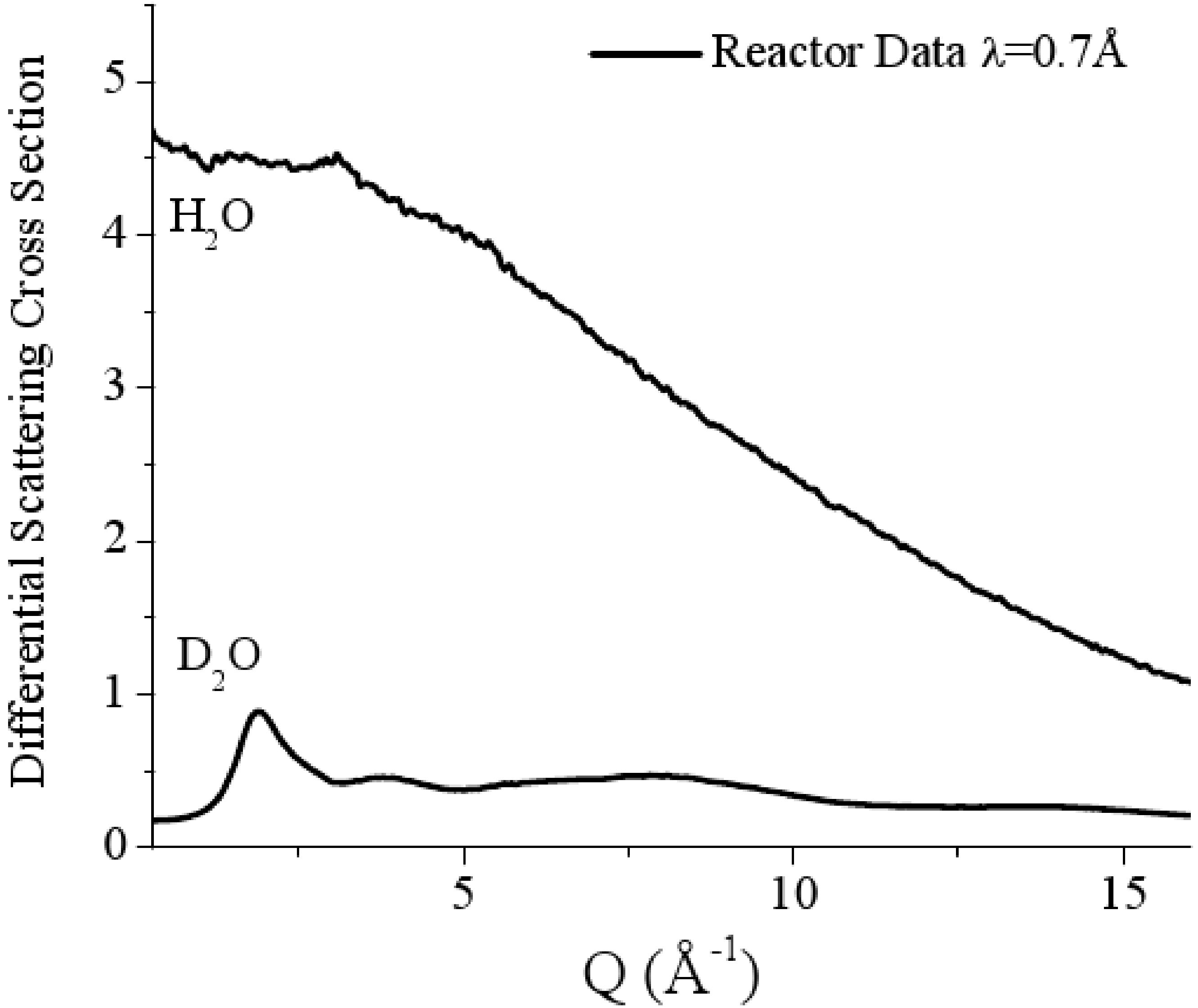

The advantage of a pulsed source diffractometer

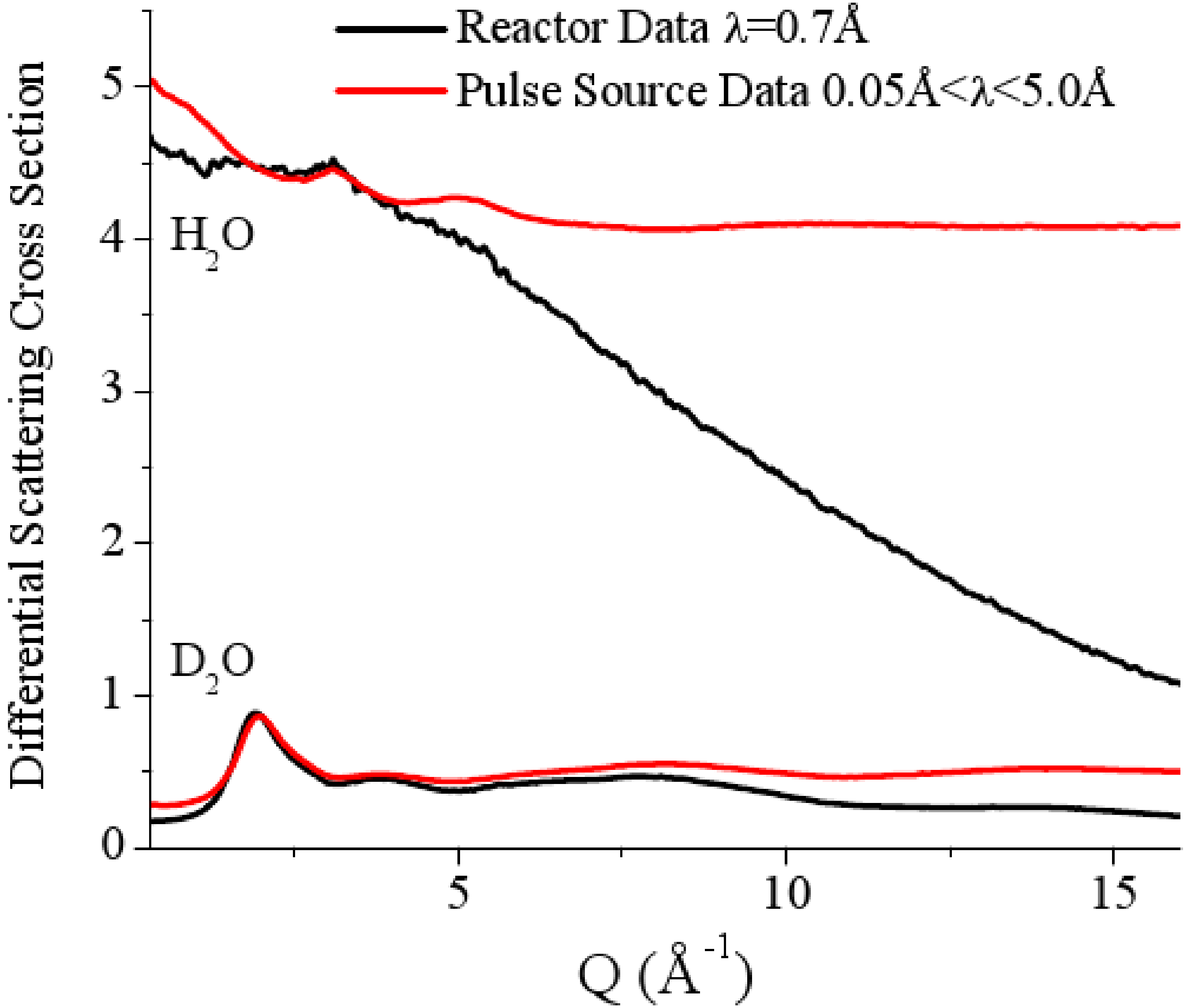

And it gets even better !

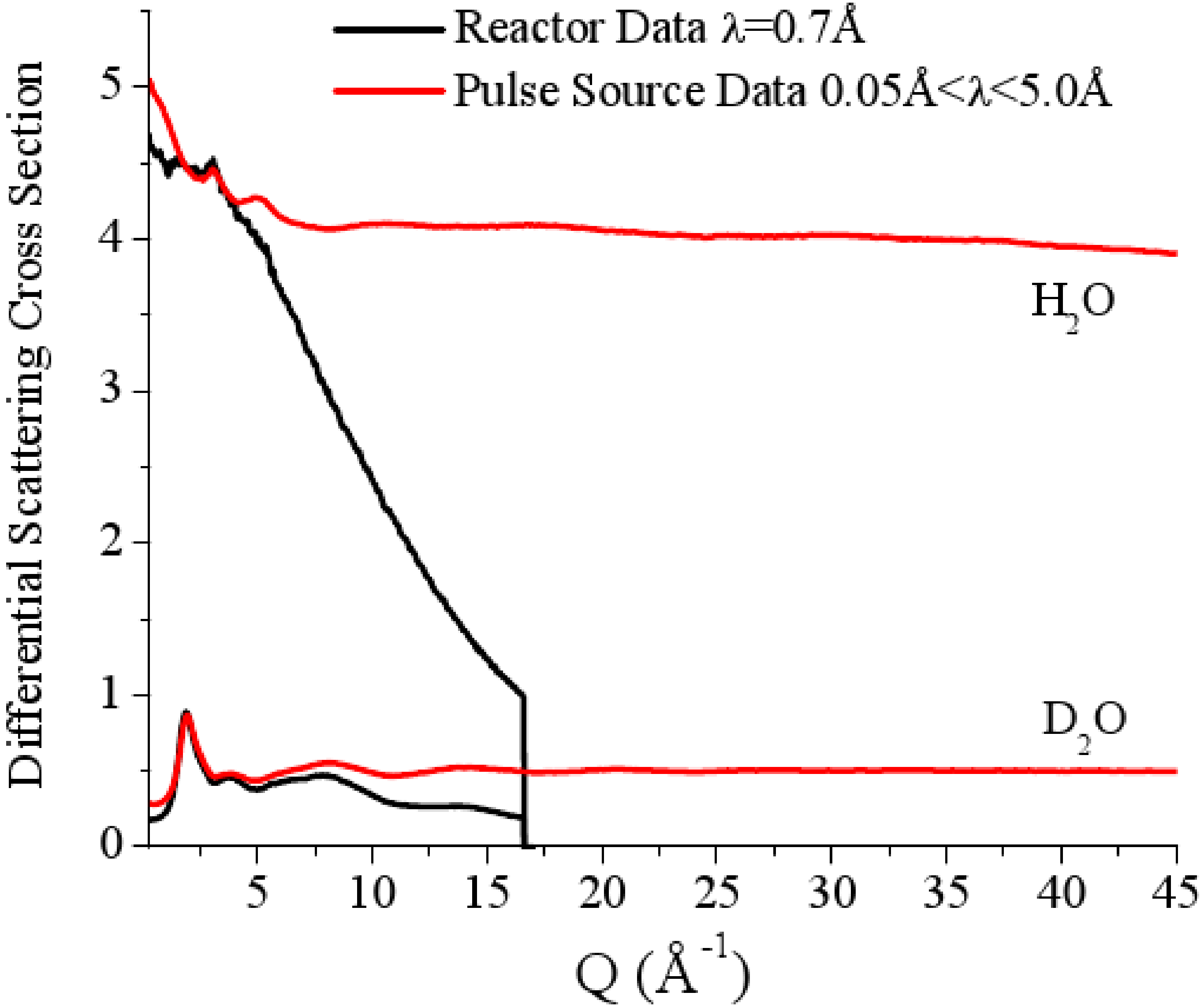

Example: The structure of liquid water

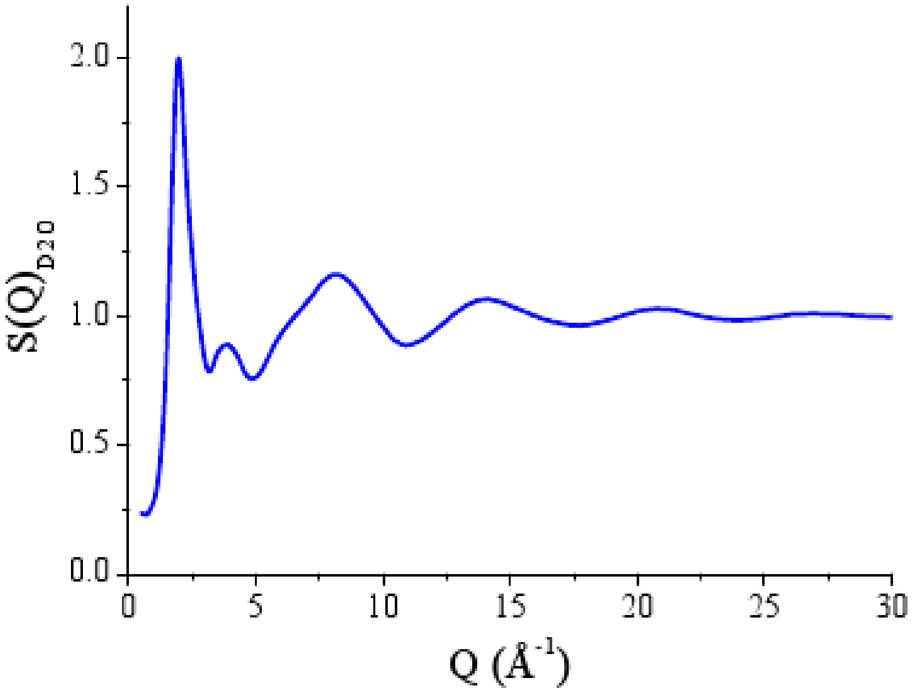

F.T.

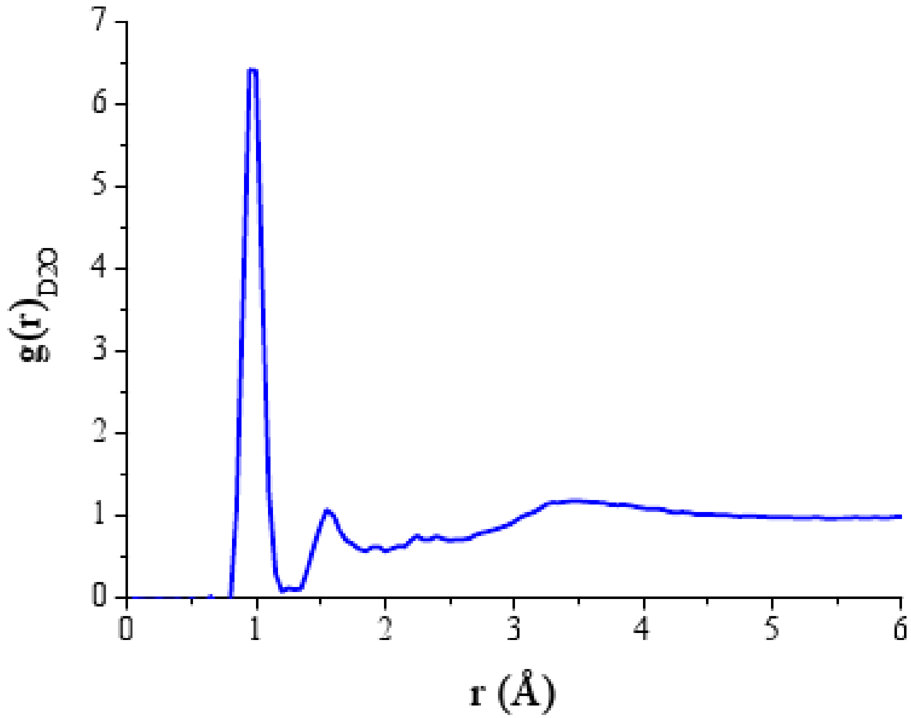

Example: The structure of liquid water

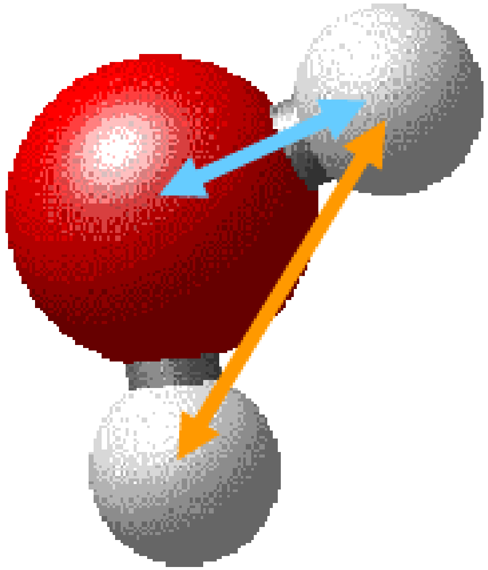

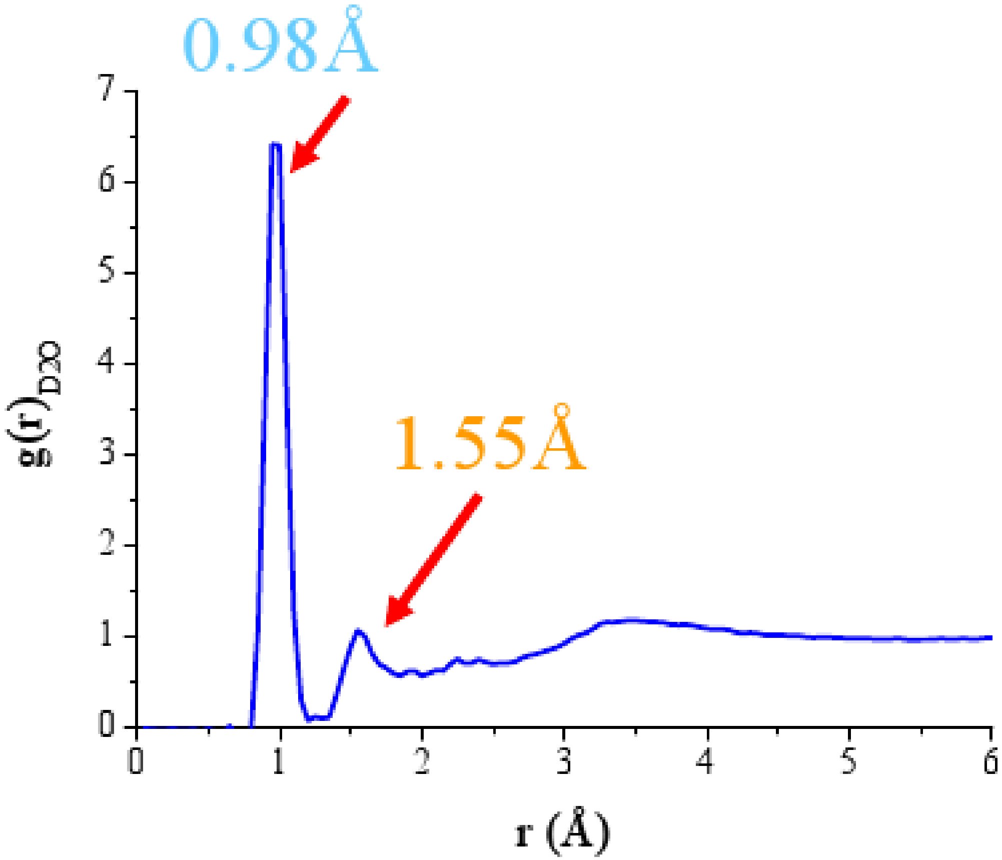

Example: The structure of liquid water

$$F_{H_2O}(Q) = c_O^2 b_O^2 [S_{OO}(Q) - 1] + 2c_O c_H b_O b_H [S_{OH}(Q) - 1] + c_H^2 b_H^2 [S_{HH}(Q) - 1]$$

$$F_{HDO}(Q) = c_O^2 b_O^2 [S_{OO}(Q) - 1] + 2c_O c_H b_O b_{HD} [S_{OH}(Q) - 1] + c_H^2 b_{HD}^2 [S_{HH}(Q) - 1]$$

$$F_{D_2O}(Q) = c_O^2 b_O^2 [S_{OO}(Q) - 1] + 2c_O c_H b_O b_D [S_{OH}(Q) - 1] + c_H^2 b_D^2 [S_{HH}(Q) - 1]$$

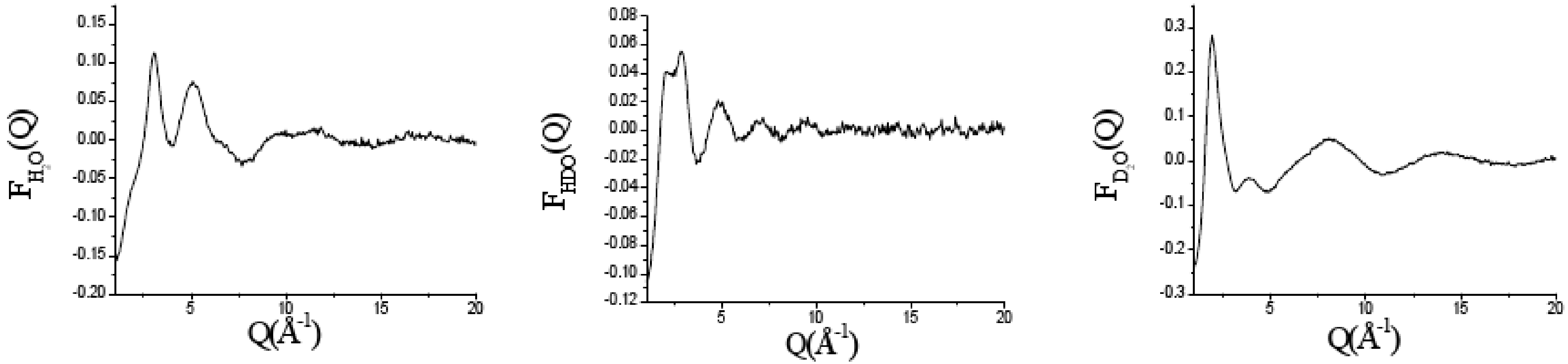

Example: The structure of liquid water

$$F_{H_2O}(Q) = c_O^2 b_O^2\left[S_{OO}(Q)-1\right] + 2c_O c_H b_O b_H\left[S_{OH}(Q)-1\right] + c_H^2 b_H^2\left[S_{HH}(Q)-1\right]$$

$$F_{HDO}(Q) = c_O^2 b_O^2\left[S_{OO}(Q)-1\right] + 2c_O c_H b_O b_{HD}\left[S_{OH}(Q)-1\right] + c_H^2 b_{HD}^2\left[S_{HH}(Q)-1\right]$$

$$F_{D_2O}(Q) = c_O^2 b_O^2\left[S_{OO}(Q)-1\right] + 2c_O c_H b_O b_D\left[S_{OH}(Q)-1\right] + c_H^2 b_D^2\left[S_{HH}(Q)-1\right]$$

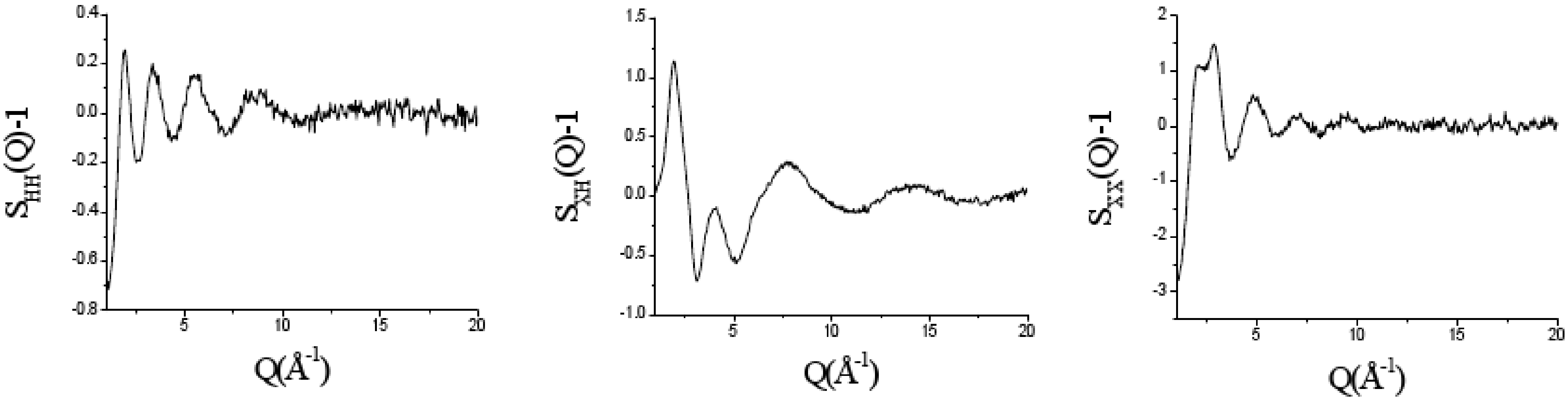

Access to intra and inter molecular distances

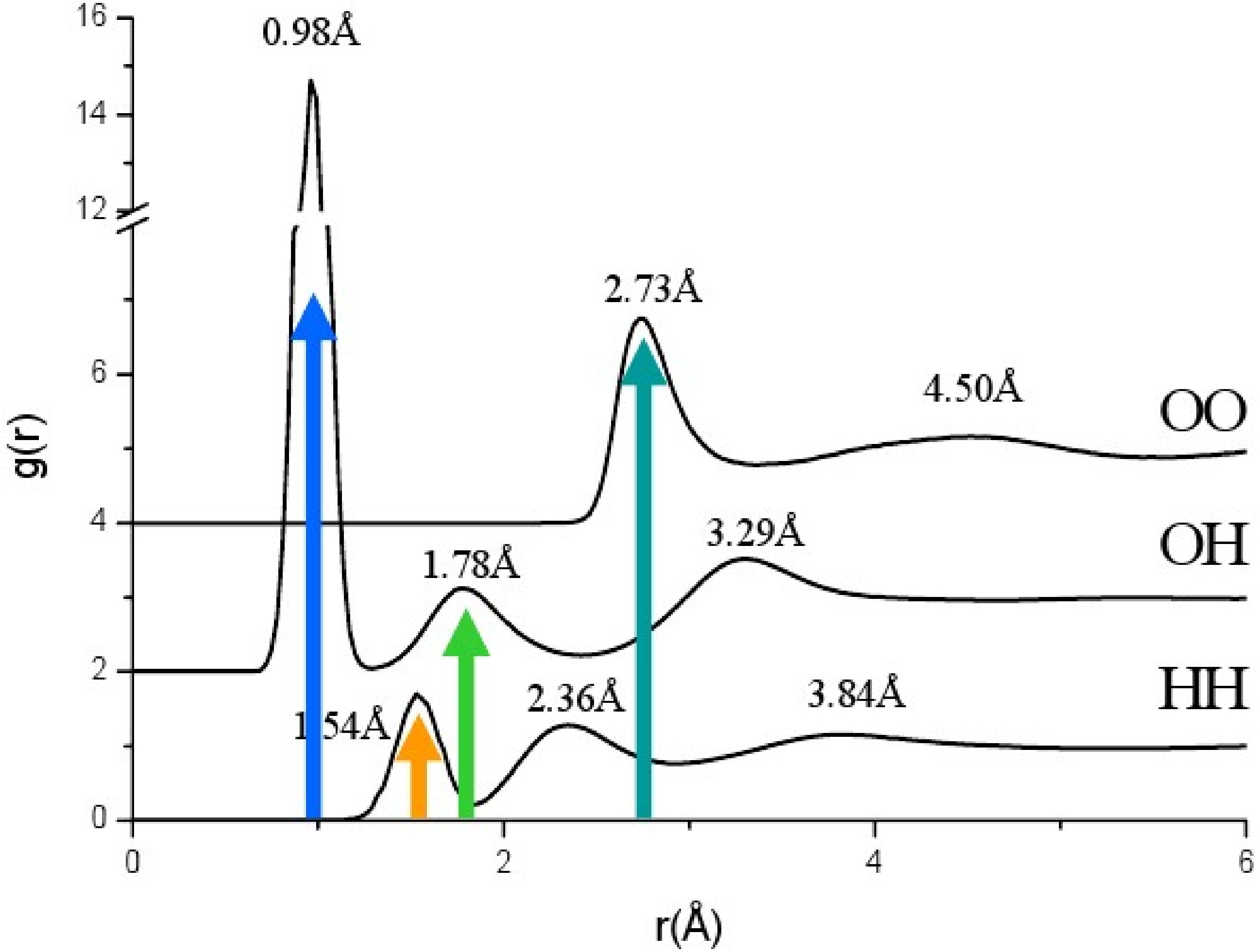

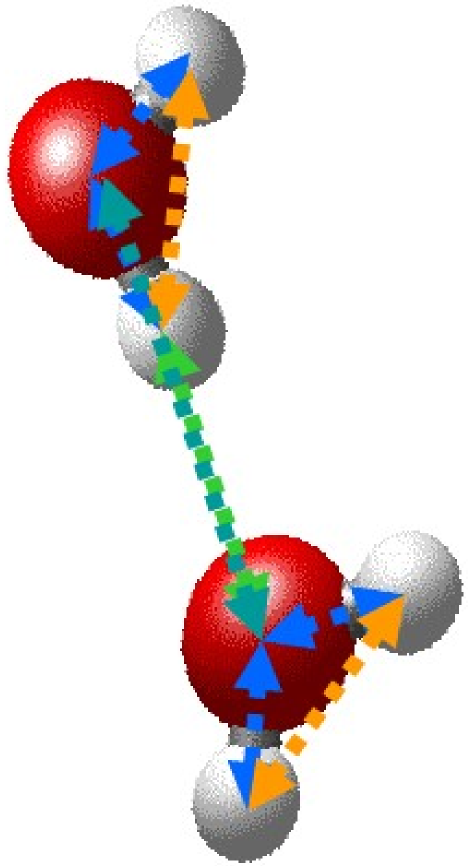

Access to number of neighbouring atoms

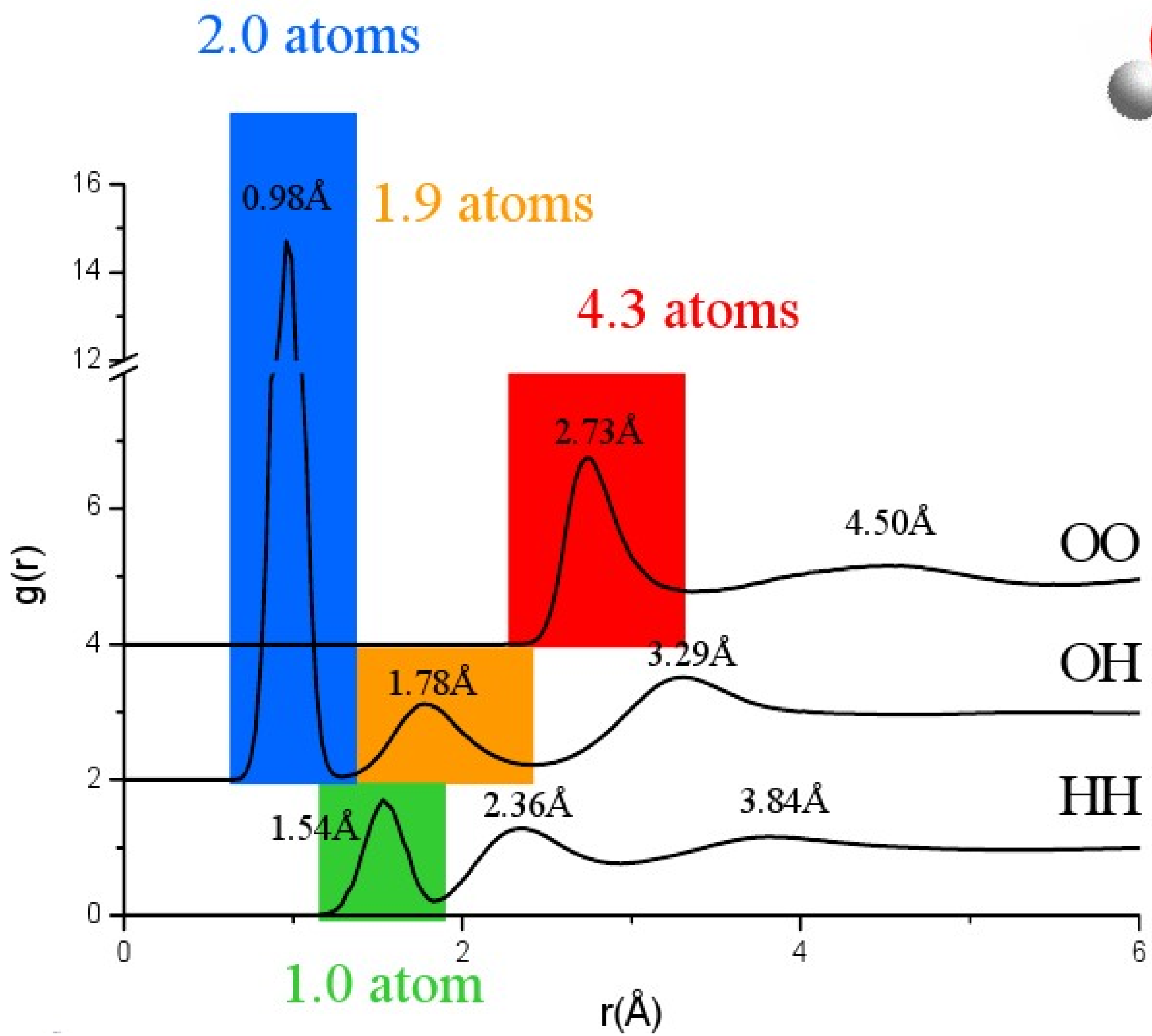

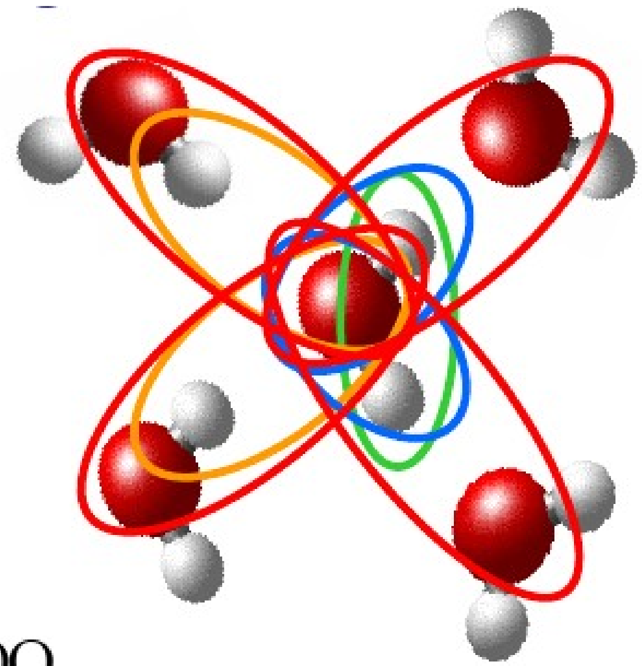

Access to angular information

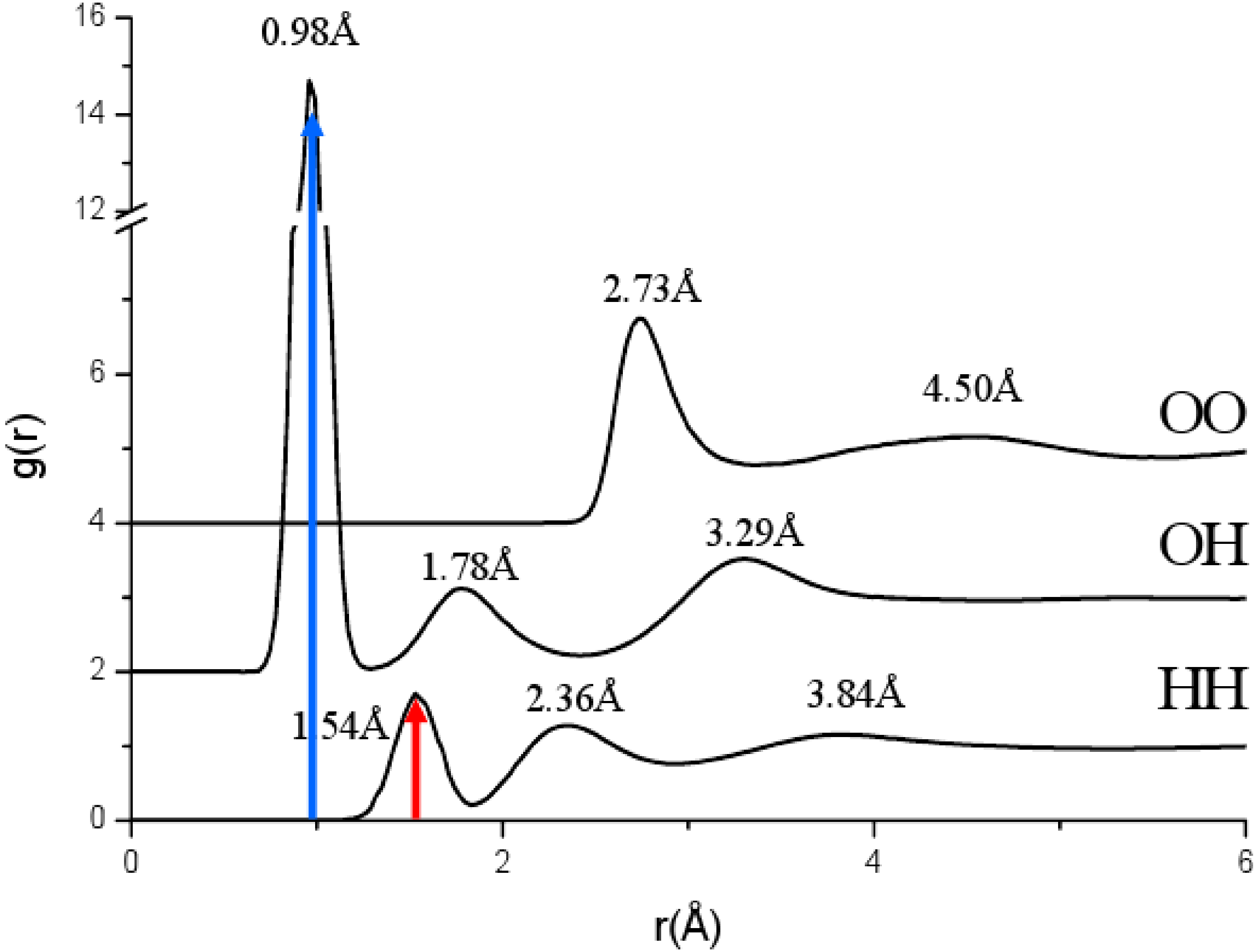

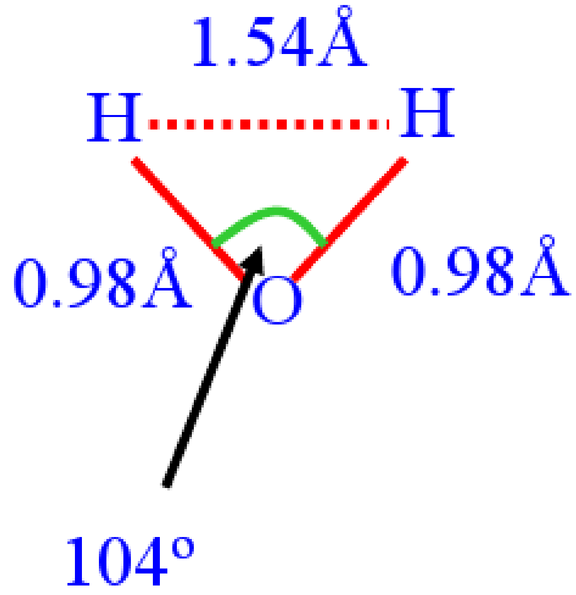

Benefits of a flat plate sample geometry: efficient use of beam

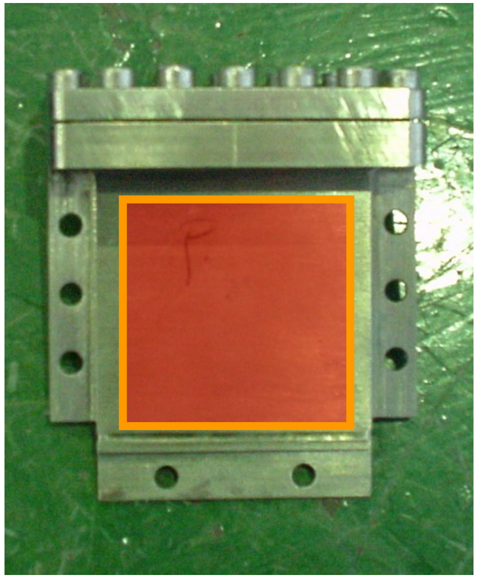

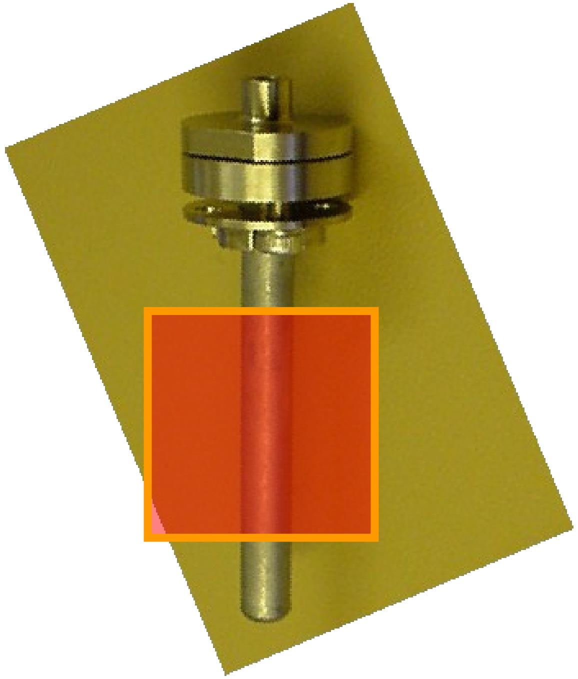

Light element diffractometers make use of the forward scattering geometry, the absence of detectors at high scattering angles allows the use of flat plate sample cells

Benefits of a flat plate sample geometry: sample diagnostics

In the flat plate sample geometry after nomalization to vanadium and correction for background, multiple scattering and attenuation, but before correction for self scattering, the measured total differential scattering intensity oscillates about the high Q limit.

$$\lim_{Q\to\infty} I(Q) = \frac{\rho t f \sum_i c_i \sigma_i}{4\pi}$$

ρ Atomic density of sample
t Sample thickness
f Packing fraction
c_i Fraction of atoms of type i
σ_i Total scattering cross section of atoms of type i

Benefits of a flat plate sample geometry: sample diagnostics

The scattering cross sections are well known and tabulated so:

Liquid samples:

As liquids by definition fill their containers, if one knows the density and thickness of the sample container → sample composition

Powder samples:

If one knows the sample composition and density and size of sample container → packing fraction

Benefits of a flat plate sample geometry: H/D sample composition

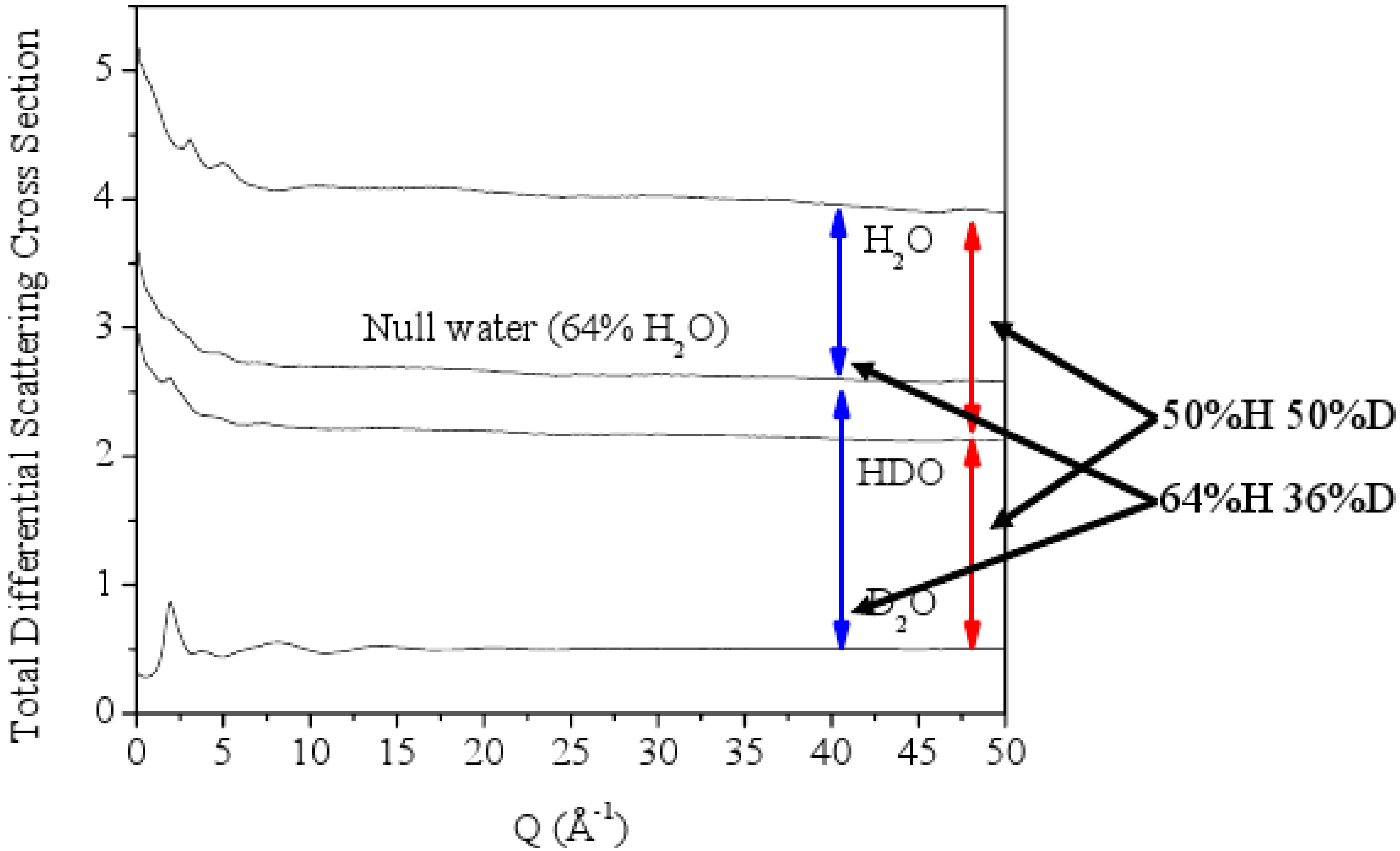

Science & Technology Facilities Council

ISIS

A selection of elements with potentially problematic neutron resonances between 0.003eV and 33eV (5Å and 0.05Å)

hydrogen 1 H 1.0079																		helium 2 He 4.0026
lithium 3 Li 6.941	beryllium 4 Be 9.0122												boron 5 B 10.811	carbon 6 C 12.011	nitrogen 7 N 14.007	oxygen 8 O 15.999	fluorine 9 F 18.998	neon 10 Ne 20.180
sodium 11 Na 22.990	magnesium 12 Mg 24.305												aluminium 13 Al 26.982	silicon 14 Si 28.086	phosphorus 15 P 30.974	sulfur 16 S 32.065	chlorine 17 Cl 35.453	argon 18 Ar 39.948
potassium 19 K 39.098	calcium 20 Ca 40.078		scandium 21 Sc 44.956	titanium 22 Ti 47.867	vanadium 23 V 50.942	chromium 24 Cr 51.996	manganese 25 Mn 54.938	iron 26 Fe 55.845	cobalt 27 Co 58.933	nickel 28 Ni 58.693	copper 29 Cu 63.546	zinc 30 Zn 65.39	gallium 31 Ga 69.723	germanium 32 Ge 72.61	arsenic 33 As 74.922	selenium 34 Se 78.96	bromine 35 Br 79.904	krypton 36 Kr 83.80
rubidium 37 Rb 85.468	strontium 38 Sr 87.62		yttrium 39 Y 88.906	zirconium 40 Zr 91.224	niobium 41 Nb 92.906	molybdenum 42 Mo 95.94	technetium 43 Tc [98]	ruthenium 44 Ru 101.07	rhodium 45 Rh 102.91	palladium 46 Pd 106.42	silver 47 Ag 107.87	cadmium 48 Cd 112.41	indium 49 In 114.82	tin 50 Sn 118.71	antimony 51 Sb 121.76	tellurium 52 Te 127.60	iodine 53 I 126.90	xenon 54 Xe 131.29
caesium 55 Cs 132.91	barium 56 Ba 137.33	57-70 *	lutetium 71 Lu 174.97	hafnium 72 Hf 178.49	tantalum 73 Ta 180.95	tungsten 74 W 183.84	rhenium 75 Re 186.21	osmium 76 Os 190.23	iridium 77 Ir 192.22	platinum 78 Pt 195.08	gold 79 Au 196.97	mercury 80 Hg 200.59	thallium 81 Tl 204.38	lead 82 Pb 207.2	bismuth 83 Bi 208.98	polonium 84 Po [209]	astatine 85 At [210]	radon 86 Rn [222]
francium 87 Fr [223]	radium 88 Ra [226]	89-102 * *	lawrencium 103 Lr [262]	rutherfordium 104 Rf [261]	dubnium 105 Db [262]	seaborgium 106 Sg [266]	bohrium 107 Bh [264]	hassium 108 Hs [269]	meitnerium 109 Mt [268]	ununnilium 110 Uun [271]	unununium 111 Uuu [272]	ununbium 112 Uub [277]		ununquadium 114 Uuq [289]				

*Lanthanide series	lanthanum 57 La 138.91	cerium 58 Ce 140.12	praseodymium 59 Pr 140.91	neodymium 60 Nd 144.24	promethium 61 Pm [145]	samarium 62 Sm 150.36	europium 63 Eu 151.96	gadolinium 64 Gd 157.25	terbium 65 Tb 158.93	dysprosium 66 Dy 162.50	holmium 67 Ho 164.93	erbium 68 Er 167.26	thulium 69 Tm 168.93	ytterbium 70 Yb 173.04
* *Actinide series	actinium 89 Ac [227]	thorium 90 Th 232.04	protactinium 91 Pa 231.04	uranium 92 U 238.03	neptunium 93 Np [237]	plutonium 94 Pu [244]	americium 95 Am [243]	curium 96 Cm [247]	berkelium 97 Bk [247]	californium 98 Cf [251]	einsteinium 99 Es [252]	fermium 100 Fm [257]	mendelevium 101 Md [258]	nobelium 102 No [259]

Challenging neutron resonances for light element diffractometers

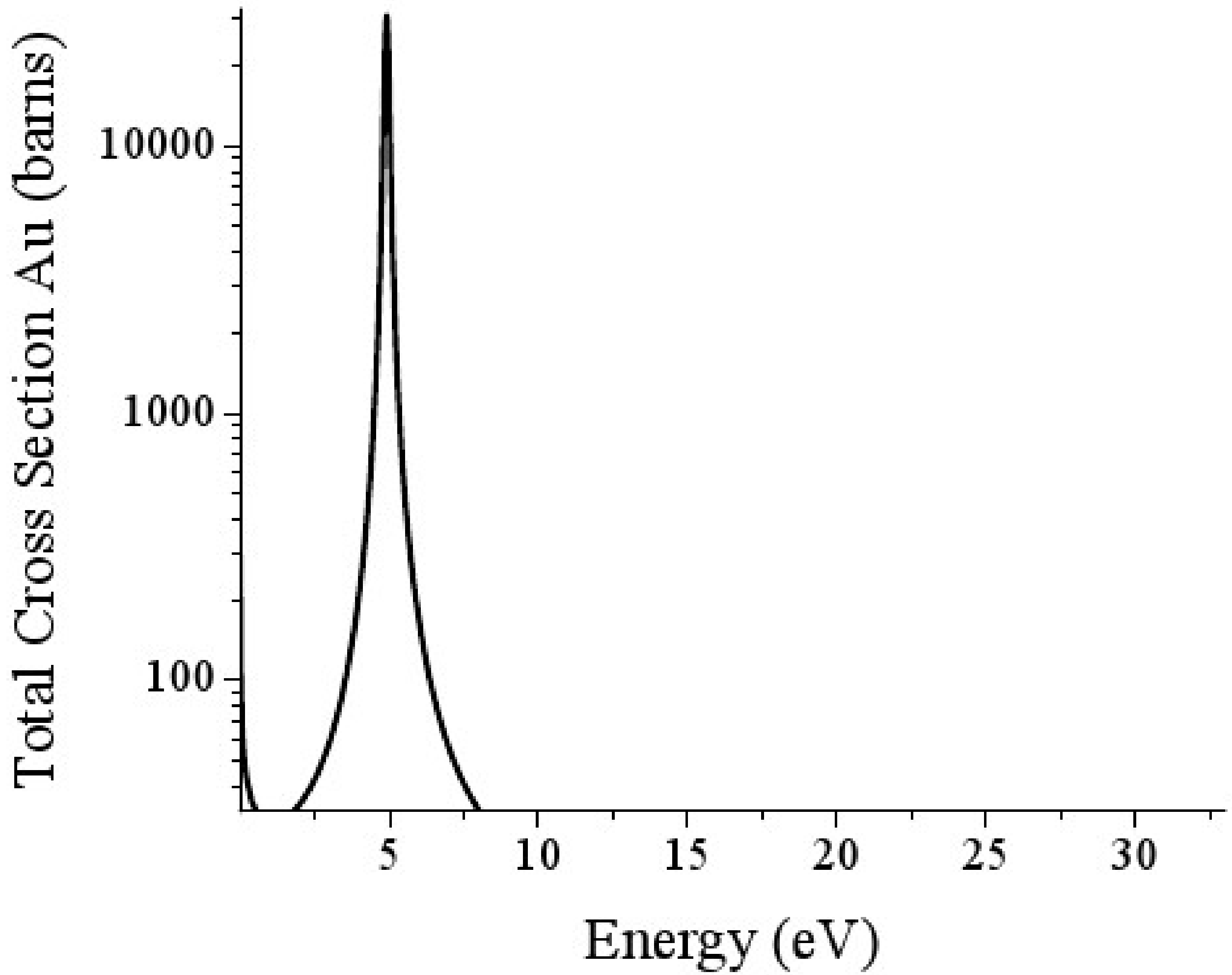

Challenging neutron resonances for light element diffractometers

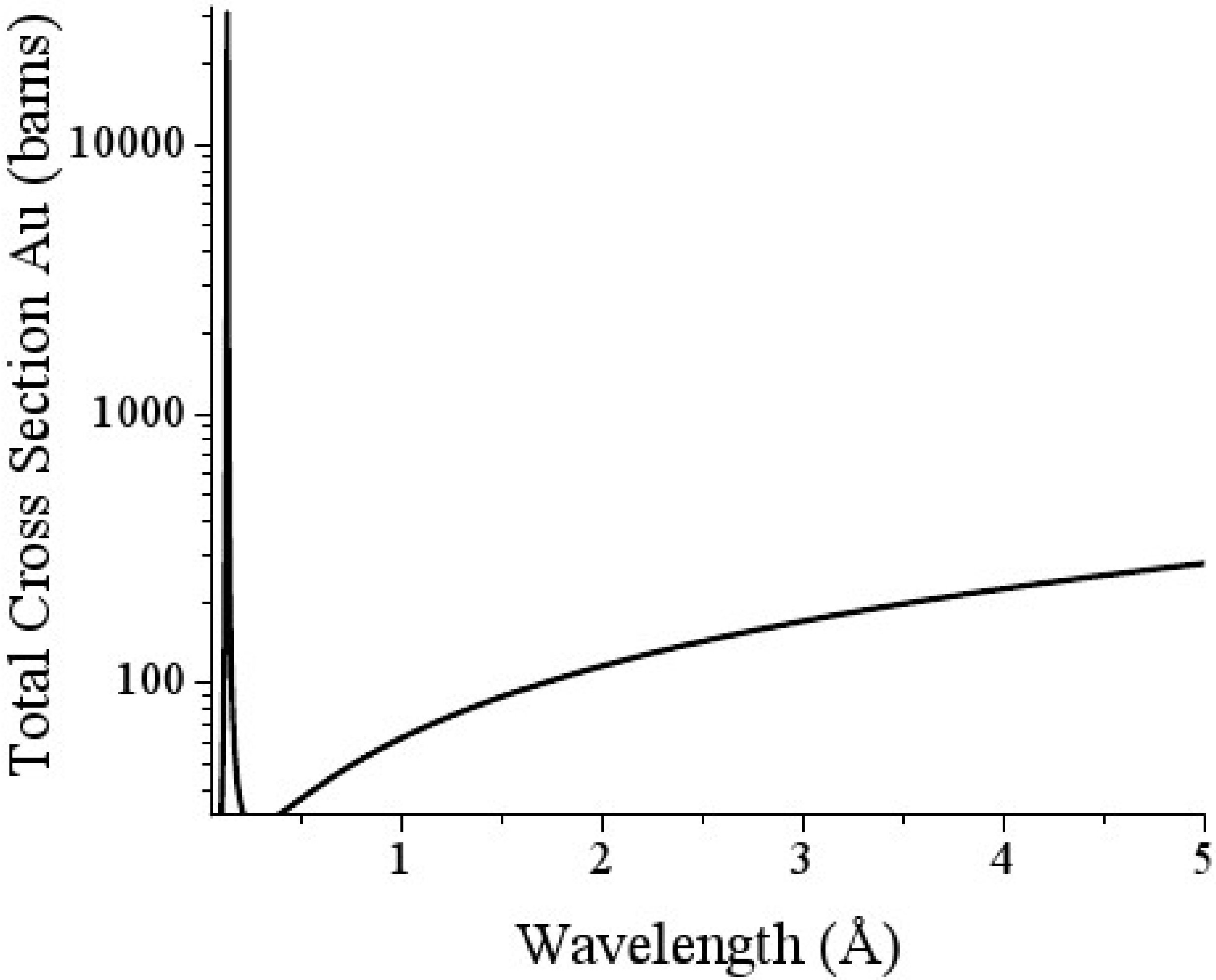

Neutron Resonance in a sample

Resonance at 4.9eV (0.13Å)

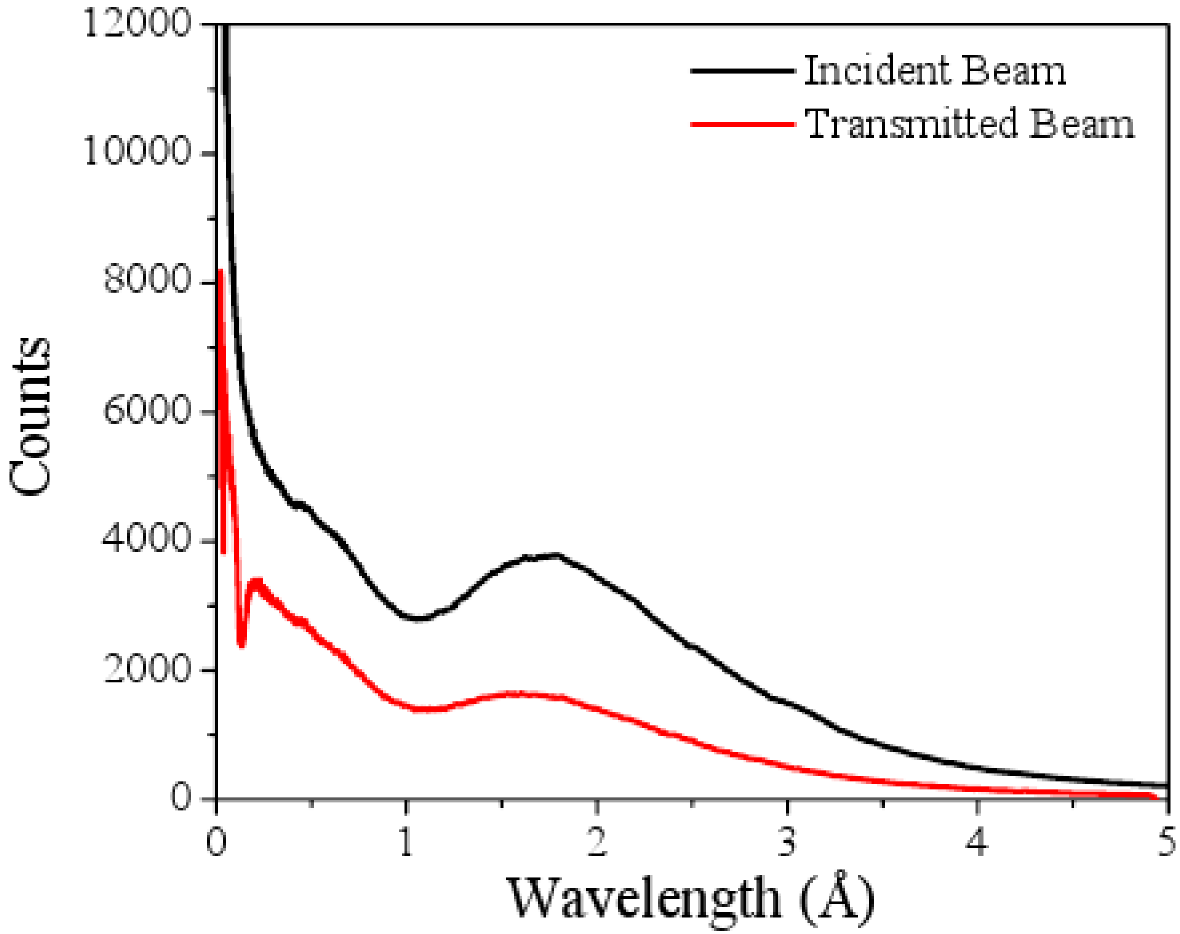

Tracking the neutron resonance across the detector array

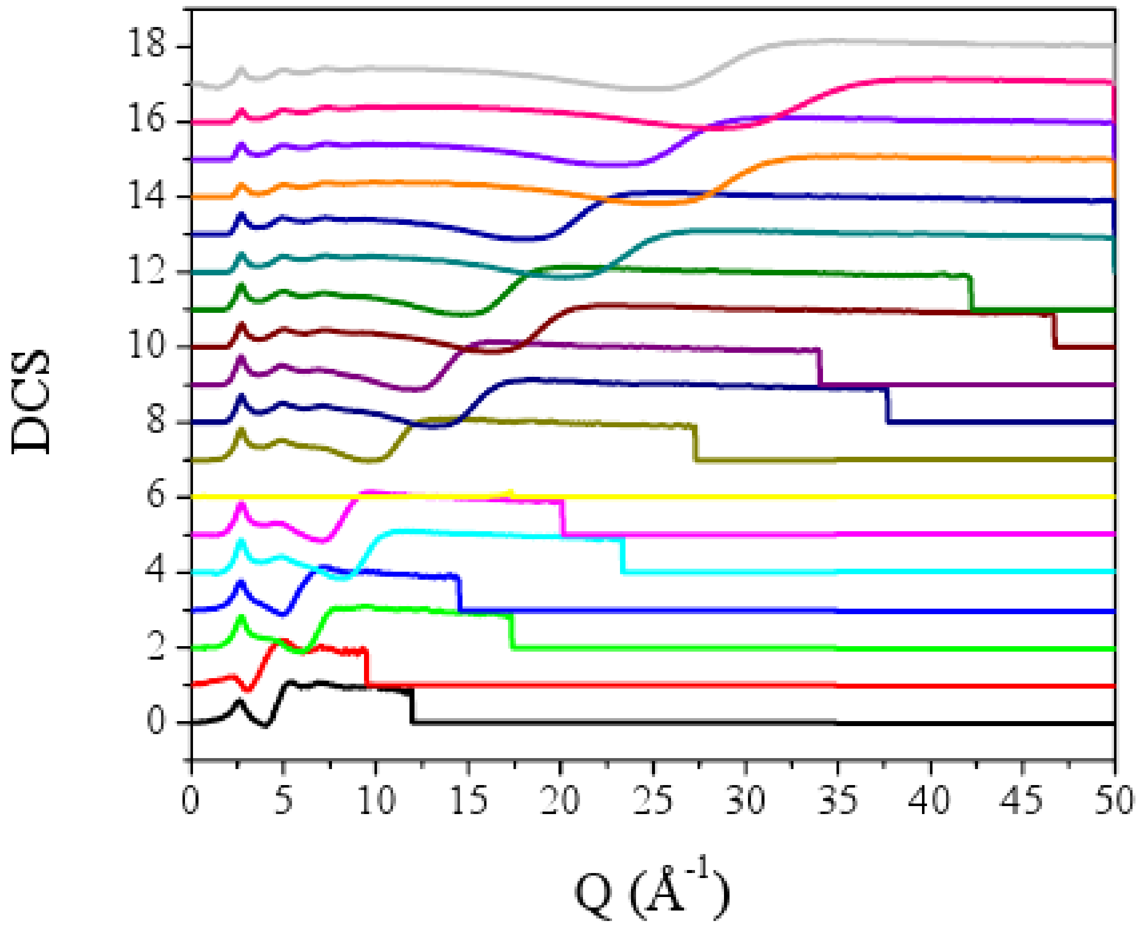

Effect of the neutron resonance on the merged DCS

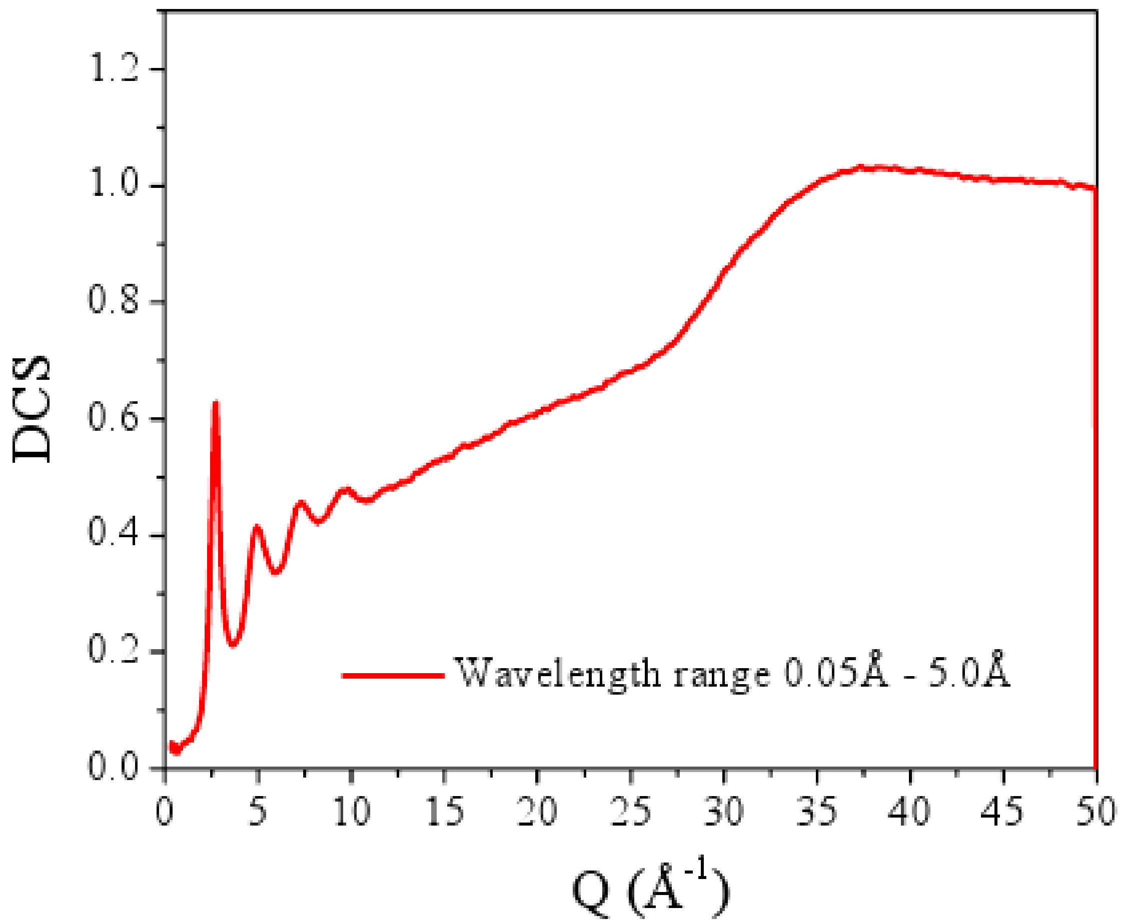

Imperfect correction of the resonance using a reduced wavelength range

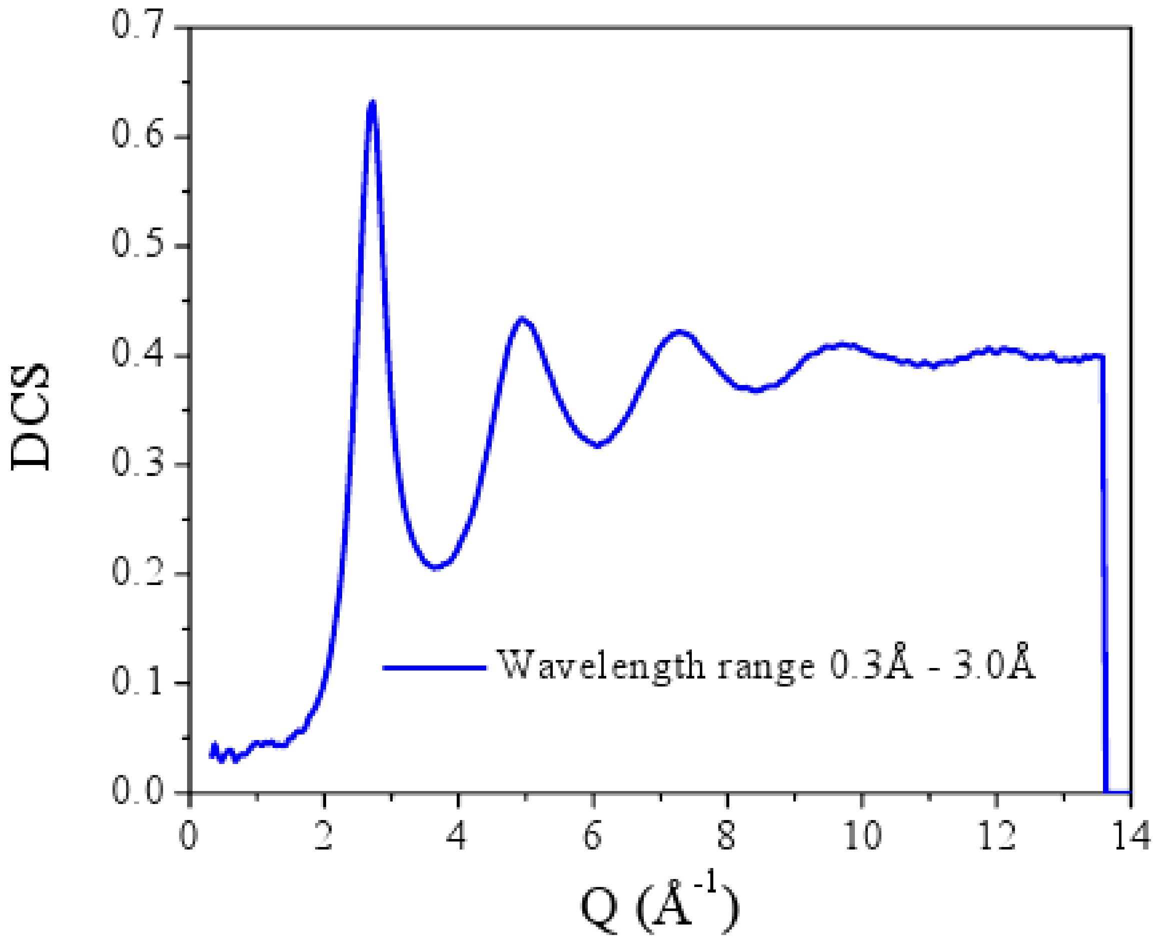

Elements suitable for isotopic substitution on a light element diffractometer

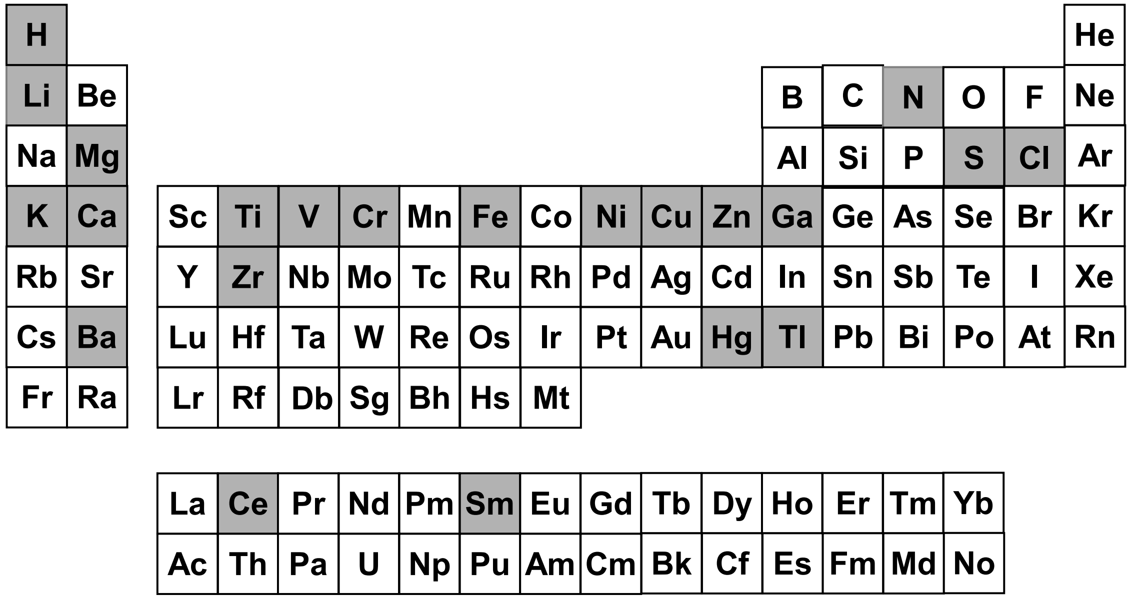

Elements with isotopes that potentially can be used for NDIS ion solvation studies ($\Delta\ b_c \geq\ 1$fm)

J.E.Enderby, *Chem. Soc. Revs.* 159 (1995)

Suitable for study on a pulsed neutron source

New directions for neutron instrumentation
NIMROD: Near and Intermediate Range Order Diffractometer

From SANDALS to NIMROD: from 40Å to 400Å (with atomic resolution)

5Å

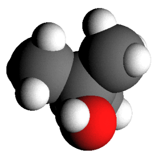

$1Å^{-1}$

10Å

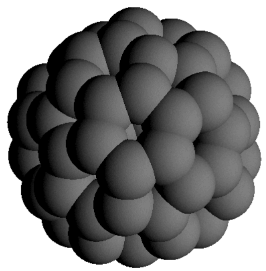

$0.6Å^{-1}$

40Å

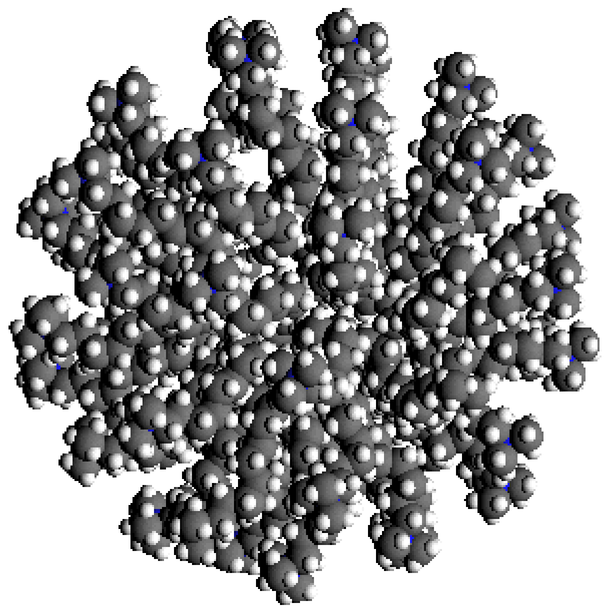

$0.15Å^{-1}$

70Å

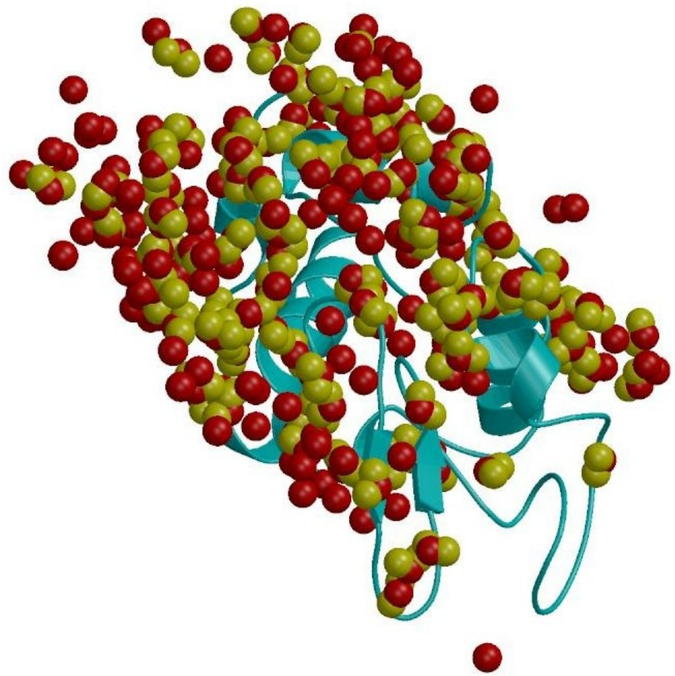

$0.09Å^{-1}$

Key Characteristics
NIMROD: Near and Intermediate Range Order Diffractometer

(1) Simultaneous access to a wide Q-range 0.01Å-1 to 50Å-1

→ access to structural correlations up to 400Å with atomic resolution

(2) Highly efficient and stable detectors (~0.1%) to allow isotopic substitution techniques on more dilute systems

(3) Forward scattering geometry using high energy neutrons to minimise undesirable inelastic scattering effects - Placzek corrections

(4) Efficient use of short and long wavelength neutrons produced by the moderators and pre-moderators of the ISIS second target station

ISIS Target Station 2

Target station monolith

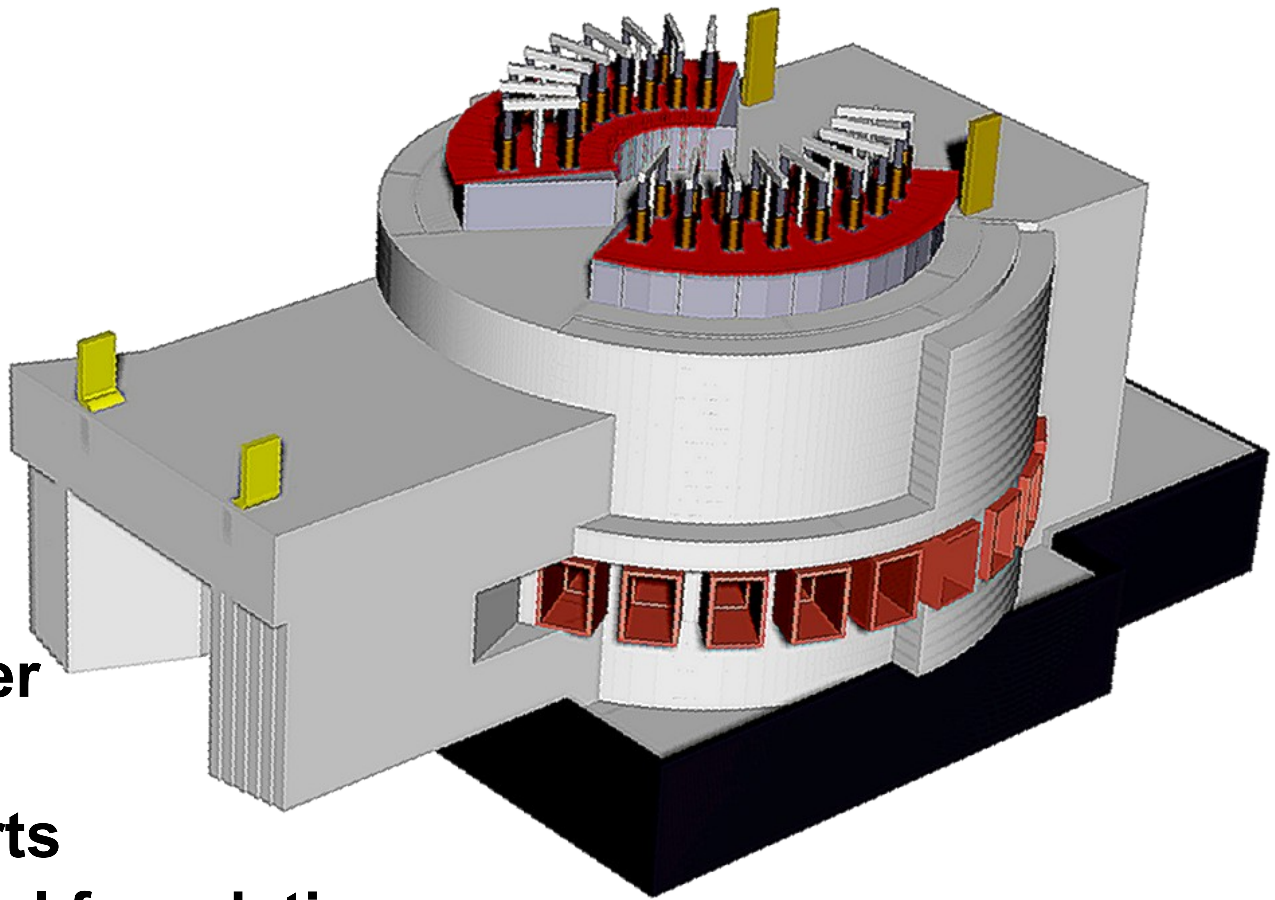

- 12m diameter
- 7m high
- 18 beam ports
- 3m deep steel foundations
- Steel and concrete construction

ISIS Target Station 2: The Target Monolith

Science & Technology Facilities Council

ISIS

ISIS Target Station 2: Target and Moderators

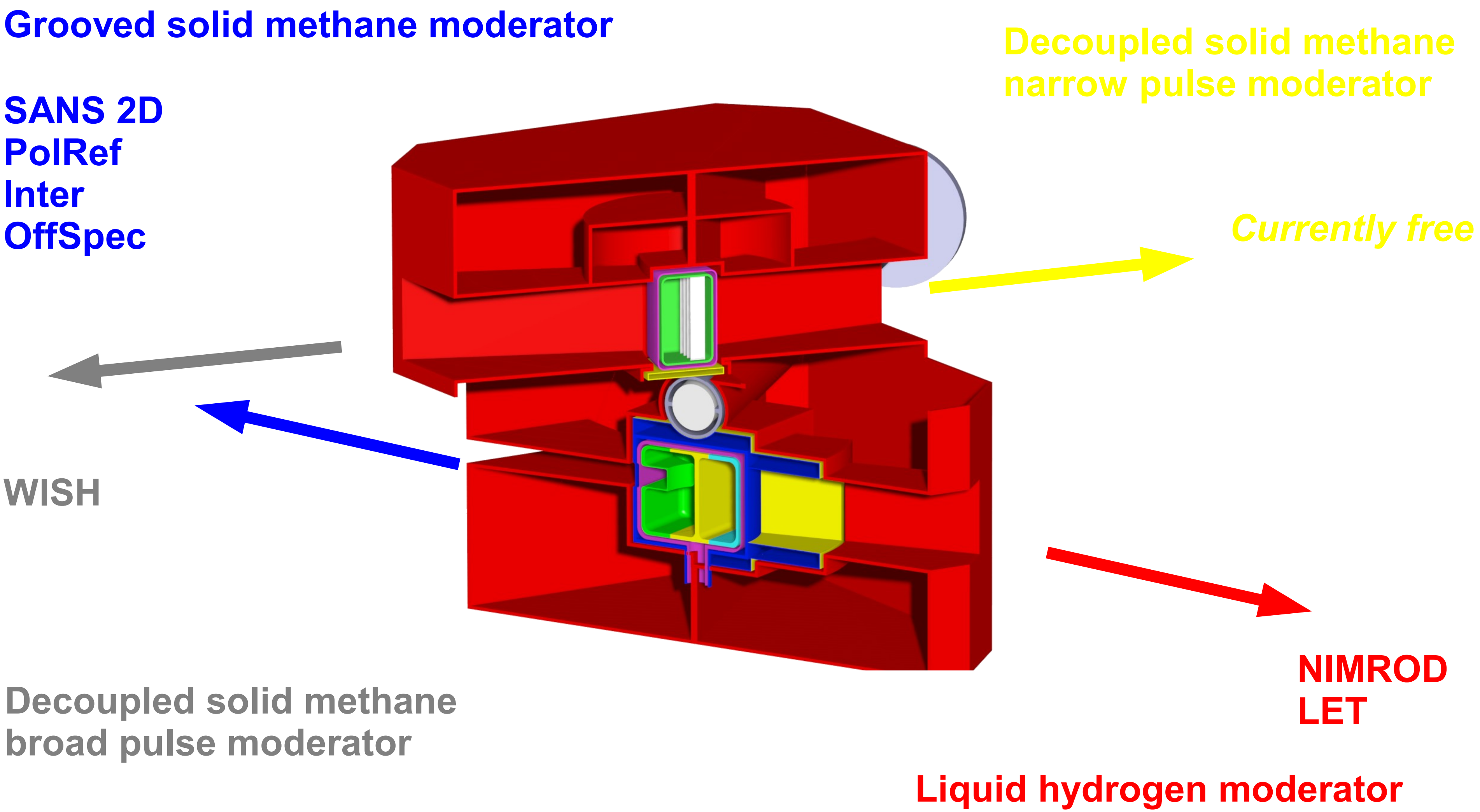

ISIS Target Station 2 Moderators: Simulated Performance

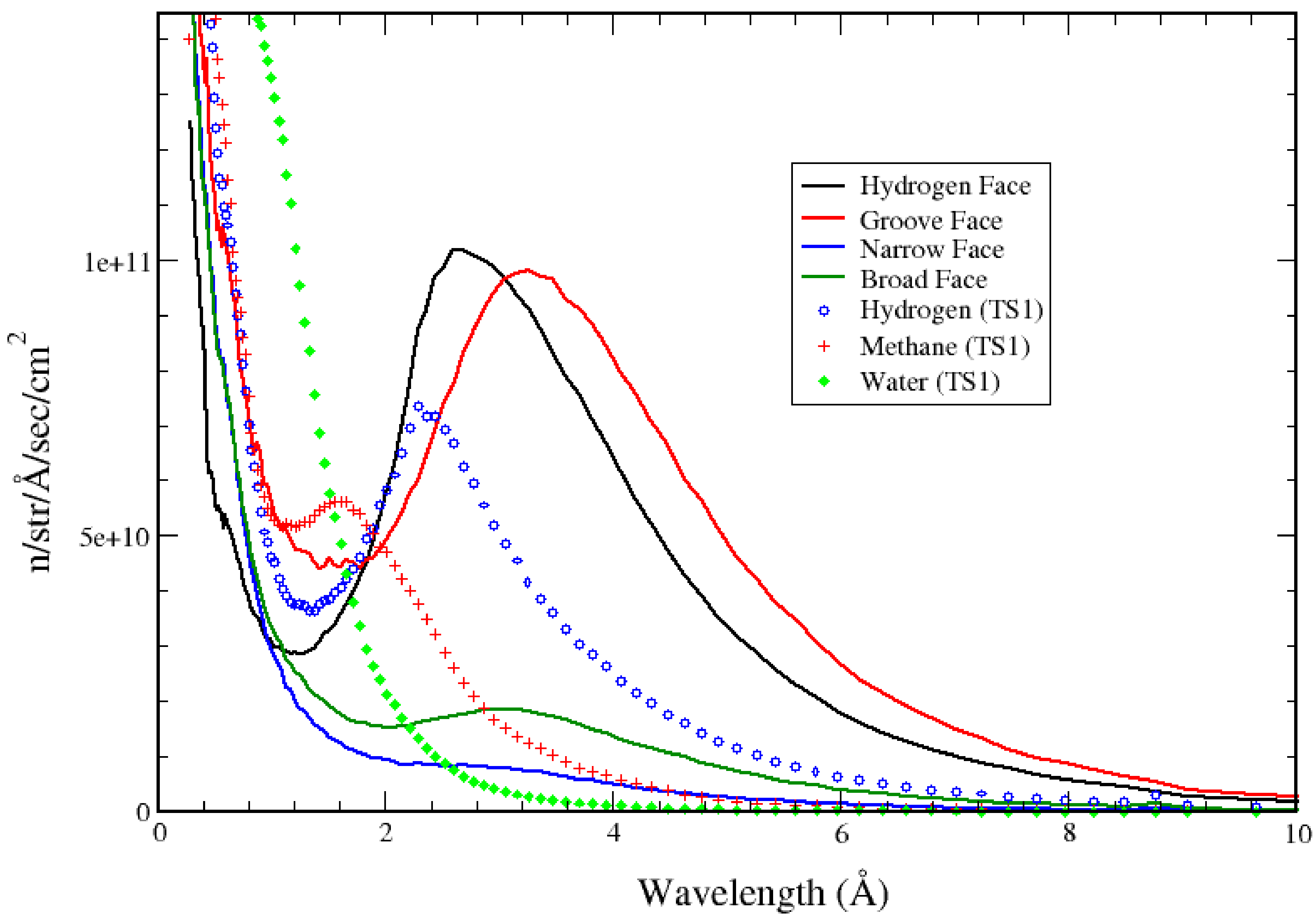

ISIS Target Station 2: Target and Moderators

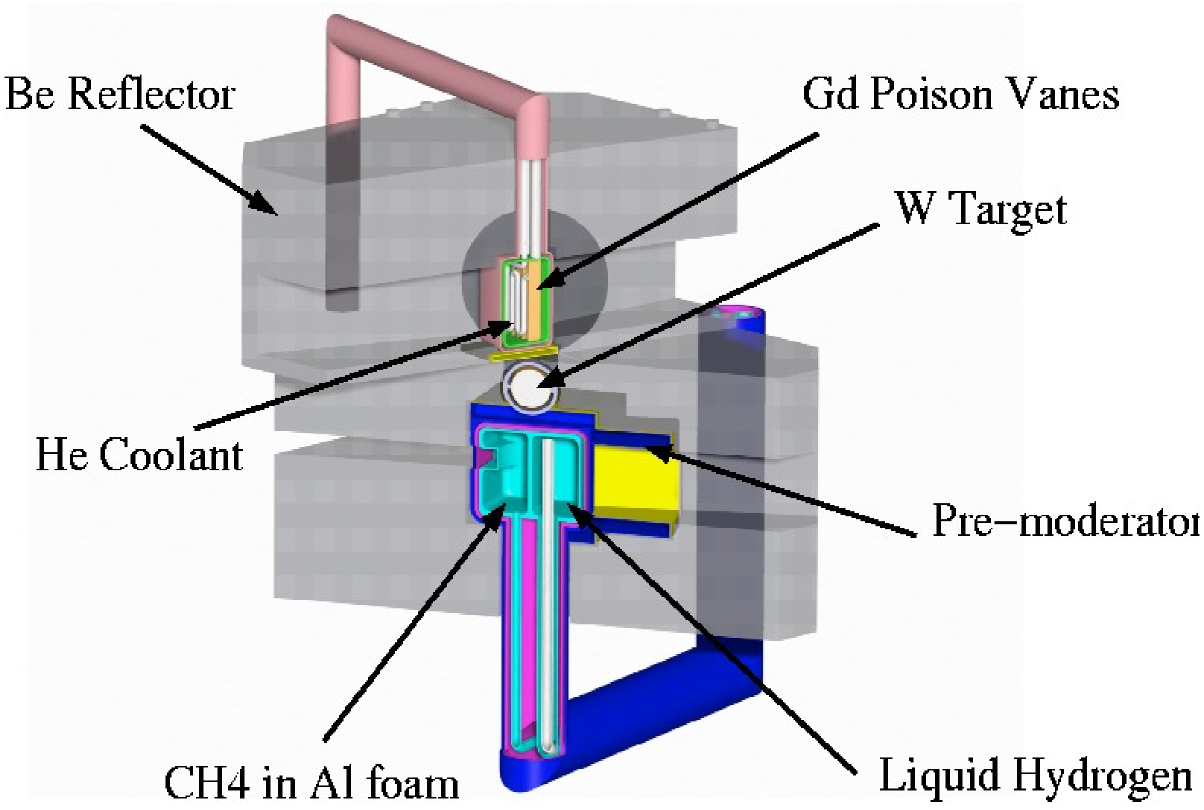

Combined view of moderator and pre-moderator
High flux across a broad wavelength range

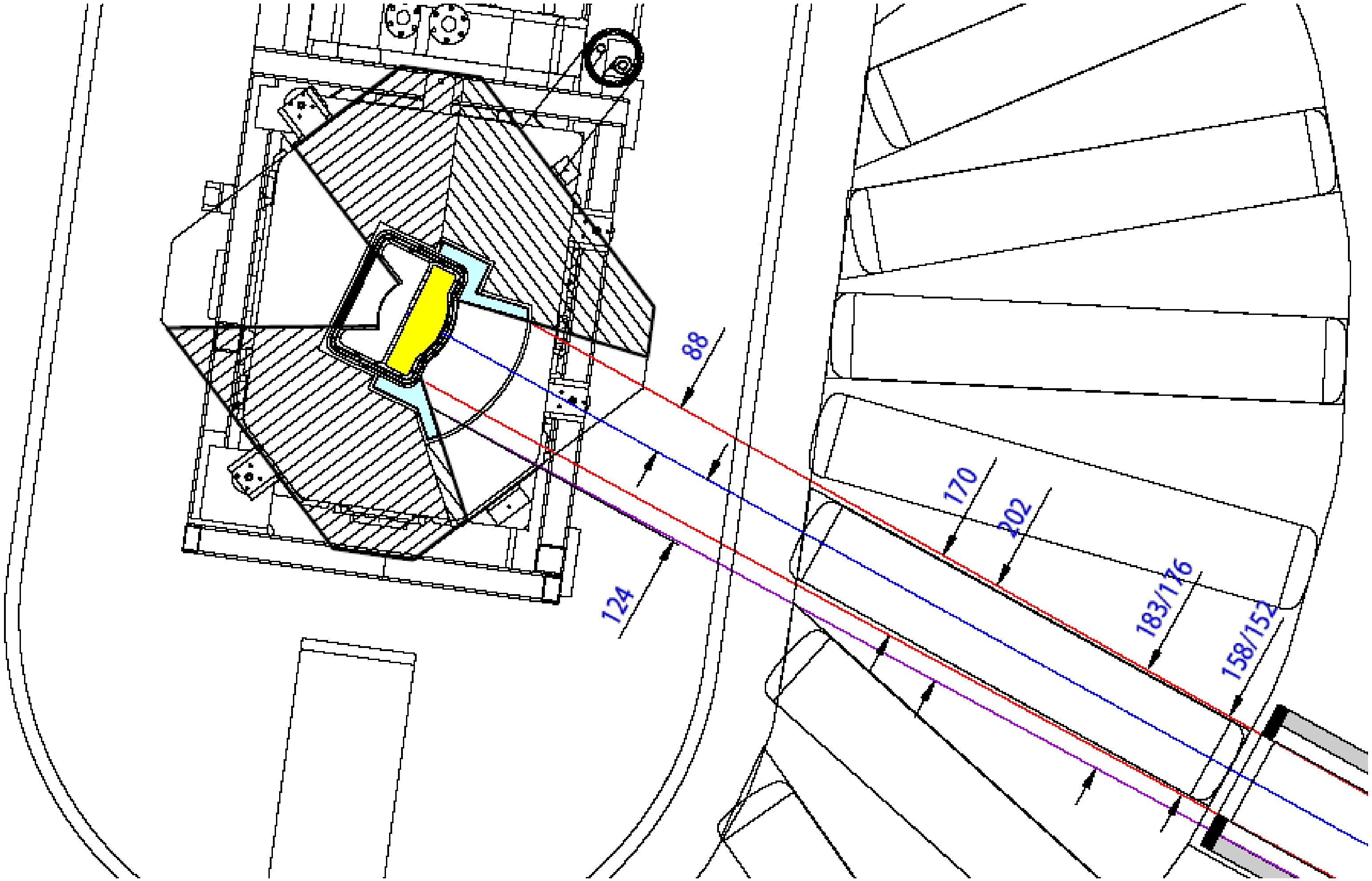

Target Insert Collimation

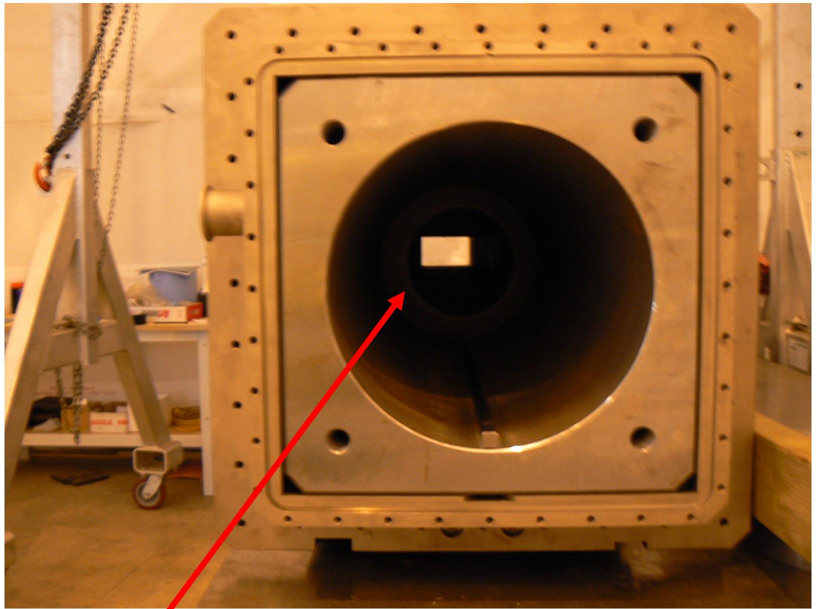

Collimated view of moderator and premoderator approximately 20cm wide x 12cm high

Combined view of moderator and pre-moderator
High flux across a broad wavelength range

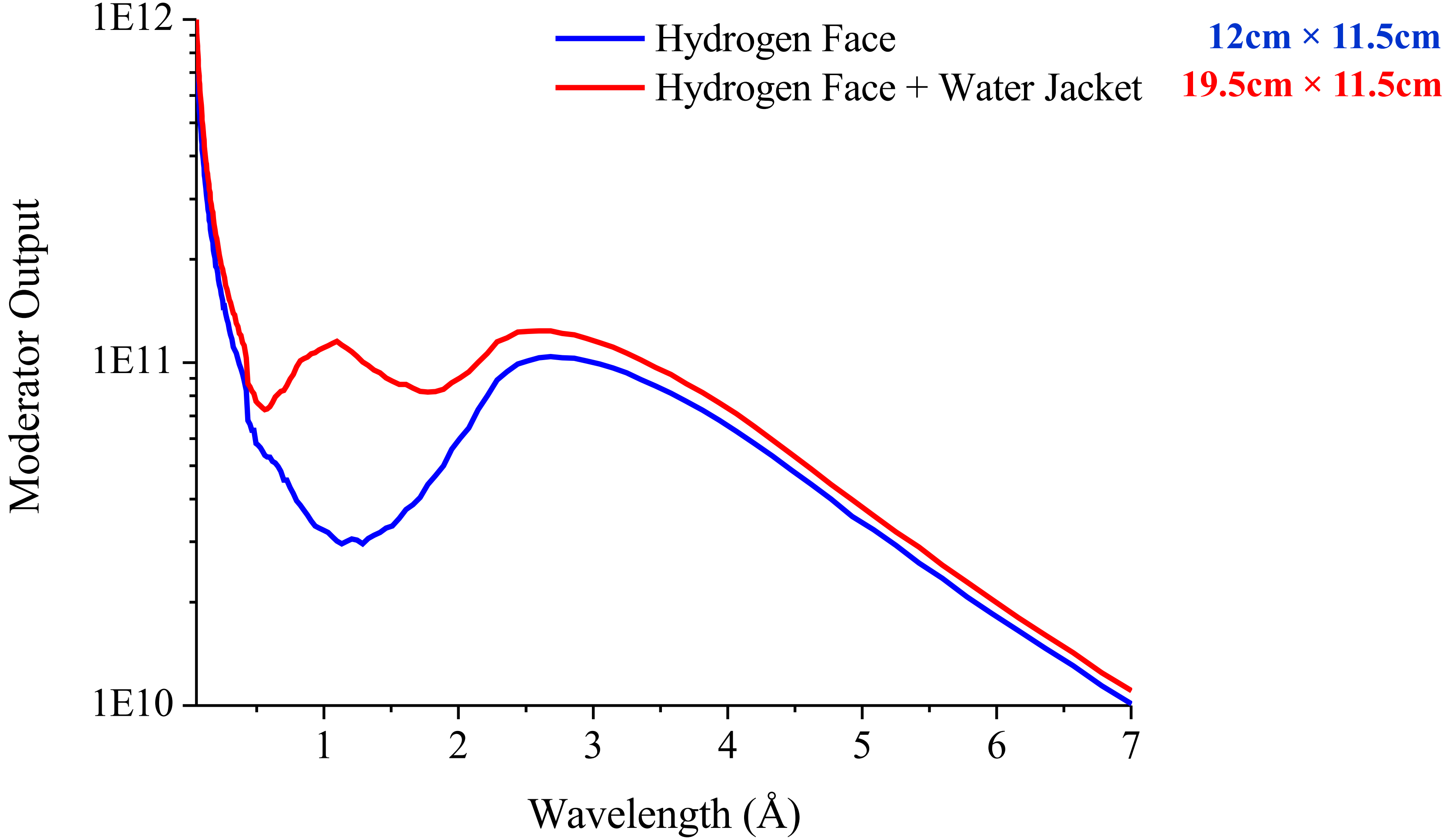

Combined view of moderator and pre-moderator
High flux across a broad wavelength range

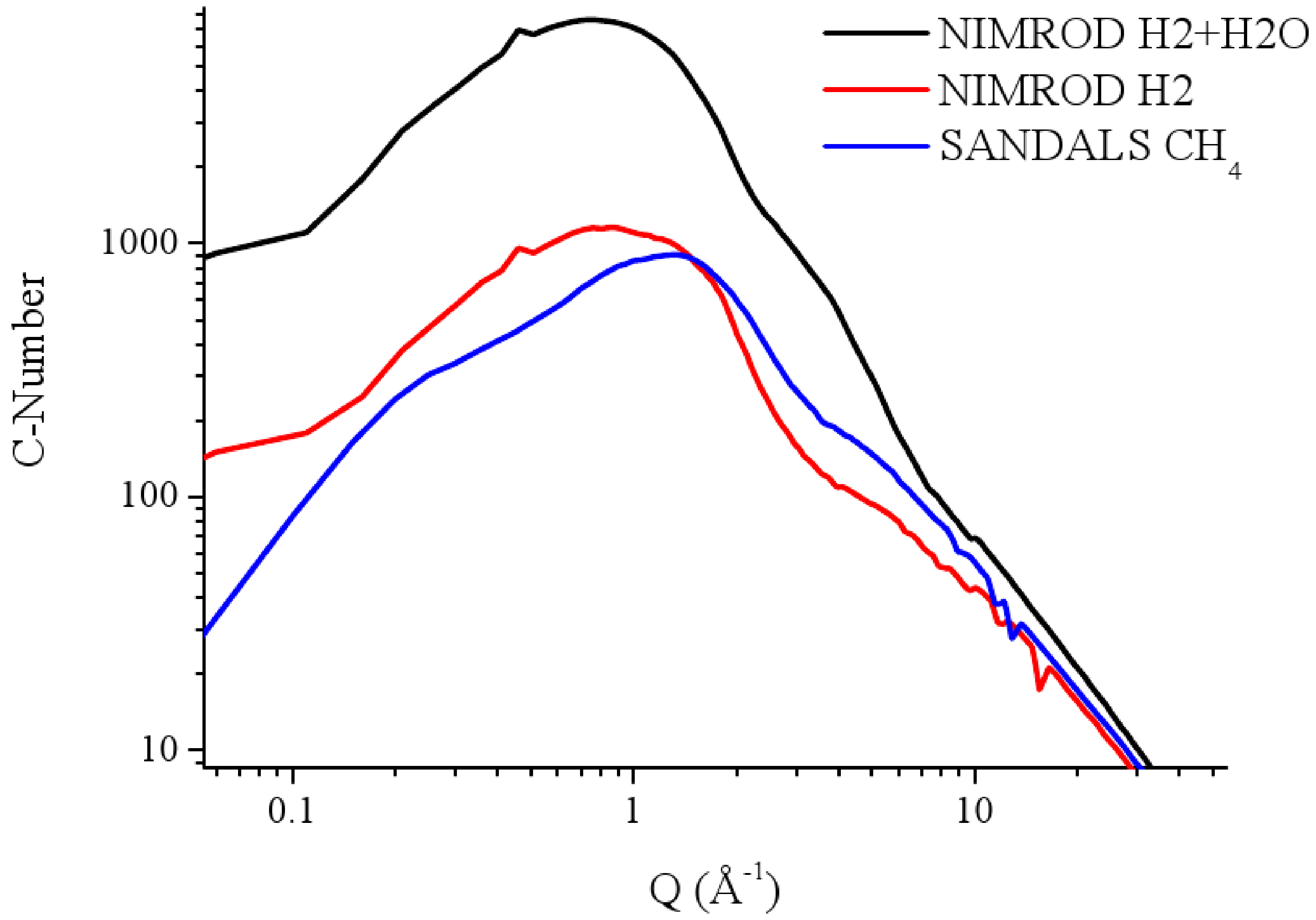

NIMROD

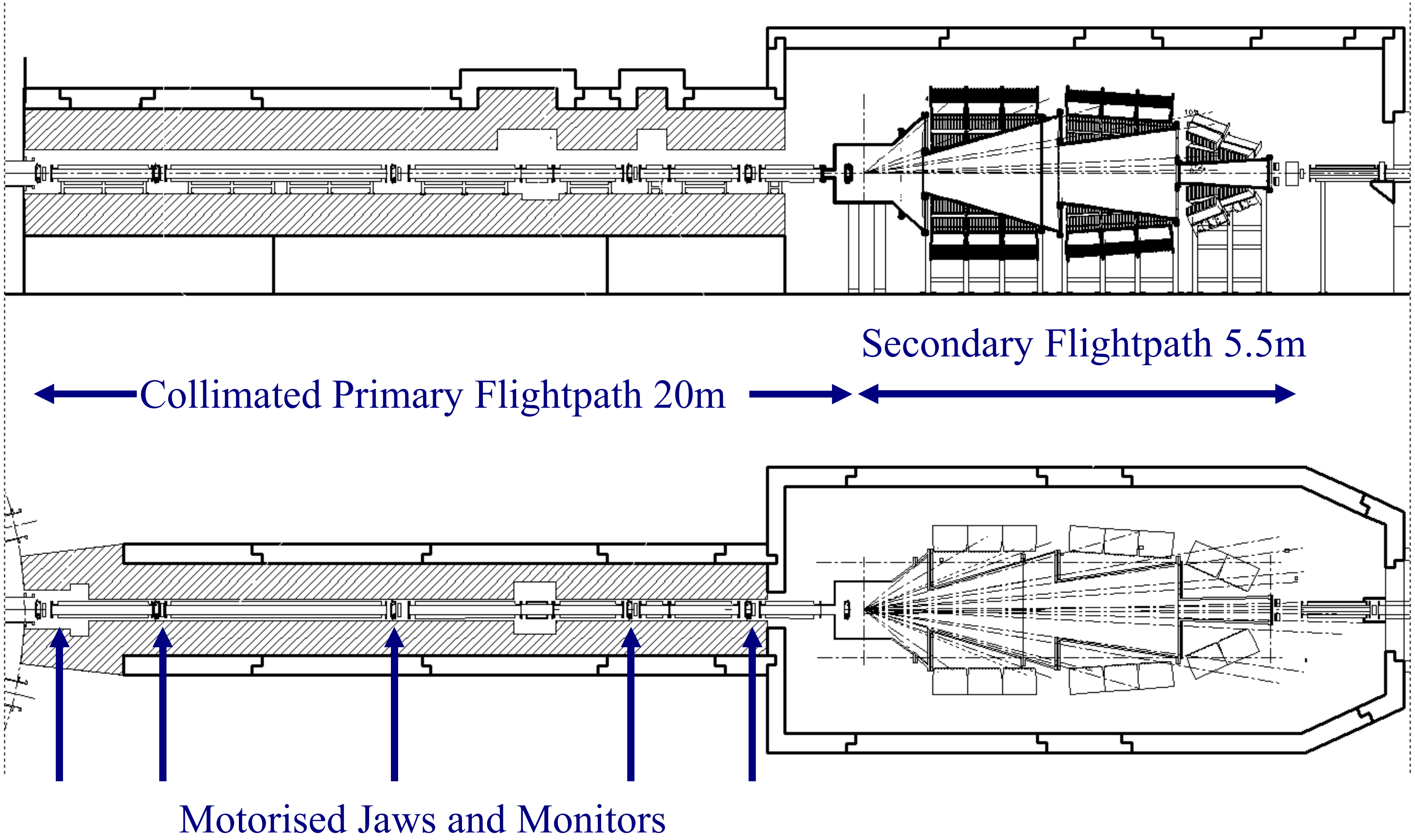

Secondary Flightpath 5.5m
Collimated Primary Flightpath 20m
Motorised Jaws and Monitors

Neutrons and gravity

Neutrons have mass (1.67×10^{-27} kg) and therefore are subject to gravity

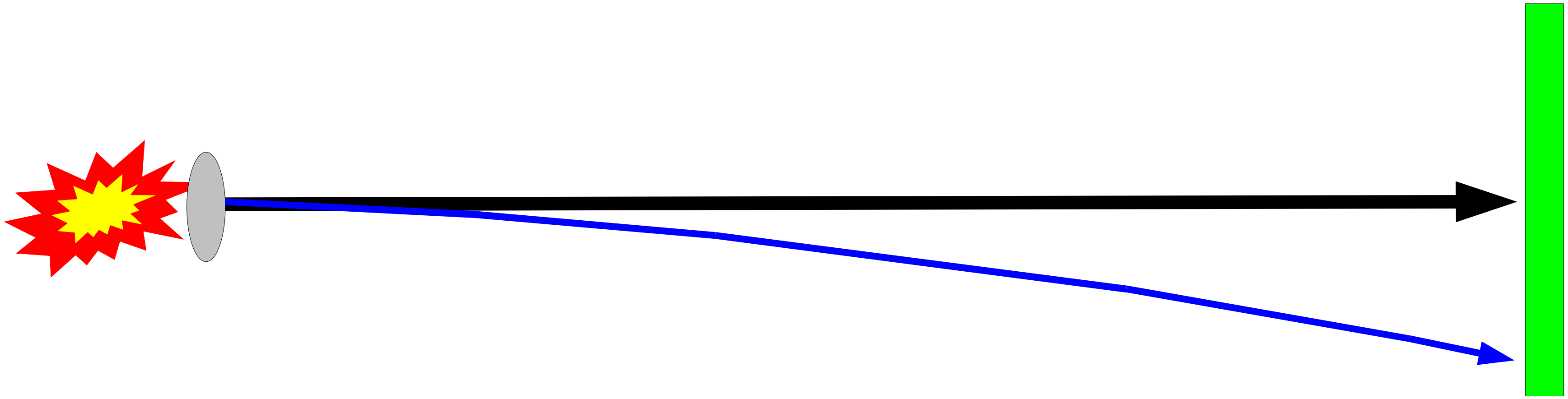

ISIS TS1

If a neutron takes 20ms to travel from the moderator to the detector, it will fall by:

1.96mm

ISIS TS2

If a neutron takes 100ms to travel from the moderator to the detector, it will fall by:

4.9cm

Primary beam collimation

Made in Spain

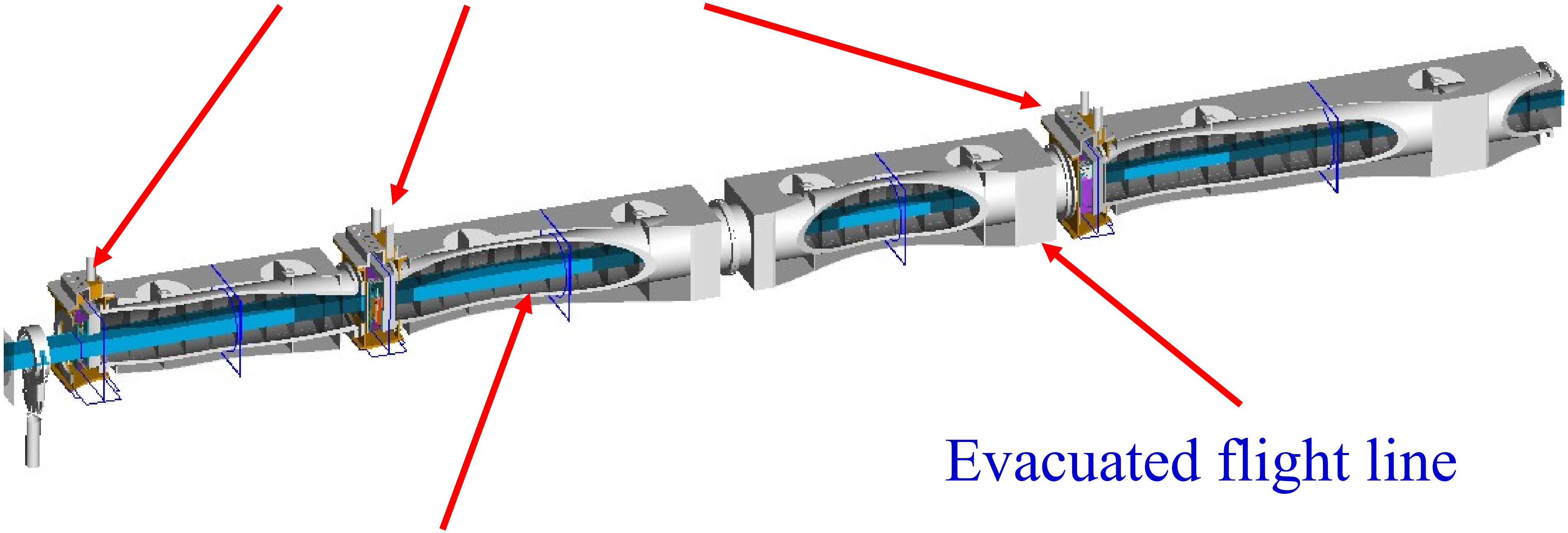

NIMROD incident flight line

NIMROD sample and detector vacuum tank

Made in Italy

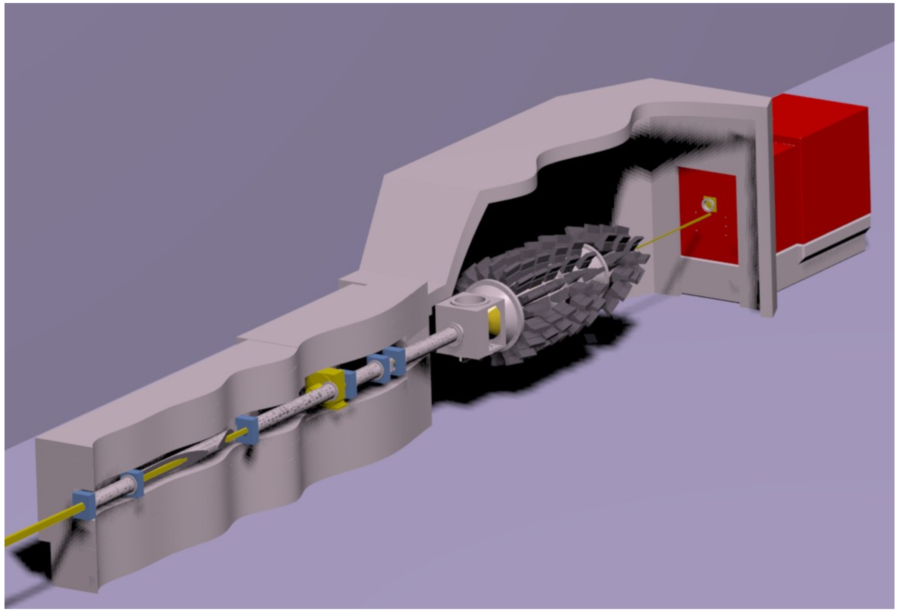

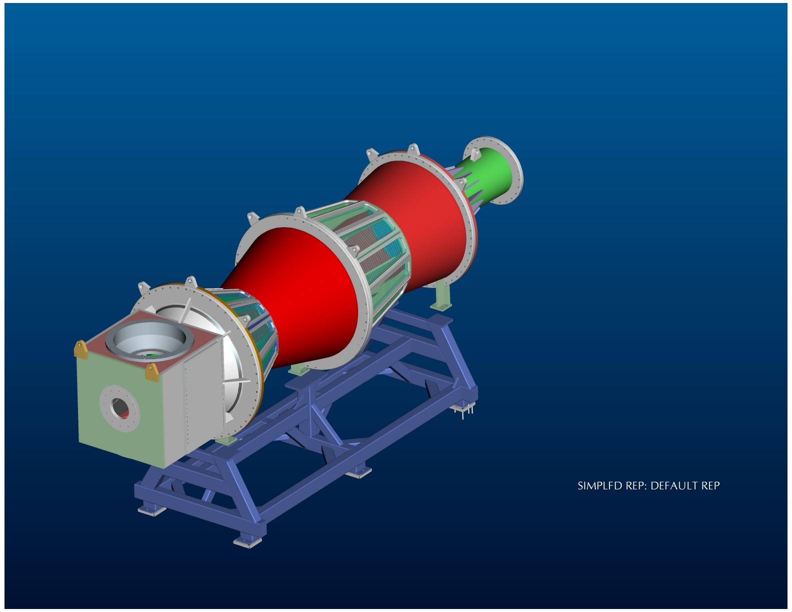

NIMROD Detector Tank

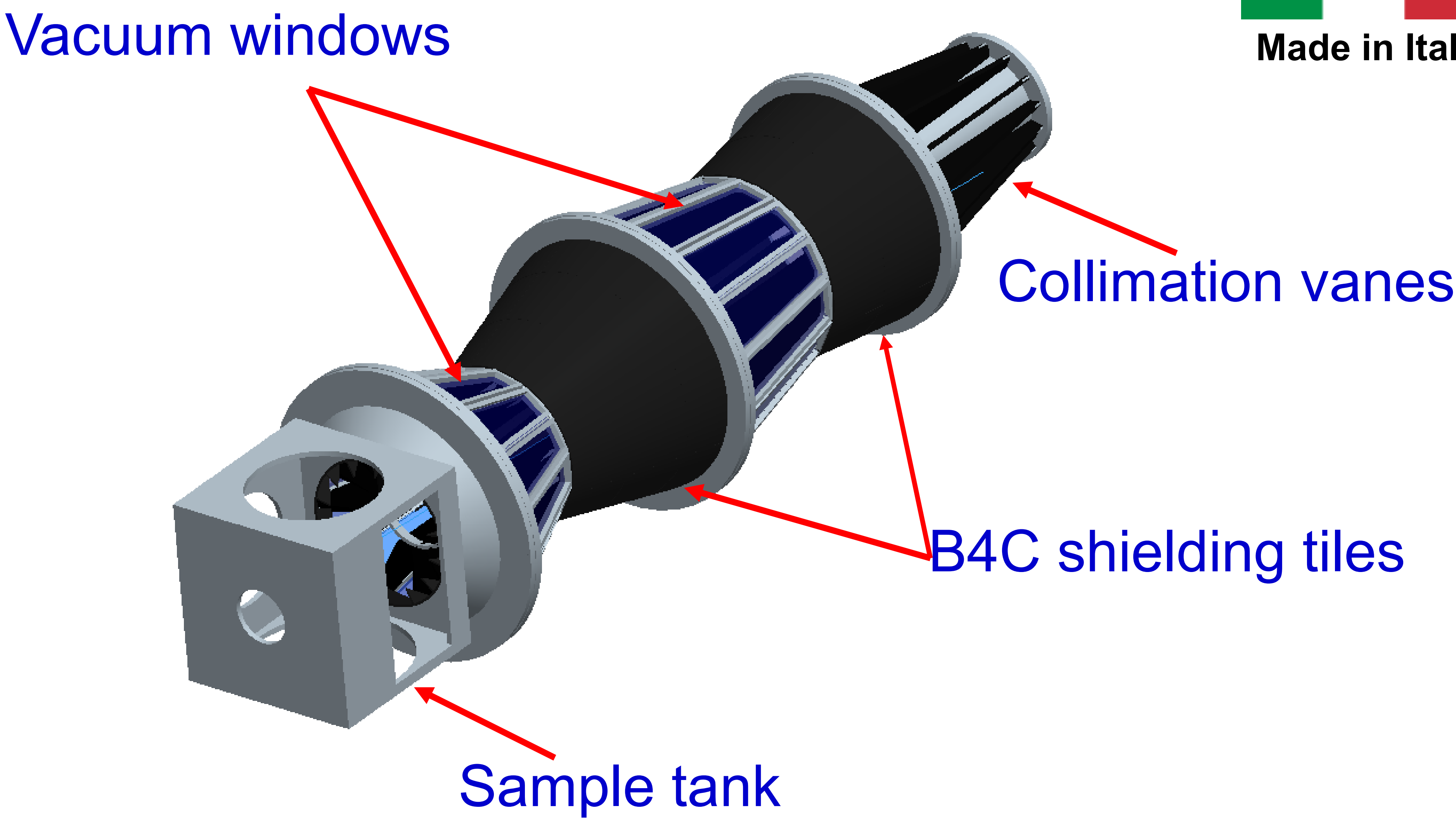

Made in Italy

NIMROD Detector Tank

Made in Italy

NIMROD Detector Modules and Mounting Frames

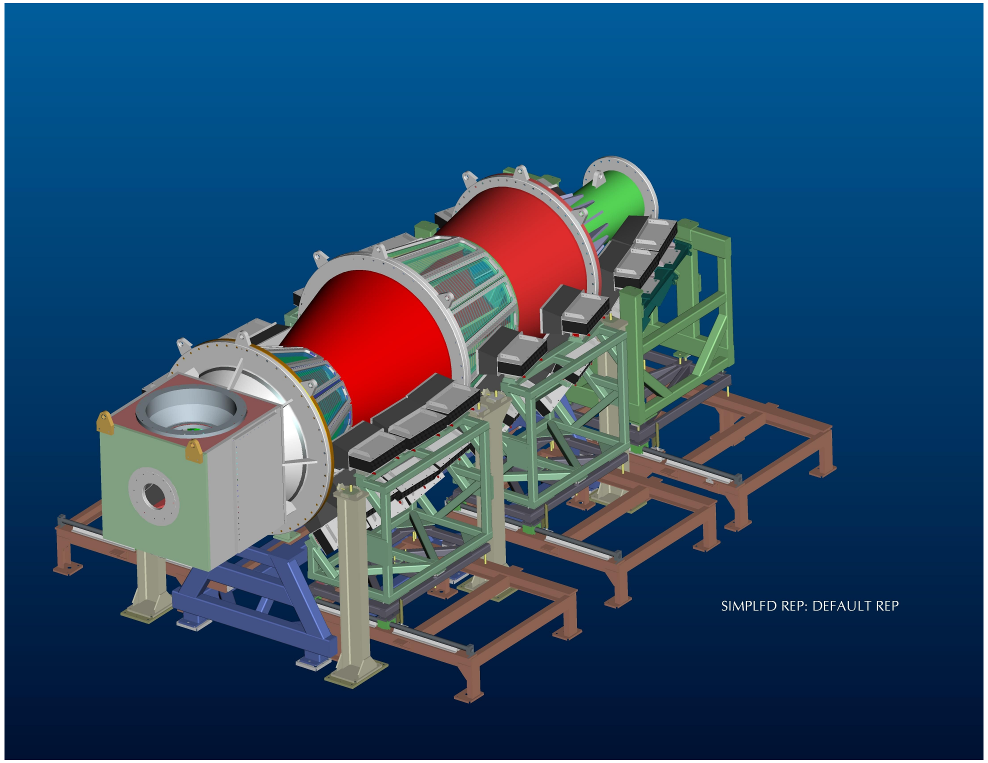

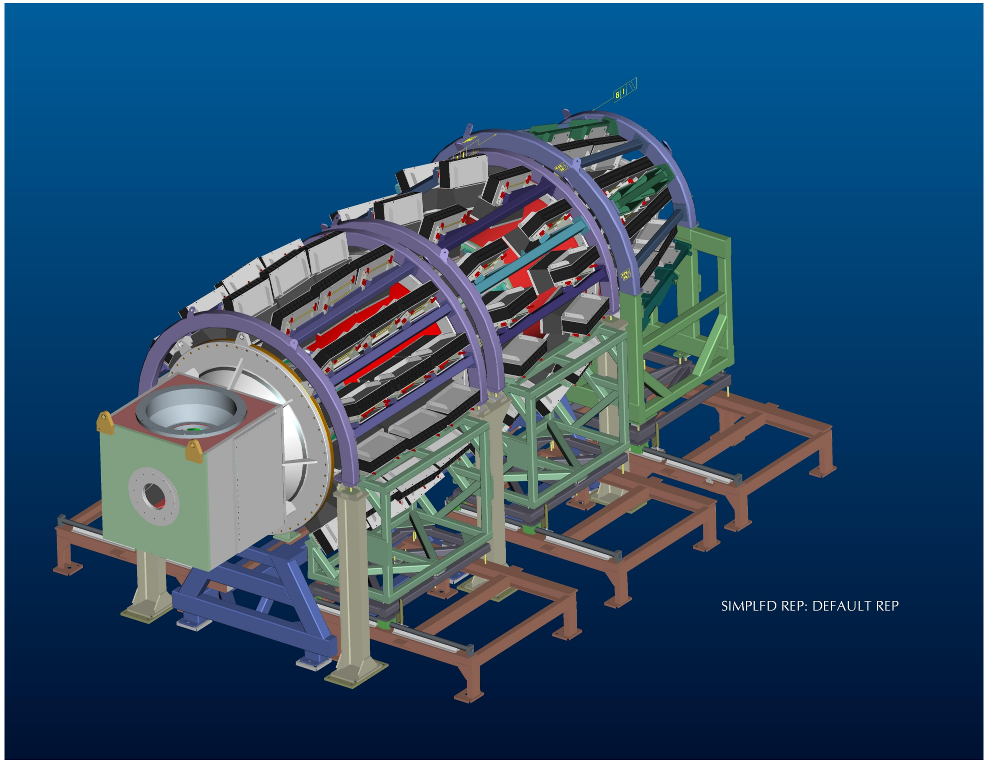

NIMROD Detector Modules and Mounting Frames

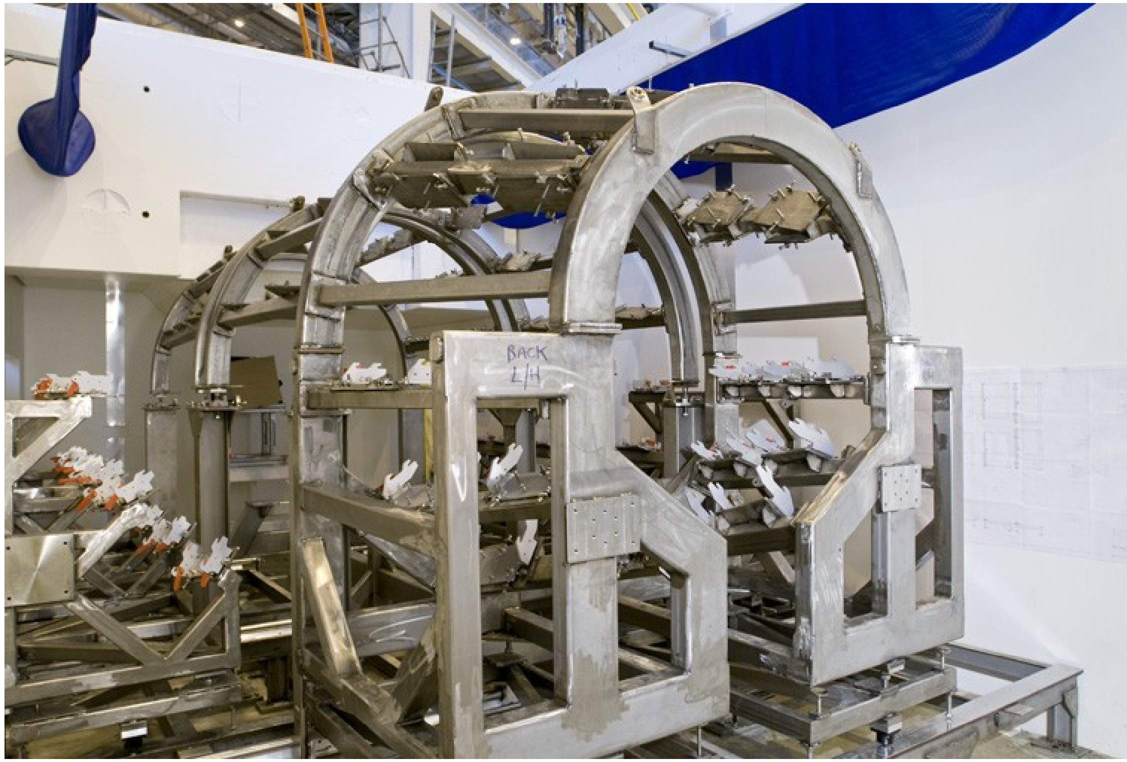

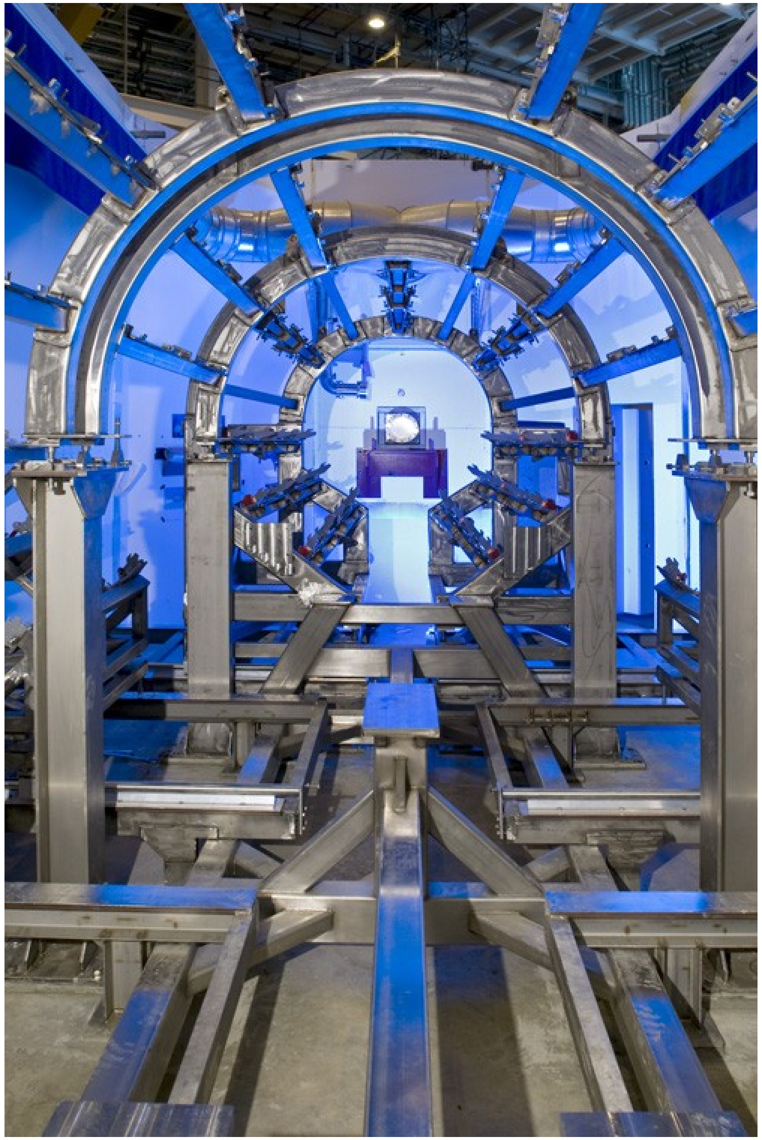

Positioning the NIMROD Detector Modules

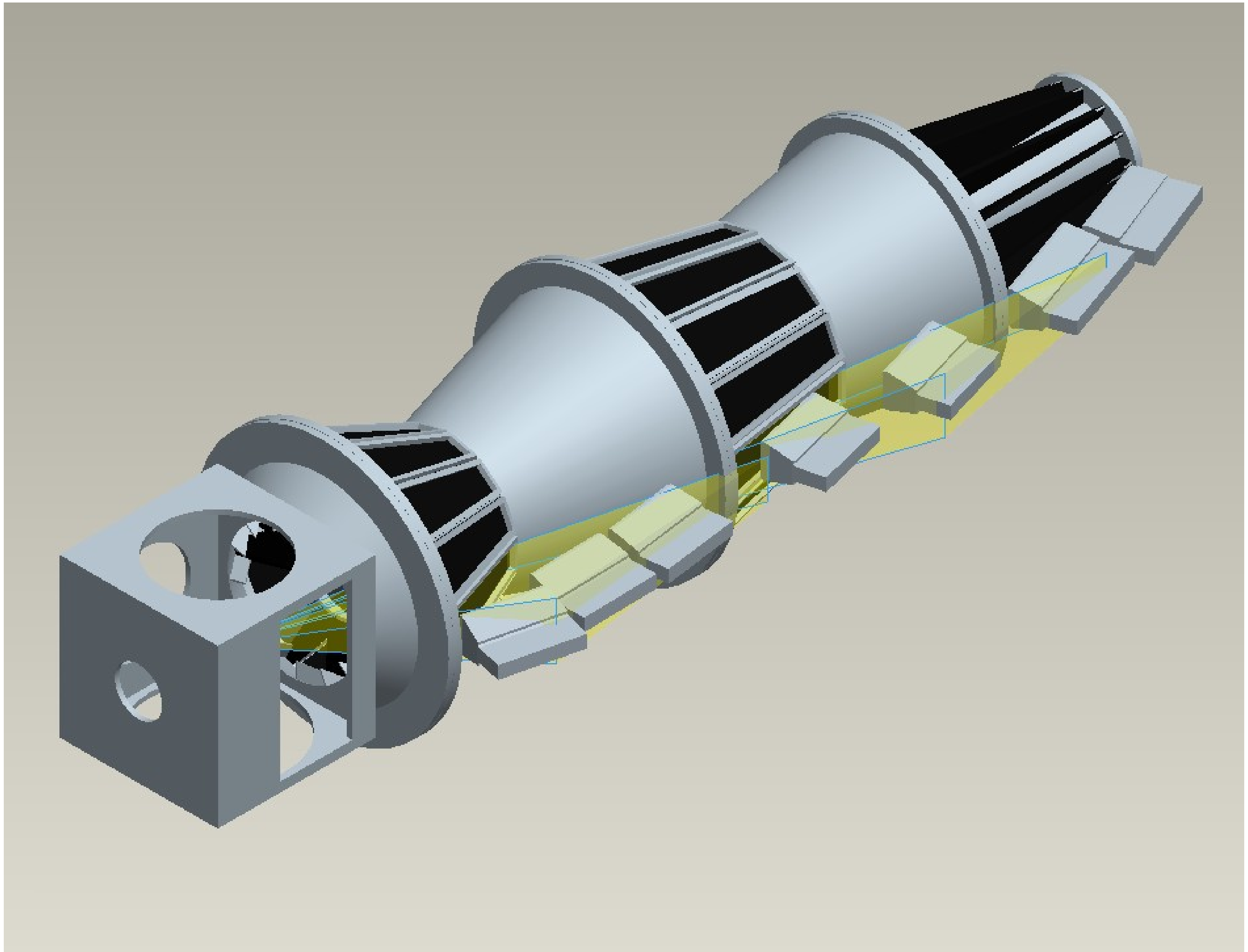

SANDALS type detector technology

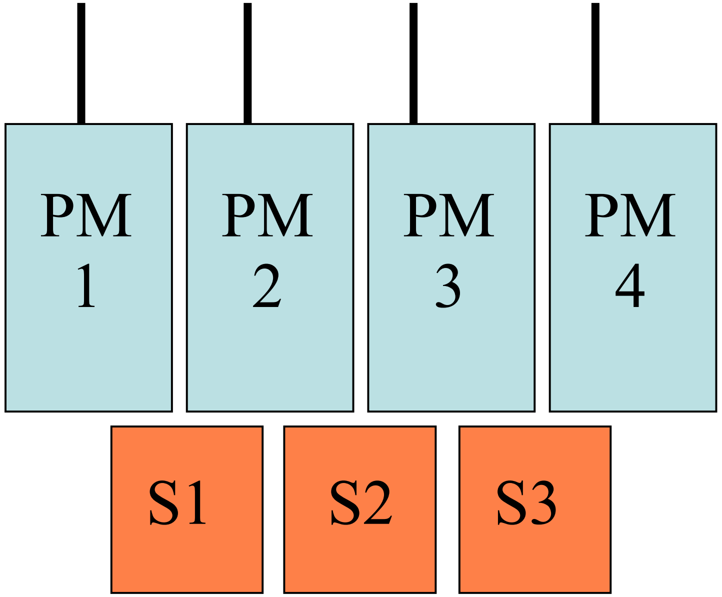

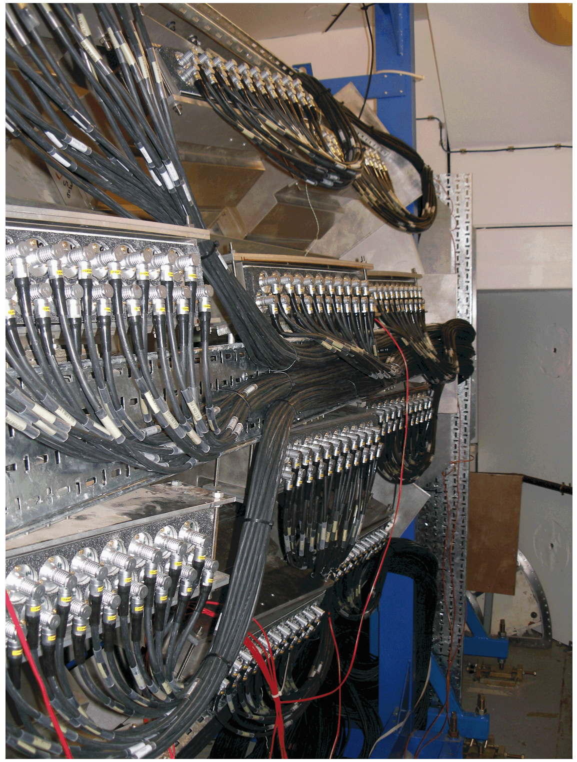

Array of high efficiency ZnS scintillators viewed by photomultiplier tubes

SANDALS type detector technology

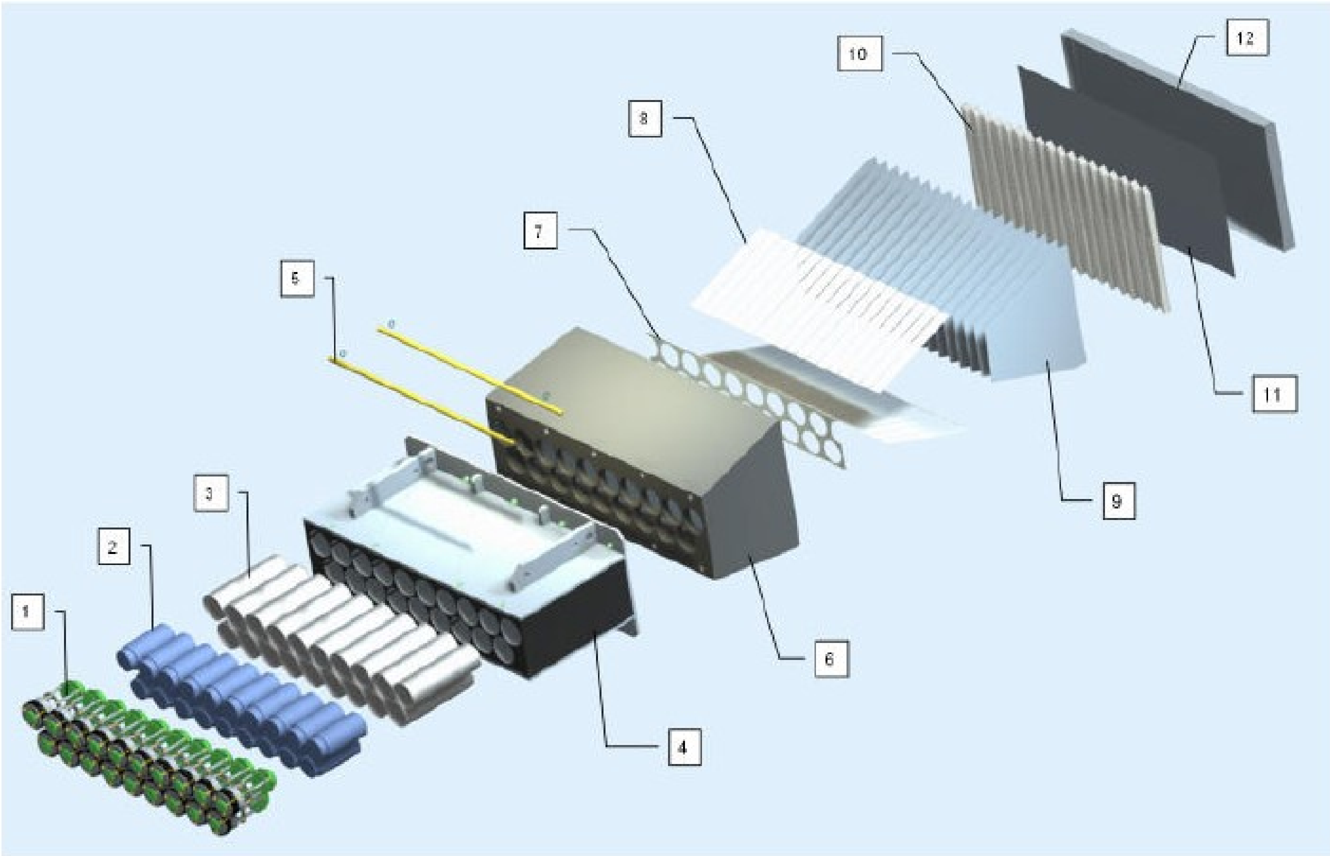

Figure 1 – NIMROD detector exploded assembly consisting of: (1) electronics assemblies; (2) PMTs; (3) mu-metal assemblies; (4) upper moulding; (5) mounting pins; (6) lower moulding; (7) upper reflective layer; (8) reflector backing plates; (9) dividing plates; (10) scintillator assemblies; (11) foil lining; (12) detector cover.

NIMROD detector modules: efficiency test

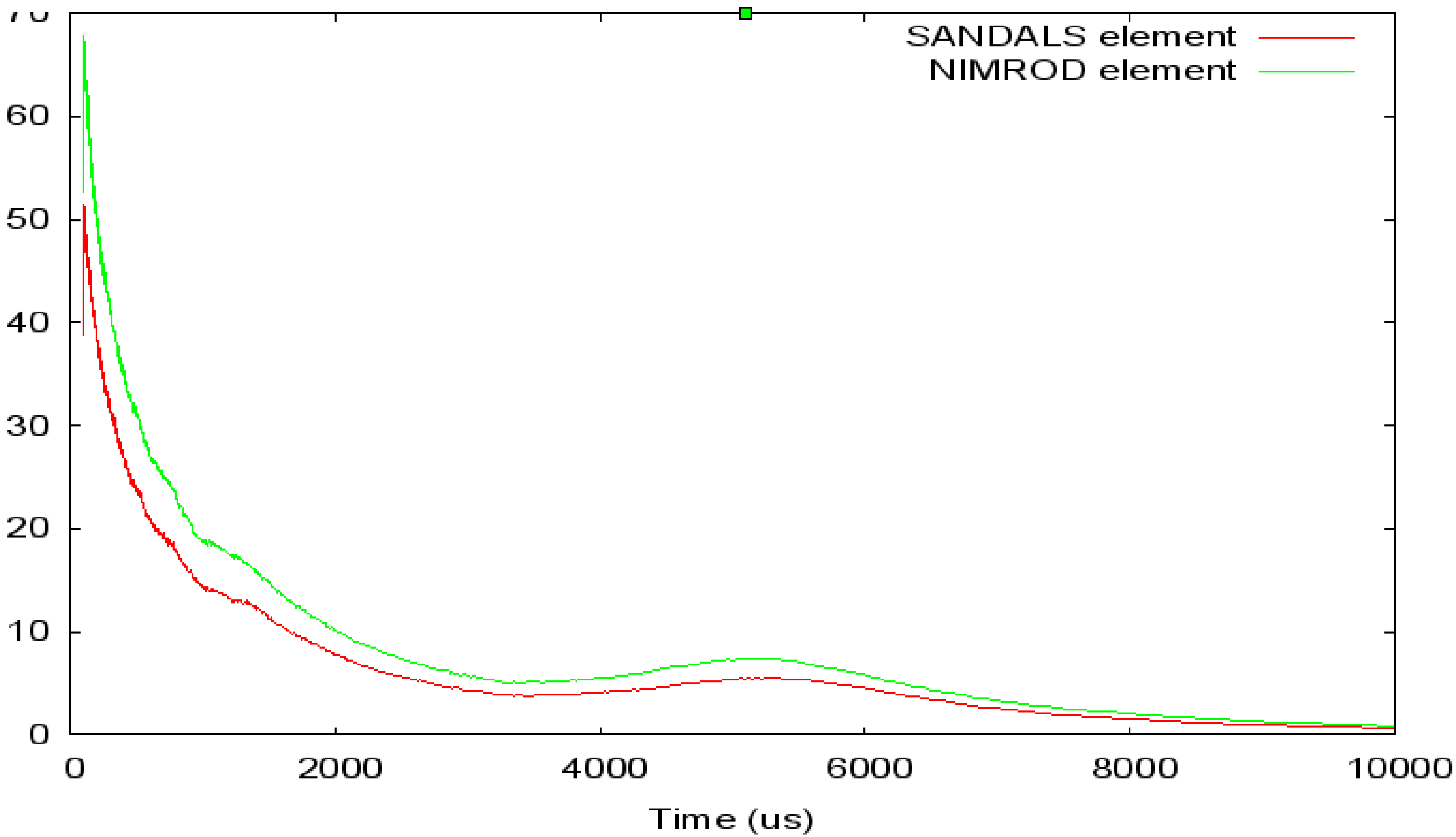

Test element approximately 30% more efficient than a SANDALS element

NIMROD detector modules: stability test

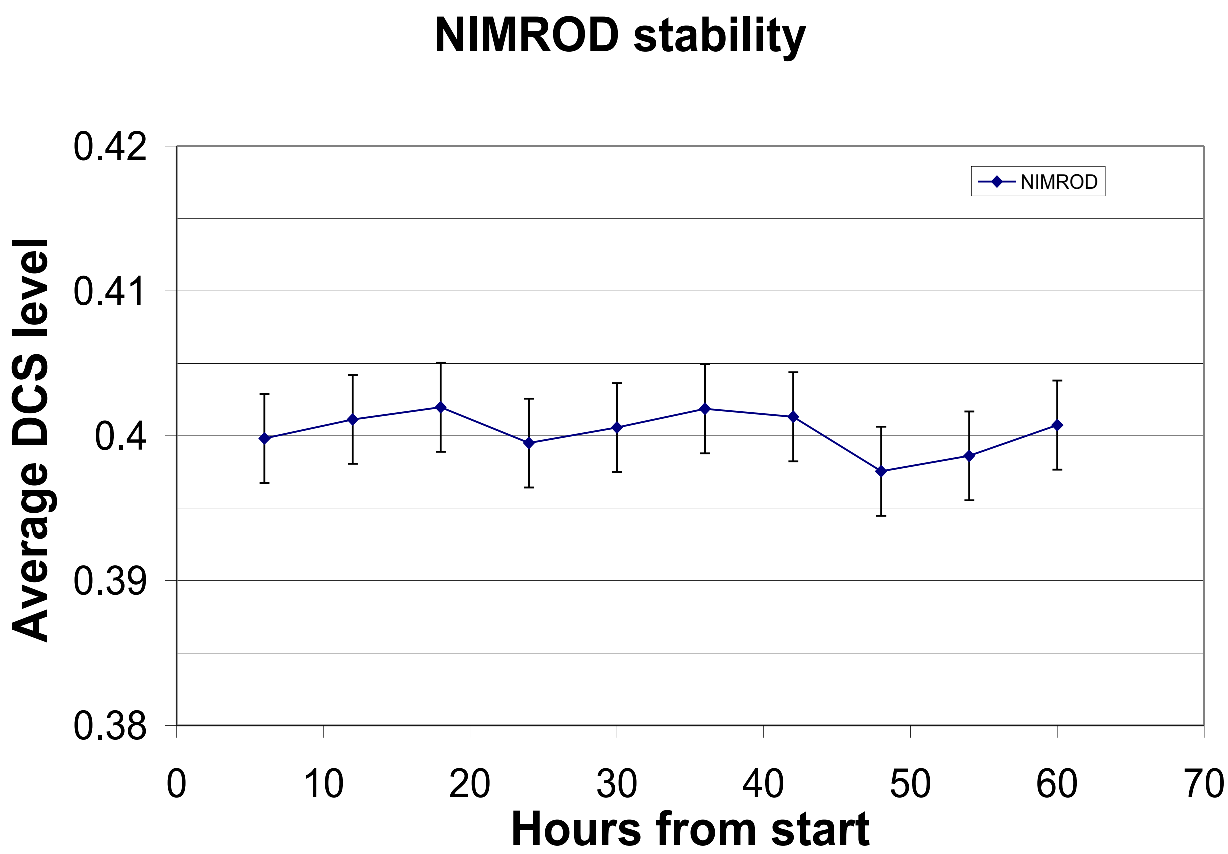

Test module at least 0.35% stable: within counting statistics

NIMROD blockhouse: environment control

To ensure the stability of the detectors it is necessary to control the temperature and humidity of the blockhouse

$\Delta T \pm 1^{o}C$
Δhumidity ± 5% (at $20^{o}C$)

NIMROD air conditioning system

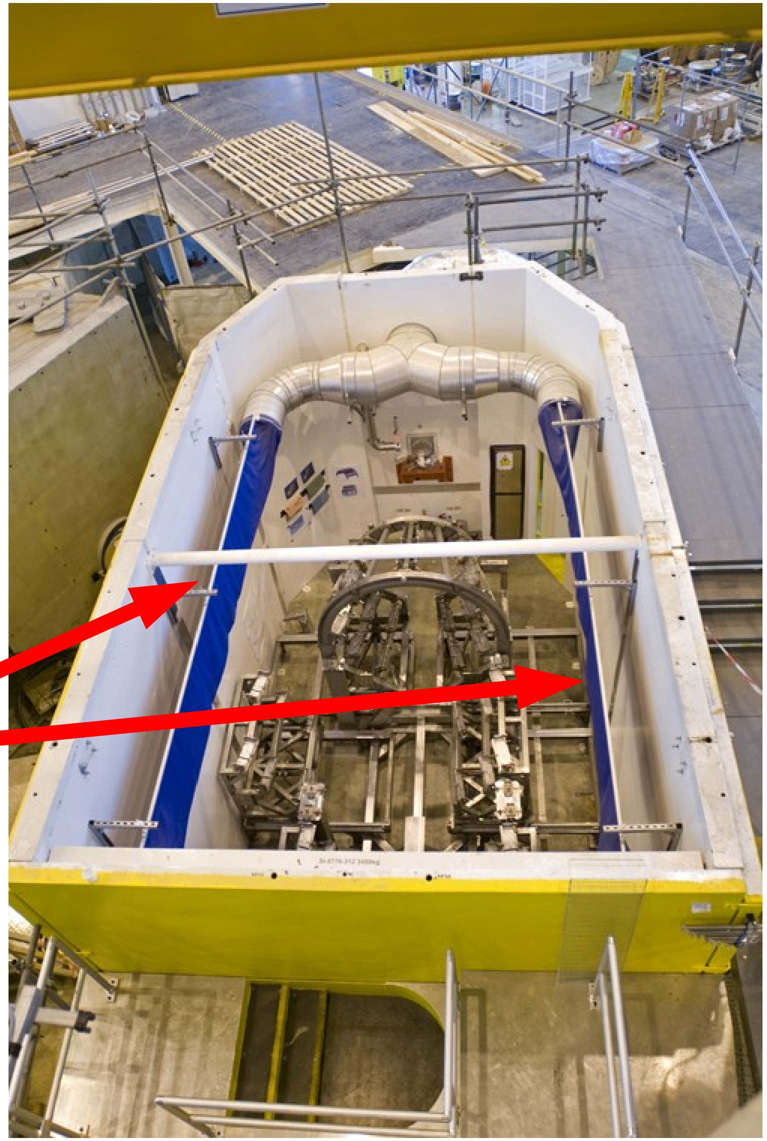

Pixellated small angle detector bank

Minimum scattering angle 0.5º

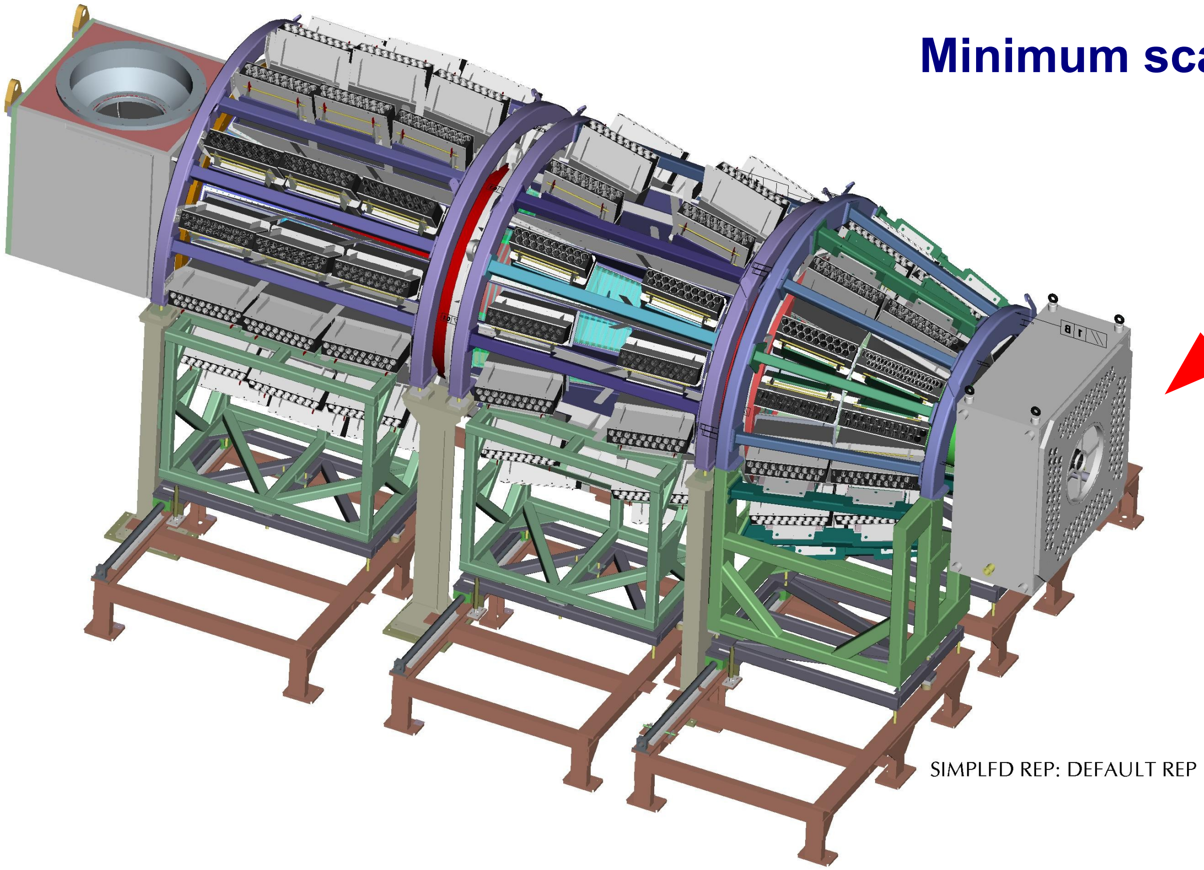

NIMROD sample point

Normal access to the sample point is from the top of the instrument, but side access options can be developed

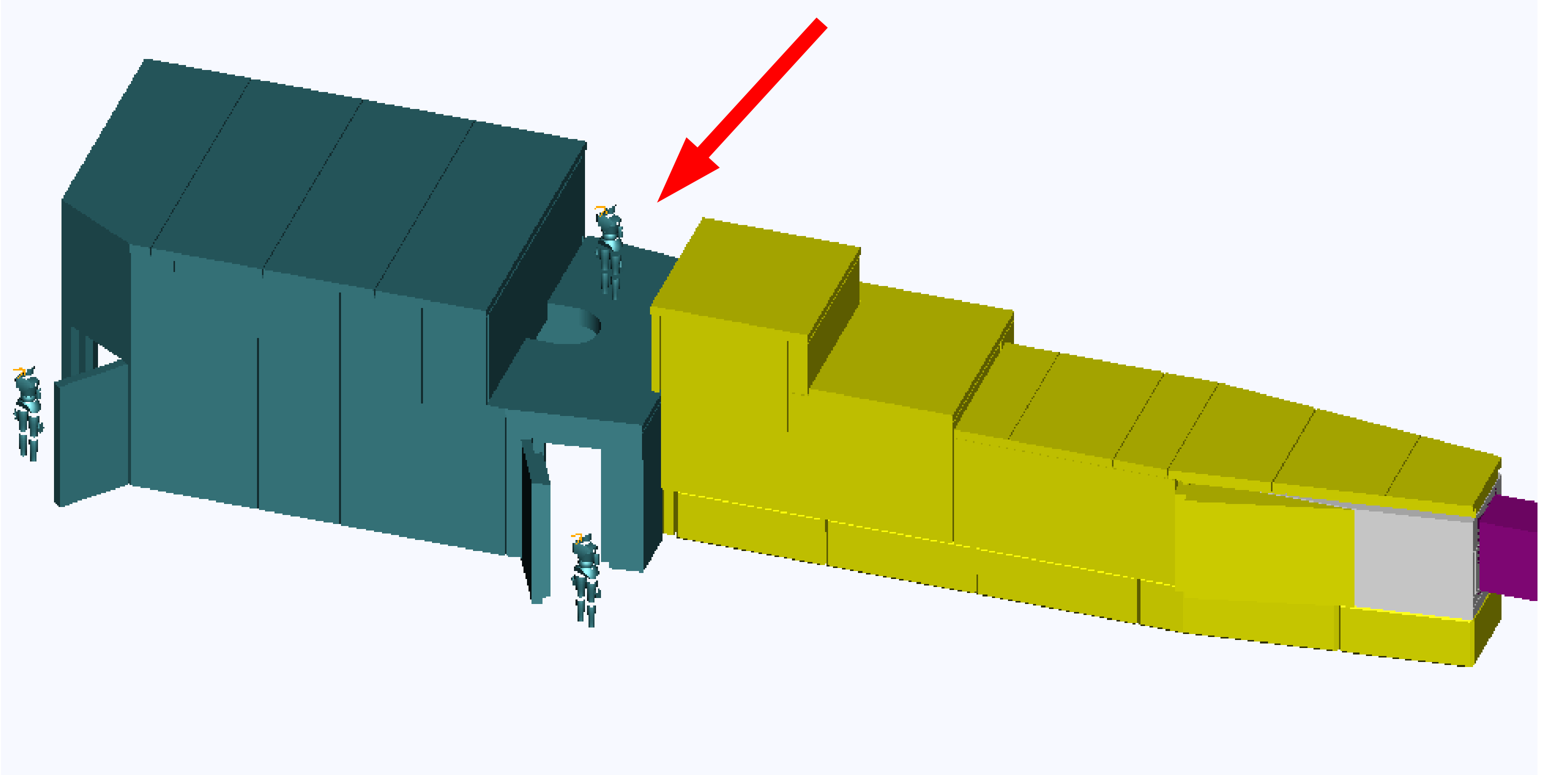

Overview of NIMROD

Counting House for DAE and detector electronics

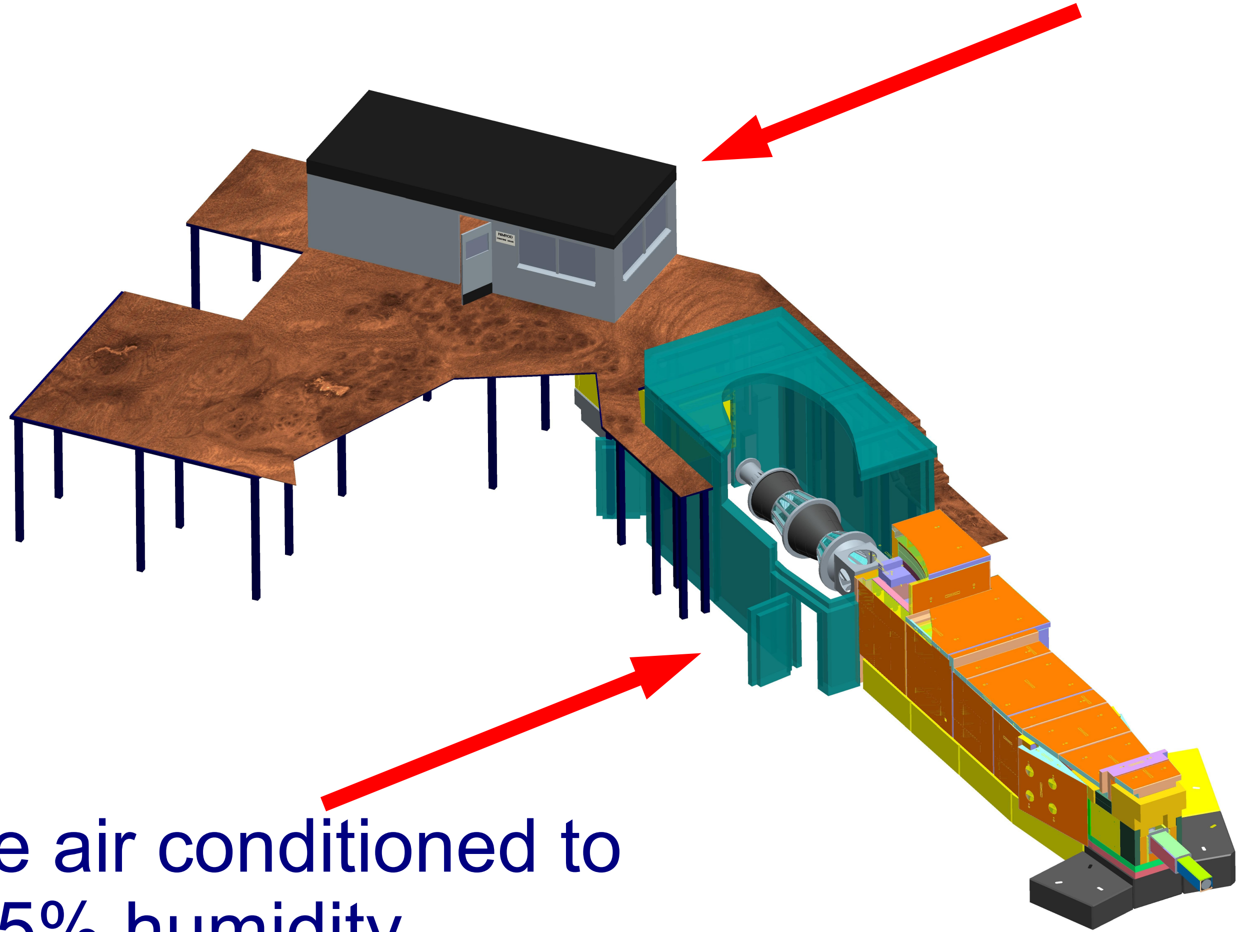

Block house air conditioned to
±1°C and ±5% humidity

Diverse areas of application

(1) Atomic and molecular liquids and liquid mixtures
(2) Glasses – atomic and molecular
(3) Structured fluids
(4) Polymers and polymer blends
(5) Mesoscale confined fluids
(6) Disordered crystals
(7) ....

Both under ambient conditions and at high and low temperatures and pressures

TS-2 Phase One Instruments

Dynamics
LET High-resolution measurement of material energy scales

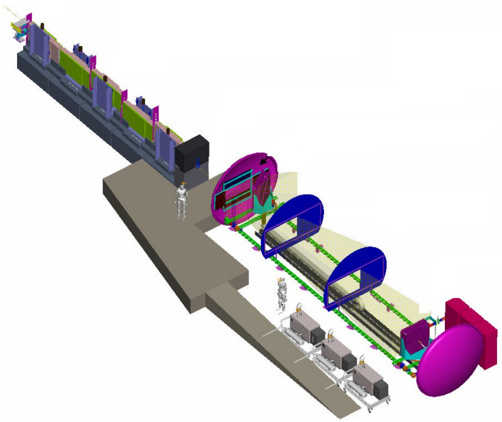

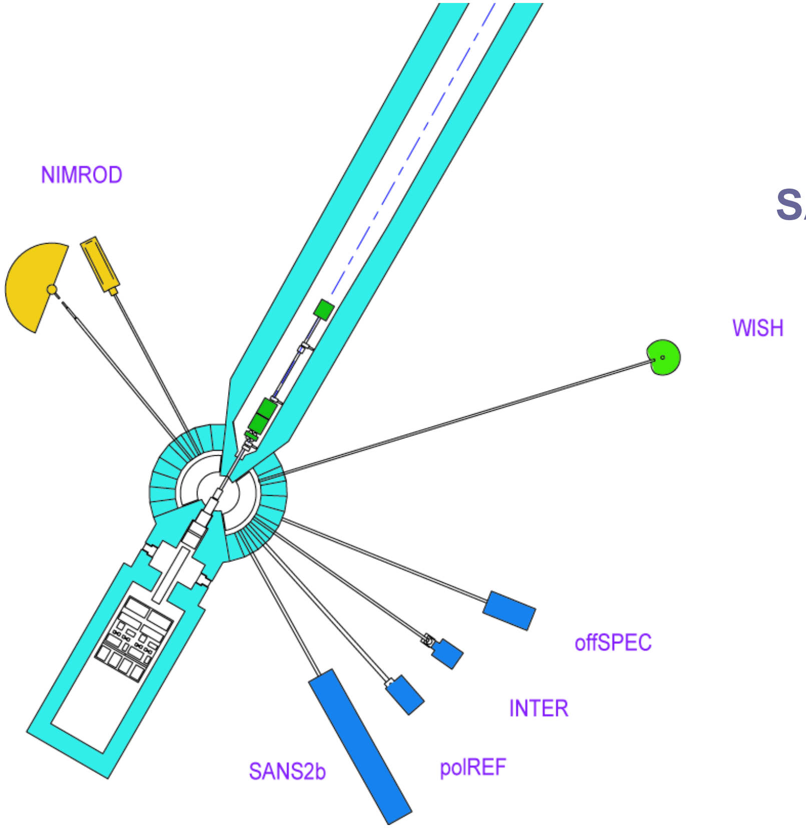

Structures
NIMROD Intermediate range order in liquids
WISH High-resolution magnetic structure
SANS2D Large molecule structure in multi-component systems

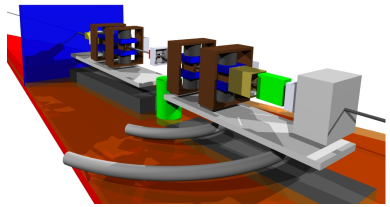

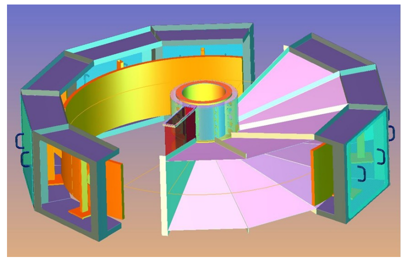

Reflectometry
INTER Air/ liquid/ solid interface interactions
OFFSPEC Structures of membrane, protein and liquid interfaces
POLREF Interface measurements in magnetic sensor devices

TS-2 Proposed Phase Two Instruments

Chipir	Atmospheric neutron research and testing
Exeed	Extreme sample environments diffractometer
Exess	Extreme sample environments spectrometer
Imat	Neutron imaging, materials science and engineering
Larmor	Multi-purpose instrument for small-angle scattering, diffraction and spectroscopy
Lmx	Large molecule crystallography
Nessie	Time-of-flight spin echo spectrometer
Zoom	High count-rate, focussing small angle scattering